CENTRAL RESEARCH LIBRARY
DOCUMENT COLLECTION

[redacted]

MARTIN MARIETTA ENERGY SYSTEMS LIBRARIES
3 4456 0360599 9

ORNL-1285
Progress
+ Errata

LABORATORY RECORDS
1954

CHEMISTRY DIVISION

QUARTERLY PROGRESS REPORT

FOR PERIOD ENDING MARCH 31, 1952

CLASSIFICATION CHANGED TO: Unc-1237
BY AUTHORITY OF: CB Clayton 1-14-61
BY:

OAK RIDGE NATIONAL LABORATORY
CENTRAL RESEARCH LIBRARY
CIRCULATION SECTION
4500N ROOM 175
LIBRARY LOAN COPY
DO NOT TRANSFER TO ANOTHER PERSON
If you wish someone else to see this report, send in name with report and the library will arrange a loan.
UCN-7969 (3 9-77)

OAK RIDGE NATIONAL LABORATORY
OPERATED BY
CARBIDE AND CARBON CHEMICALS COMPANY
A DIVISION OF UNION CARBIDE AND CARBON CORPORATION
UCC
POST OFFICE BOX P
OAK RIDGE, TENNESSEE

[redacted]

[redacted]

ORNL-1285
Errata

This document consists of 5 pages.
Copy 8 of 136 copies. Series A.

INV.

CHEMISTRY DIVISION QUARTERLY PROGRESS REPORT

FOR PERIOD ENDING MARCH 31, 1952

Errata

[redacted]

[redacted]

ERRATA SHEET

CHEMISTRY DIVISION QUARTERLY PROGRESS REPORT FOR PERIOD ENDING MARCH 31, 1952
ORNL-1285

PAGE NO.	COLUMN NO.	LINE NO.	ERRATA
8	1	24-31	read: ... It seemed of interest to confirm these results at higher temperatures and to obtain estimates of the temperature coefficients of the equilibrium constant for the dimerization reaction and of the activity coefficients of the monomer and dimer.
8	2	Eq. 1	for: $\ln \frac{y_\beta}{\gamma_\alpha}$
			read: $\ln \frac{y_\beta}{y_\alpha}$
		10-11	and delete: ... γ is the activity coefficient (molality scale)...
8	2	Eq. 1	for: v
8	2	12	read: $\overline{v}$
9	2	39	
10	1	4	
13	1	33	
13	1	39	
8	2	Ref. 7	for: y_+
			read: $y_\pm$
9	1	43	for: ϕ
			read: θ
10	1	17-22	read: This series was selected in such a way that the concentration ranges of the various solutions at equilibrium overlapped with only moderate changes in concentration for each experiment.
11	2	7	for: ~0.4
			read: ~4.0

[redacted]

[redacted]

PAGE NO.	COLUMN NO.	LINE NO.	ERRATA
15	1	17	for: for example read: i.e.
17	2	6-13	read: ... Since one expects that the diffusion of thallium(I) and thallium(III) in mixtures would be essentially independent of each other, one expects that the diffusion current constants vary linearly with % thallium(III) in the solutions, as observed.
31	1	3	for: reactor read: pile
31	1	17-18	for: ..., which is read: .... This is most
59	2	8-11	read: The value u = 0.53 was completely unsatisfactory, indicating that the displacement of Br is toward the approaching hydrogens....
60	1	Table 21, Col. 3	read: I_{obs} 1600 129 3285 129 157 143 0 0 276 }* 533 }* 260 }* 57 }* 365 }* 84 }* 151 }* 132 }*
62 64	2 1	25-26 1-4	read: ... The couplings are consistent with the earlier chloromethane values[9] and can be explained by variations in ionic character in the carbon-chlorine bond as a function of chemical composition....

[redacted]

[redacted]

PAGE NO.	COLUMN NO.	LINE NO.	ERRATA
72	2	21-25	read: ... Analysis of this phase by hydrogen evolution and alkalinity gave good agreement for a barium excess over $BaCl_2$ of 23 ± 1 mole per cent.
73	2	14-20	read: ... X-ray diffraction was also used to search for a subhalide in attempts similar to those by Wöhler and Rodewald[4] to separate a phase different from $CaCl_2$ by treatment with various mixtures of ethyl iodide and bromo form....
73	2	31-37	read: ... On the other hand, the more recent work of the California group indicating an appreciable solubility in the molten state, though greatly below that corresponding to 100% subhalide formation, is being confirmed to a large extent....

[redacted]

[redacted]

ORNL-1285

This document consists of 132 pages.

Copy 8 of 136 copies. Series A.

Contract No. W-7405-eng-26

CHEMISTRY DIVISION

QUARTERLY PROGRESS REPORT

for Period Ending March 31, 1952

S. C. Lind, Acting Director

G. E. Boyd, M. A. Bredig, Associate Directors

DATE ISSUED

NOV 12 1952

OAK RIDGE NATIONAL LABORATORY

Operated by

CARBIDE AND CARBON CHEMICALS COMPANY

A Division of Union Carbide and Carbon Corporation

Post Office Box P

Oak Ridge, Tennessee

[redacted]

ORNL-1285
Progress

INTERNAL DISTRIBUTION

1. G. T. Felbeck (GCCC)
2-3. Chemistry Library
4. Physics Library
5. Biology Library
6. Health Physics Library
7. Metallurgy Library
8-9. Training School Library
10-13. Central Files
14. Reactor Experimental Engineering Library
15. C. E. Center
16. C. E. Larson
17. W. B. Humes (K-25)
18. L. B. Emlet (Y-12)
19. A. M. Weinberg
20. E. H. Taylor
21. E. J. Murphy
22. E. D. Shipley
23. S. C. Lind
24. F. C. Vonderlage
25. R. C. Briant
26. J. A. Swartout
27. F. L. Steahly
28. A. H. Snell
29. A. Hollaender
30. M. T. Kelley
31. G. H. Clewett
32. K. Z. Morgan
33. J. S. Felton
34. A. S. Householder
35. C. S. Harrill
36. C. E. Winters
37. D. W. Cardwell
38. E. M. King
39. J. A. Wethington
40. G. E. Boyd
41. M. A. Bredig
42. R. W. Stoughton
43. R. B. Briggs
44. G. W. Parker
45. C. J. Borkowski
46. G. H. Jenks
47. K. A. Kraus
48. H. A. Levy
49. R. S. Livingston
50. T. E. Willmarth
51. C. H. Secoy
52. C. J. Hochanadel
53. D. K. Neville
54. [illegible] H. Baldwin
55. [illegible] R. Brosi
56. [illegible] N. Lyon
57. S. A. Reynolds
58. P. F. Thomason
59. E. G. Bohlmann
60. C. [illegible] Keim
61. C. [illegible] Susano
62. D. [illegible] Cowen
63. P. [illegible] Reyling
64. R. Livingston
65. G. H. Cartledge
66. E. R. VanArtsdalen
67. S. D. Schiffman (K-25)
68. E. P. Wigner (consultant)

[redacted]

EXTERNAL DISTRIBUTION

69-76. Argonne National Laboratory
77-84. Atomic Energy Commission, Washington
85-88. Brookhaven National Laboratory
89-92. Carbide and Carbon Chemical Company (Y-12 Area)
93-96. E. I. du Pont de Nemours and Company
97-98. Knolls Atomic Power Laboratory
99-104. General Electric Company, Richland
105. Idaho Operations Office (Phillips Petroleum Co.)
106-109. Los Alamos
110. Mound Laboratory
111-113. New York Operations Office
114. Patent Branch, Washington
115. Savannah River Operations Office, Wilmington
116-130. Technical Information Service, Oak Ridge
131-134. University of California Radiation Laboratory
135-136. Westinghouse Electric Corporation

[redacted]

[redacted]

[redacted]

Chemistry Division quarterly progress reports previously issued in this series are as follows:

ORNL-65	March, April, May, 1948
ORNL-176	June, July, August, 1948
ORNL-229	September, October, November, 1948
ORNL-336	December, 1948, January and February, 1949
ORNL-286	Period Ending June 30, 1949
ORNL-499	Period Ending September 30, 1949
ORNL-607	Period Ending December 31, 1949
ORNL-685	Period Ending March 31, 1950
ORNL-795	Period Ending June 30, 1950
ORNL-870	Period Ending September 30, 1950
ORNL-1036	Period Ending December 31, 1950
ORNL-1053	Period Ending March 31, 1951
ORNL-1116	Period Ending June 30, 1951
ORNL-1153	Period Ending September 30, 1951
ORNL-1260	Period Ending December 31, 1951

[redacted]

[redacted]

TABLE OF CONTENTS

PAGE

SUMMARY 1

INORGANIC CHEMISTRY 7

Thorium Hydrolysis Studies of Solid Thorium Salts 7
Ultracentrifugal Measurements of Uranyl Fluoride Solutions 8
Heat and Entropy of Hydrolysis of Uranium(IV) 13
Determination of the Stability of Complex Ions with Cation Exchange Resins 15
Polarography of Thallium 15
Chemistry of Technetium 18
Magnetic Studies on Technetium Compounds 24
Br_2-BrO_3 Exchange in Acid Media Using Br^{82} as Tracer 25
Thermodynamics of Complex Ions 27
Entropies of Aqueous Ions 27
Chemistry of Fused Salts 27
Bond Strengths in Silicon Compounds 28

NUCLEAR CHEMISTRY 28

Half Life and Mass Assignment of Argon-39 28
Neutron Capture Cross Section of Proactinium-233 30
Preparation of Technetium and Promethium Compounds for Exhibition . . . 32
A Specific Solvent Extraction Method for Technetium 33
Gamma Radiation from 36.5-h Rhodium-105 35
Half Life and Radiations of Technetium-100 38

RADIO-ORGANIC CHEMISTRY 40

Radiation Chemistry 40
Isotope Effect Studies 43
Comparison of the isotope effects in the decarboxylation of malonic-1-C^{14} acid and malonic-2-C^{14} acid at 154°C 43
Dehydration of formic-C^{14} acid 48
Alkaline hydrolysis of *meta*- and *para*-substituted ethyl benzoates labeled with carbon-14 in the carboxyl groups 50
Decomposition of hydrogen peroxide 52
Isotope effect in the carbonation of organometallic compounds 53
Migration ratios in the rearrangement of 2,2-diarylethanols 54
Thermal stabilities of organic compounds 54

[redacted]

[redacted]

[redacted]

SEPARATION PROCESSES 57

Organic Chemistry of Solvents 57
Protium-Deuterium Exchange in Ion-Exchange Resins 57

CHEMICAL PHYSICS 58

Neutron Diffraction Studies 58
Radio-Frequency Spectroscopy 62
Alkyl chlorides 62
Chlorates 64

RADIATION CHEMISTRY 64

Peroxide Production in Reactor-Irradiated Uranyl Sulfate Solution . . . 64
Peroxide Production in Gamma-Irradiated Ice 65
Some Effects of Cobalt Gamma Rays in 0.8 *N* Sulfuric Acid Solutions . . 66
Some Effects of Cobalt Gamma Rays on UO_2SO_4 Solutions 68
Some Effects of Cobalt Gamma Rays on CCl_4-H_2O System 69
Gamma-Ray Dosimetry 70
Preparation of Alpha-Ray Deuterio-Cuprene 70

CHEMISTRY OF THE SOLIDS STATE 71

High Temperature X-ray Diffraction 71
Remote-Control X-ray Diffraction Spectrometer 71
Effects of Radiation on Crystal Structure 72
Metal-Metal Halide Systems 72
Determination of the High-Temperature Glaserite-Type Crystal Structure of Some A_2BX_4 Compounds 76
Miscellaneous X-ray Diffraction Work 77

INSTRUMENTS 77

Gamma-Ray Energy Resolution with Sodium Iodide Scintillation Spectrometers 77
Linear Amplifier for Scintillation Spectrometry 88

REACTOR CHEMISTRY 89

Homogeneous Recombination of Hydrogen and Oxygen in Solutions 89
Kinetics of the Decomposition of Hydrogen Peroxide in Uranyl Sulfate Solutions 94

[redacted]

[redacted]

[redacted]

Radiation Chemistry of Aqueous Reactor Solutions 97
Gas Kinetics of In-Reactor Radiation Studies 99
Plutonium Solubilities in Uranyl Salt Solution 108
Fission-Product Solubilities in Uranyl Sulfate Solutions 111
Calculated Fission-Product Buildups for a Homogeneous Reactor-
Experimental Solubilities of Fission-Product Mixtures in
Uranyl Sulfate Solutions 113
Two-Liquid-Phase Temperatures for the Deuterium Oxide-Uranyl
Sulfate and Uranyl Fluoride Systems 115
Conductivity of Uranyl Sulfate and Uranyl Fluoride in
Aqueous Solution 118
Vapor Pressures of Uranyl Sulfate Solutions 118
Density-Weight Percent-Molarity Relationships at 25.0°C and
Between 100 and 300°C for Aqueous Uranyl Sulfate Solutions 121
Experiments with High-Temperature Electrodes 122

[redacted]

[redacted]

CHEMISTRY DIVISION
QUARTERLY PROGRESS REPORT

SUMMARY

INORGANIC CHEMISTRY

Debye-Scherrer x-ray photographs of solid basic thorium perchlorate, $Th(OH)_2(ClO_4)_2$, indicate that it probably does not belong to the cubic, tetragonal, or hexagonal systems.

Products of dehydration and hydrolysis of thorium nitrate hydrate, $Th(NO_3)_4 \cdot 4.8H_2O$, under various conditions, include $Th(NO_3)_4 \cdot 3H_2O$, $Th(NO_3)_4 \cdot 2.3H_2O$, $Th(OH)_{1.9}O_{0.4}(NO_3)_{1.3}$, and $Th(OH)_{1.1}O_{1.2}(NO_3)_{0.5}$.

Activity coefficients for UO_2F_2 were determined at 30°C by ultracentrifugation. From the data the equilibrium constant for the dimerization reaction was found to be K = 4.3, and estimates for the activity coefficients for the monomer and dimer were obtained. By using the earlier freezing-point data, the heat and entropy of dimerization were estimated to be 4500 cal and 21 e.u. In potassium fluoride solution, uranyl fluoride appears to exist predominantly as a dimeric species at concentrations that would result in only slight dimerization in water alone.

From spectrophotometric measurements of the hydrolysis of uranium(IV) at temperatures of 10.0, 25.0, and 43.0°C, the heat and entropy of the hydrolysis reaction

$$U^{+4} + 2H_2O \longrightarrow U(OH)^{+3} + H_3O^+$$

were estimated to be ΔH = 11,000 cal and ΔS = 30 e.u. at an ionic strength of 0.5. If ΔH is the same at 250°C as at the lower temperatures, uranium(IV) in the absence of complexing agents would be completely hydrolyzed, even in strongly acidic solutions.

Earlier conclusions in regard to the considerable complexing of zinc by chloride ions at low ionic strength were confirmed by cation-exchange experiments with Dowex-50 at room temperature and at 80°C.

Cobalt, like zinc and cadmium, is less strongly adsorbed from chloride solution than from perchlorate solutions, suggesting the formation of a weak chloride complex.

The cathodic diffusion current of thallium(III) was found to be linear with concentration and could be used for the analytical determination of thallium(III) concentrations by the polarographic method.

Work on the Br-BrO_3 exchange in acid media using Br^{82} as tracer was continued. In order to be able to interpret spectrophotometric data concerning the rate of growth and destruction of HBrO in the system $HBrO_3$-Br_2-$HClO_4$, extinction coefficients of Br_2, Br_3^-, HBrO, and $HBrO_3$ were determined.

Calorimetric measurements of the heat of combustion of technetium metal, and of the heats of solution and dilution in water of several technetium compounds were performed. The heat of formation of Tc_2O_7 (*s*) from elemental technetium and oxygen gas was found as −266.1 ± 2.6 kcal per mole of Tc_2O_7. The heat of formation of aqueous pertechnic acid was −173.0 ± 1.7 kcal per mole of $HTcO_4$.

Magnetic measurements on $TcO_2 \cdot 2H_2O$ and $ReO_2 \cdot 2H_2O$ showed technetium and rhenium in these compounds to have a susceptibility of only about one-tenth that found for $MnO_2 \cdot 0.48H_2O$ suggesting

that a large change in the number of unpaired electrons must occur between manganese and the heavier members of Group VIIB. Susceptibility determinations on complex chloride and thiocyanate ions of technetium(IV) and rhenium(IV) showed these to be paramagnetic and to possess a magnetic moment approximately that expected for three unpaired electrons on the basis of the "spin only" formula. The susceptibilities of metallic technetium and rhenium were both appreciably smaller than that for metallic manganese.

A research program on pure molten salts and their mixtures, involving the measurement of electrical conductivity, ionic transport, complex formation, and other physical-chemical properties has been started.

The equilibration constant for the reaction between the bis- and tris-pentanedione complexes of the manganese(III) ion has been measured at various temperatures.

A theoretical study has been made of the correlation of the entropy of aqueous ions with the ionic potential. The correlation appears to be useful not only for purposes of the empirical interpolation but also for an interpretation of the action of the ions upon their aqueous environment.

On the basis of thermochemical data from the more recent literature, the silicon-to-oxygen bond strength in compounds containing carbon-to-silicon and oxygen-to-silicon bonds was calculated to be of the order of 80 to 100 kcal/mole.

NUCLEAR CHEMISTRY

A tentative mass of 39 previously assigned to an argon isotope decaying with an alpha type of forbidden beta spectrum has been confirmed, and its half life has been determined to be 265 ± 30 years. The log (ft) value is 9.9 and log $[(W_0^2 - 1)ft]$ is 10.4, that is, within the range of values given in the literature for beta transition where $\Delta l = 1$ and $\Delta I = 2$.

In order to determine the neutron-capture cross section of Pa^{233}, an intermediate in the transformation of Th^{233} into U^{233}, slugs of thorium were irradiated for varying periods of time in the LITR. Calculations were made that show that after a cooling period of three months it will be possible to obtain this cross section with reasonable accuracy by determining the U^{234}-to-U^{233} and U^{233}-to-Th ratios through isotopic analysis.

A number of technetium and rhenium compounds were prepared in quantities ranging from 1 to 75 mg for exhibition at the American Academy of Arts and Sciences in Boston, Massachusetts.

A specific solvent-extraction method for technetium has been developed in which tetraphenylarsonium pertechnetate is precipitated from nitric acid solution and extracted in chloroform.

The decay of 36.5-h $Rh^{105}(g)$ was examined and shown to occur with the emission of a 320-kev gamma ray in about 10% of its disintegrations. A new, short-lived technetium activity, Tc^{100}, was produced by neutron irradiation of purified fission-product $Tc^{99}(g)$. The half life observed was 15.8 ± 0.2 sec. Beta rays of 2.8 ± 0.2 Mev together with gamma radiations were found.

RADIO-ORGANIC CHEMISTRY

Radiation Chemistry. A Co^{60} shield and source-holder have been constructed. The source has been calibrated for intensity of radiation at three positions.

The irradiation of samples of aqueous acetic acid has been continued in order to explain the mechanism of succinic acid formation.

Exploratory experiments have been carried out in which aqueous solutions of methanol, oxalic acid, and succinic acid were irradiated.

Isotope Effect Studies. The isotope effects in the decompositions of malonic-1-C^{14} acid and malonic-2-C^{14} acid at 154°C have been determined by two different methods. The results indicate that the isotope effect is the same during the decomposition of the two differently labeled acids.

The previously reported isotope effect in the decomposition of formic-C^{14} acid has been redetermined in a refined apparatus. The present results are in essential agreement with the earlier data.

The isotope effects in the alkaline hydrolyses of five *meta*- or *para*-substituted carboxyl-labeled ethyl benzoates are reported for 25°C. With the exception of the data for ethyl benzoate, a quantitative correlation with the Hammett equation is indicated. The isotope effect in the hydrolysis of carboxyl-labeled ethyl benzoate has been determined at 25°C and at 1°C, and a temperature coefficient has been demonstrated.

One run has been made with the purpose of determining the isotope effect in the decomposition of hydrogen peroxide-O^{18}. Data will be presented in a subsequent report.

A normal-isotope effect has been demonstrated conclusively in the carbonation of 1-methyl-9-fluorene-sodium with carbon-C^{14} dioxide.

Migration Ratios in the Rearrangements of 2,2-Diarylethanols. The migration ratios in the Wagner rearrangements of six additional 2,2-diarylethanols have been determined.

Thermal Stabilities of Organic Compounds. An apparatus has been constructed for use in determining the thermal stabilities of organic compounds.

CHEMISTRY OF SEPARATIONS PROCESSES

Extractions of various cations (Fe, Al, Ba, La, and Na) from aqueous solution with carbon tetrachloride containing 0.75 *M* tributyl phosphine oxide do not show as high selectivity as with solvents that do not extract so completely. It is believed, however, that selectivity can be varied with the structure of the organic molecule and with the anionic character of the aqueous solution.

A method for the determination of the equivalent weight of salts of organic or inorganic acids by cation exchange as recently suggested in the literature was found useful.

CHEMICAL PHYSICS

The crystal structures of the tetragonal phase (III) and of the high-temperature, cubic phase (I) of deutero-ammonium bromide have been determined by neutron diffraction at −78°C and at 200 to 250°C.

Improvements have been made in the apparatus for radio-frequency spectroscopy. Chlorine quadrupole couplings, consistent with the earlier chloromethane values, were observed in a variety of substituted ethanes and related compounds and can be explained by variations in ionic character in the carbon-chlorine bond.

The effect of environment and/or distortion of the ClO_3 anion on the

chlorine quadrupole resonance is being studied for $NaClO_3$, $KClO_3$, $AgClO_3$, $Ba(ClO_3)_2 \cdot H_2O$, $Cu(ClO_3)_2 \cdot 6H_2O$, and $Ni(ClO_3)_2 \cdot 6H_2O$. The effects of paramagnetic cations in random and antiferromagnetic structures are given special attention.

RADIATION CHEMISTRY

Measures taken to prevent decomposition of the hydrogen peroxide formed by reactor irradiation of uranyl sulfate solutions, by immersing the irradiated solution in liquid nitrogen for the period of radioactive decay before analysis, led to a peroxide yield of 0.97 molecules per 100 ev. When compared with the hydrogen yield of 0.98 molecules/ev, the result suggests that the initial products are H_2 and H_2O_2 rather than H_2 and O_2.

The results of experiments on the irradiation of ice at various temperatures between 0 and −196°C seem to indicate that although the initial rate of production of H_2O_2 decreases continuously with decreasing temperature, at least when oxygen is present, the tendency toward recombination of the products decreases even more rapidly, resulting in a higher steady-state concentration of H_2O_2 at low temperatures.

Some studies are reported on effects of gamma rays on 0.8 *N* H_2SO_4 and also on solutions of ferrous sulfate and ceric sulfate in 0.8 *N* H_2SO_4. Uranyl sulfate lowers the yield of molecular H_2 and H_2O_2 produced in water by gamma radiation but has little effect on the yield of free radicals H and OH that are available to react with solutes. Uranyl sulfate was also shown to be a solute that is relatively inefficient in reacting with H- and OH-free radicals.

In saturated solutions of carbon tetrachloride in water, 9 to 12 molecules of HCl were found to have been formed per 100 ev of gamma radiation.

The observed yield of 15.6 ferrous ions oxidized per 100 ev, as used in gamma-ray dosimetry, was found to be independent of intensity over a wide range.

The production of deutero-cuprene in a specially designed apparatus by irradiation with radon alpha particles of deutero-acetylene, for the purpose of studying the structure of cuprene by neutron diffraction, has been initiated and is progressing satisfactorily.

CHEMISTRY OF THE SOLID STATE

Further attempts are being made to increase the operating temperature of the high-temperature x-ray-diffraction spectrometer beyond 2100°C.

Difficulties in the operation of the remote-control x-ray-diffraction spectrometer are being overcome.

Further control tests in the absence of radiation indicate that the previously reported transformation of yellow lead oxide into the red form on exposure in the Chalk River reactor was very likely due to the failure to maintain a low ambient temperature rather than to neutron collisions.

In the study of halogen-deficient salt melts, the solubilities of calcium and barium metals in their molten chlorides were found to be of the order of 8 and 25 mole %, respectively. The figures are much lower than those reported in the older literature but are in essential agreement with data from more recent work.

The solubilities at 860°C of potassium metal in the binary eutectic NaF-KF and in the ternary eutectic LiF-NaF-KF were found to be 3.0 and 1.6 mole%, respectively. Thermodynamic estimates indicate the amounts would be sufficient to suppress metallic corrosion and mass transfer by molten fluorides which, according to similar estimates as well as actual observations, can be caused by shifts in reaction equilibria such as

$$Fe + 2KF \rightleftharpoons FeF_2 + 2K$$

with temperature.

The x-ray-diffraction study of the crystal structure of glaserite $(K,Na)_2SO_4$, isotypic with the high-temperature forms of Na_2BeF_4 and K_2BeF_4, is progressing.

INSTRUMENTATION

A new method of crystal preparation and mounting was developed that gives long-time surface stability and good energy resolution to thallium-activated, sodium iodide, scintillation spectrometers.

Difficulties in the building of a practical unit of the new linear amplifier for scintillation spectrometry, largely associated with the problem of getting good overload characteristics, have been overcome.

Equipment for use in nuclear quadrupole measurements is being designed.

REACTOR CHEMISTRY

The study of recombination of hydrogen and oxygen in uranyl sulfate solution in the absence of radiation as the function of total pressure, partial pressures, catalyst concentration, temperature, wall surface, and diffusion rate led to the establishment of first-order reactions with respect to hydrogen, and copper ion, or iodine ion, catalyst concentration, and of a second- and one-half-order reaction with respect to silver ion catalyst concentration. Reaction rate constants (±20%) can be expressed as follows:

$$k(\text{soln}) = [Cu]^{1.0} \times 5.9 \times 10^{13}\, e^{-24000/RT},\ hr^{-1},$$

$$k(\text{soln}) = [I]^{1.0} \times 1.2 \times 10^{11}\, e^{-18500/RT},\ hr^{-1},$$

and

$$k(\text{soln}) = [Ag]^{2.45} \times 2.2 \times 10^{10}\, e^{-9000/RT},\ hr^{-1},$$

Other ions tested and shown to have no significant catalytic activity are: Co, Zn, Cd, Pb, As, Li, Rb, Cl, K, Br, and Mg.

Thermal decomposition in uranyl sulfate solutions from 0.0045 to 0.17 *M* of hydrogen peroxide over a concentration range of 4×10^{-4} to 5×10^{-3} *N* was found to be a first-order reaction with respect to the hydrogen peroxide and to be independent of the uranyl sulfate concentration from 0.0175 to 0.176 *M*.

The rate of gaseous hydrogen and oxygen production in fissioning uranium solutions was found under constant neutron flux to decrease with an increase in uranyl sulfate (fluoride) concentration and a decrease in enrichment (U^{235} content) and to be independent of temperature between 30 and 250°C.

Cupric ion does not decrease the rate of gas formation; rather it increases it slightly. The decrease in equilibrium pressure over fissioning UO_2SO_4 solutions containing copper is caused by a chemically induced back reaction, the recombination of hydrogen and oxygen to form water.

Equations representing the rate of gas formation during in-reactor radiation studies of uranyl sulfate solutions as a function of neutron flux, volume, diffusion coefficient, and of various constants such as fission cross section, fission-product recoil energy, rate of hydrogen production per 100 ev, Henry's law constant, etc. were set up. The nature of the dP/dt vs. P graph serves to indicate the state of the system. It was found that mixing between gas and liquid phase is about ten times better than that which would result from simple diffusion alone.

Hydrolysis of plutonium(IV) sulfate in 2.73 *M* uranyl sulfate solution was found to be a first-order reaction at temperatures varied from 100 to 150°C, with an activation energy of 31 kilocalories. The hydrolysis in uranyl fluoride solution is also a first-order reaction.

Gamma radiation was found to enhance the rate of the reaction $Pu(III) + Pu(V) \rightleftharpoons Pu(IV)$ in plutonium(IV) sulfate solution.

An extremely large reduction of the solubility of cesium sulfate in 1.26 *M* uranyl sulfate solution at temperatures between 170 and 285°C as compared with that in 0.126 *M* solution has been noted.

The change in the differential heat of solution above 100°C of various fission-product sulfates such as $Y_2(SO_4)_3$, $La_2(SO_4)_3$, Cs_2SO_4, $CdSO_4$, Ag_2SO_4, and $Ce(SO_4)_2$ in uranyl sulfate solution of increasing molarity was found to be positive.

The build-up of fission products that might precipitate as sulfates was calculated for a 50-kw/l reactor running continuously for one month or for one year, both for the case of 0 and 100% gas removal.

Solubility measurements in mixtures of sulfate solutions also containing 1.26 *M* UO_2SO_4 of ten of the most important fission products indicate that cerium, zirconium, ruthenium, barium, and niobium will be the first to precipitate of the elements studied.

On the basis of new measurements of the two-liquid-phase transition temperatures in water and deuterium oxide-uranyl sulfate and fluoride solutions, there is believed to be an effect of impurities on these temperatures. There is also a significant 10°C lowering of the transition temperature for the D_2O system as compared with water.

Electrical conductivity measurements of aqueous solutions of uranyl sulfate and fluoride in concentrations ranging from 0.0001 *N* to 6 *N* at temperatures between 0 and 125°C indicate that both are weak electrolytes, with sulfate being the more highly dissociated salt.

Measurements of the vapor pressures of saturated uranyl sulfate solutions at temperatures ranging from 50 to 100°C have been started. Empirical density-weight per cent-molarity conversion equations have been determined for uranyl sulfate-water solutions at 25.0°C and between 100 and 300°C from available density data.

Silver, silver sulfate and mercury, mercury sulfate electrodes were developed for high-temperature potential measurements and were found suitable for observations of the stability of passive films on stainless steel in hot uranyl sulfate solutions.

INORGANIC CHEMISTRY

THORIUM HYDROLYSIS STUDIES OF SOLID THORIUM SALTS

W. C. Waggener R. W. Stoughton

Basic Thorium Perchlorate. Solid thorium perchlorate prepared by fuming hydrated thorium nitrate with perchloric acid at 200 to 215°C has the empirical formula, $Th(OH)_2(ClO_4)_2$.[1,2] Debye-Scherrer x-ray photographs of the compound indicate that it probably does not belong to the cubic, tetragonal, or hexagonal systems. Thus far, efforts to prepare single crystals for further x-ray studies have been unsuccessful.

In one attempt to prepare large crystals, a sample of thorium perchlorate in concentrated perchloric acid was heated to constant weight in a vacuum oven at 117°C and a pressure of 1 to 2 mm Hg. The sample changed from a colorless, viscous liquid to a glassy solid that, over a period of a week, fell to a white powder. This final product was similar in appearance to the solid perchlorate prepared at 200°C, with a molecular weight approaching 466.0 as compared to 465.1 for $Th(OH)_2(ClO_4)_2$. Powder photographs and analysis of the charge of the hydrolyzed cation[2] are being utilized to compare the material with that prepared at the higher temperature.

Thorium Nitrate. Experiments are being performed in which thorium nitrate hydrate is heated to determine the existence and nature of partially hydrolyzed species, which may exist in the solid state of this salt, similar to those of the stable, half-hydrolyzed perchlorate. Thorium nitrate hydrate appears to be more susceptible to thermal decomposition than indicated in the literature. For example, at 113 to 115°C in air, 60-mg samples of $Th(NO_3)_4 \cdot 4.8H_2O$ were 70% hydrolyzed in three days, whereas 1.5-g samples were 87.5% hydrolyzed in about one month.

Samples of water-recrystallized thorium nitrate (with Maywood, and Baker and Adamson, reagent-grade salts used as starting materials) have been heated at 113 to 115°C in air for varying periods of time. Both the weight loss and the magnitude of the cation charge have been followed as a function of time. These experiments are incomplete; however, tentative results from the data are now available:

1. Water-recrystallized thorium nitrate dried in vacuum at room temperature contains $4.8H_2O$, and is certainly less than 1% hydrolyzed.

2. At 114°C, $1.8H_2O$ is lost within 30 min to give $Th(NO_3)_4 \cdot 3H_2O$. Very little hydrolysis of the nitrate occurs in this short time, and the salt will revert to $Th(NO_3)_4 \cdot 4.8H_2O$ if allowed to stand overnight in a hygrostat having a relative humidity of 35%.

3. Decomposition of $Th(NO_3)_4 \cdot 3H_2O$ occurs slowly at 114°C with resultant hydrolysis of the thorium cation, the rate being a function of sample and particle size. A graph of the charge of the hydrolyzed cation vs. weight loss becomes linear below a charge of 3.5. Moreover, the curve indicates that the decomposition involves internal hydrolysis of $Th(NO_3)_4 \cdot 2.3H_2O$, with loss of HNO_3.

---

(1) W. C. Waggener and R. W. Stoughton, *Chemistry Division Quarterly Progress Report for Period Ending September 30, 1951*, ORNL-1153, p. 7.

(2) W. C. Waggener and R. W. Stoughton, *Chemistry Division Quarterly Progress Report for Period Ending December 31, 1951*, ORNL-1260, p. 1.

4. Broad plateaus in the graphs of weight loss vs. heating time have been found at 38 and 47% weight loss. By combining the data on the hydrolyzed cationic charges with the weight-loss figures, the two compositions of particular stability correspond to $Th(OH)_{1.9}O_{0.4}(NO_3)_{1.3}$ and $Th(OH)_{1.1}O_{1.2}(NO_3)_{0.5}$.

X-ray diffraction photographs will be used to verify the existence of the species postulated above. The studies are being extended to the halide hydrates.

ULTRACENTRIFUGAL MEASUREMENTS OF URANYL FLUORIDE SOLUTIONS

J. S. Johnson K. A. Kraus

Activity coefficients of UO_2F_2, calculated from freezing-point depressions of aqueous solutions,[3,4] indicated that at concentrations above 0.1 *m*, the solute exists primarily as an equilibrium mixture of unionized monomer and dimer. Therefore confirmation of these results at higher temperatures and estimates of the temperature coefficients of the equilibrium constant for the dimerization reaction and of the activity coefficients of the monomer and dimer seemed to be of interest.

The activity coefficients of UO_2F_2 in water and in the presence of supporting electrolytes were measured by ultracentrifugation to equilibrium. This method, in which the concentration distribution of the solute is measured as a function of the radius of rotation, x, at sedimentation equilibrium, has been used for inorganic salts by Pedersen[5] and Drucker.[6] The ratios of activity coefficients for various concentrations of the solute at different positions alpha and beta in the cell can be calculated from the equation

$$\ln \frac{y_\beta}{\gamma_\alpha} = \frac{M\,(1 - v\rho)\omega^2}{2RT} = (x_\beta^2 - x_\alpha^2) - \ln \frac{c_\beta}{c_\alpha}, \quad (1)$$

where y is the activity coefficient (molarity scale), γ is the activity coefficient (molality scale), M the molecular weight of the solute, v the partial specific volume of the solute, ρ the density of the solution, ω the angular velocity of the centrifuge (2π times the number of revolutions per second), R the gas constant, T the absolute temperature, and c the molarity.[7] The subscripts α and β refer to radii of rotation. From a knowledge of the activity coefficient at one concentration and the ratios determined by Eq. 1, values of y at other concentrations may be calculated.

The concentration interval from 0.15 *M* to saturated was studied for uranyl fluoride-water solutions. In addition, a few centrifugation equilibrium experiments of uranyl fluoride in sodium perchlorate and potassium fluoride solutions were also conducted.

The solutions were centrifuged in a Specialized Instrument Corporation

(3) J. S. Johnson and K. A. Kraus, *op. cit.*, ORNL-1260, p. 3.

(4) J. S. Johnson and K. A. Kraus, *Undissociated Species and Dimerization in Aqueous Solutions of Uranyl Flouride*, AECD-3236 (1951).

(5) K. O. Pedersen, *Z. Physik. Chem.* **A170**, 41 (1934); K. O. Pedersen in T. Svedberg, *The Ultracentrifuge*, Oxford University Press (1940), p. 53.

(6) C. Drucker, *Z. Physik. Chem.* **A180**, 359 (1937).

(7) If mean ionic activity coefficients, y_+, of a solute dissociated into ions are measured, the mean molecular weight M/ν (where ν is the number of moles of ions per mole of solute) appears in Eq. 1 instead of M.

("Spinco") Model E ultracentrifuge[8] operated at approximately 27,700 rpm. The average speed over a period of several hours was determined by means of a counter, which indicated that the speed was constant within ±20 rpm during an experiment.

The solutions were placed in cells with quartz windows, which are standard equipment with this instrument. The centerpieces were made of Kel-F plastic to avoid corrosion. Cells with 12-mm thickness, h, of solution in the direction of observation (perpendicular to plane of rotation) were used with dilute solutions and 3-mm cells with the more concentrated solutions. The midpoints of the cells were 65 mm from the center of rotation.

The machine is equipped with a Philpot-Svensson[9] optical system, which gives a (photographic) plot of a distance, Z, proportional to the gradient of the refractive index, n, as a function of radius of rotation, x, or dn/dx. This distance, Z, represents the displacement of the shadow of an inclined bar resulting from the refractive index gradients in the cell. The base line from which the displacement is measured is obtained in a "background" equilibrium experiment in which the solute is absent from the solution in the cell.

The optical constants for the centrifuge are as follows: radial magnification of the cell at the photographic plate, 2.04; magnification, ϕ, of the bar by the cylindrical lens, 4.47; and optical distance from the upper collimating lens to the bar (optical lever arm, L), 58.1 cm. Angles, ϕ, of 45 to 65 deg, complementary to those between the bar and the axis of the cylindrical lens were used. The optical constants allow[9] conversion of Z to dn/dx by the equation

$$\frac{dn}{dx} = \frac{Z \tan \theta}{Lh\phi} . \qquad (2)$$

Determinations of the refractive index of uranyl fluoride solutions were carried out with an Abbe refractometer.

The photographic plates were examined with a Gaertner toolmaker's microscope or an equivalent comparator, either of which permitted measurements of distances to ±0.002 mm in mutually perpendicular directions. This procedure is considerably better than the accuracy warranted, considering the definition of the bar shadows in the photographs.

The temperature of the solutions during equilibration could not be readily controlled. Measurements taken after the experiments indicated that equilibrium temperatures were 30 ± 3°C.

The time necessary to attain equilibrium varied from about three days for the more dilute solutions to approximately ten days for a saturated solution of uranyl fluoride. Equilibrium was considered to have been attained when three photographs taken at least 4 hr apart indicated no significant change in the bar-shadow displacement, Z.

The densities of uranyl fluoride-water solutions as measured by Marshall, Gill, and Secoy[10] were used for the computations according to Eq. 1. The partial specific volume, v, of uranyl fluoride was calculated from these data and found to be 0.125 over almost the whole concentration range, and

[8] E. G. Pickels, *Machine Design* **22**, 102 (1950).

[9] H. Svensson, *Koll. Z.* **87**, 181 (1939); H. Svensson, *Koll. Z.* **90**, 141 (1940).

[10] W. L. Marshall, J. S. Gill, and C. H. Secoy, *Chemistry Division Quarter Progress Report for Period Ending June 30, 1950*, ORNL-795, p. 22.

this value was used throughout. Errors introduced by deviations from this value are probably small, since $(1 - v\rho)$ is between about 0.75 and 0.88.

The same uranyl fluoride preparations were used in these experiments as in the previous freezing-point measurements.[3] One was prepared by Harshaw Chemical Company and the other by the Chemistry Department of the Electromagnetic Plant at Y-12.

Uranyl Fluoride in Water. A series of ultracentrifugal equilibrium experiments were conducted using solutions with initial concentrations of 0.234, 0.755, 1.57, and 2.97 *M* and saturated uranyl fluoride. The series was selected so that, for each experiment, the concentration ranges of the various solutions at equilibrium could be made to overlap by moderate changes in concentration. The concentration gradient, dc/dx, was calculated as a function of x, the distance from the center of rotation, by using the displacements of the bar shadow, Z, and the refractive index measurements of the uranyl fluoride solutions. A c vs. x diagram was constructed by normalizing to the known total quantity of solute in the cell. In the case of the saturated solution, normalization was achieved by assuming that the uranyl fluoride solution was 5.17 *M* at the maximum value of x, a value obtained from the data of Marshall, Gill, and Secoy.[10]

Activity coefficient ratios were calculated for the concentration range 0.15 to 4.5 *M* by using Eq. 1. From these ratios a set of activity coefficients, y^* (molarity scale) and γ^* (molality scale), was calculated, where the asterisk indicates that the reference value is an assigned value at a finite concentration, not $y = \gamma = 1$ at infinite dilution. The assignment, $c\,y^* = m\gamma_f^*$ at $c = 0.15$, was made where $\gamma_f^* = 0.890$ in order to make a comparison with the activity coefficients, y_f^*, determined from the freezing-point depressions. The activity coefficients, together with those obtained earlier from the freezing-point measurements,[3] are given in Table 1.

The accuracy of the activity coefficient ratios obtained is somewhat difficult to estimate. Measurements of the quantities in the first term on the right of Eq. 1, of the dependence of n on c, and of Z might be expected to cause an error of less than 2 to 3% in $(1 - \gamma^*/0.890)$. Uncertainties inherent in the optical system and the fact that equilibrium was attained at different temperatures for different experiments introduced additional errors. In the experiments with the more concentrated solutions, the densities were high (greater than 2 at saturation), consequently, the quartz windows of the cell were subjected to much higher pressures than in the background runs and may have contributed different increments to the refractive index gradients.

Table 1

ACTIVITY COEFFICIENTS

m	c (30°C)	y^* (30°C)	γ^* (30°C)[a]	γ_f^*
0.1511	0.150	0.895	0.890	0.890
0.3	0.296	0.75	0.74	0.801
0.5	0.490	0.64	0.63	0.719
0.7	0.679	0.58	0.56	0.666
1.0	0.960	0.52	0.50	0.613
1.5	1.418	0.47	0.45	0.566
2.0	1.865	0.45	0.42	0.545
2.5	2.30	0.44	0.41	0.539
3.0	2.70	0.44	0.40	0.543
3.5	3.07	0.45	0.39	0.554
4.0	3.44	0.46	0.40	0.570
4.5	3.81	0.48	0.40	0.590
5.0	4.17	0.49	0.41	0.614

[a] cy^* is assigned the same value as $m\gamma_f^*$ at $c = 0.15$.

It is apparent from Table 1 that the activity coefficients at the freezing points and 30°C show similar variation with concentration. However, at 30°C they decrease more sharply at low concentrations and rise more slowly at high concentrations than at the freezing point. These observations suggest that the same interpretation[3] applies at the two temperatures, although the parameters are different. It was previously assumed that dissociation of uranyl fluoride into ions is small and that the downward trend of γ^* from 0.1 to 2.5 *M* is due to dimerization of uranyl fluoride according to the equation

$$2\ UO_2F_2 \rightleftharpoons (UO_2F_2)_2\ , \qquad (3)$$

with an equilibrium constant

$$K = \frac{a_2}{a_1^2}\ , \qquad (4)$$

where a is the activity and the subscripts 1 and 2 refer to the monomer and dimer. The increase of γ^* above 2.5 *m* was ascribed to an increase of the activity coefficients γ_1 and γ_2 of the monomer and dimer. These activity coefficients were assumed to follow the equations

$$\log \gamma_1 = b_1 m\ ,$$

$$\log \gamma_2 = b_2 m\ ,$$

and

$$2b_1 = b_2\ , \qquad (5)$$

where b_1 and b_2 are constants and m is the molality of UO_2F_2. From these assumptions, it was shown that the equation

$$\log a^* - \log \frac{\sqrt{8Km + 1} - 1}{4K} = b_1 m - \log \beta \qquad (6)$$

should hold, where $a^* = m\gamma^*$ and $\beta a^* = a = \gamma m$. If the interpretation is correct, there should be a value of K for which the left side of Eq. 6 plotted against m would result in a a straight line with slope b_1.

Equation 6, plotted for various values of K, indicated best linearity for $K = \sim 0.4$ with a slope $b_1 = \sim 0.055$. Activity coefficients calculated from these constants show satisfactory agreement with the experimental results (Fig. 1). Values for K between 3.5 and 4.5 with slightly different b's also appear to give agreement within probable experimental error. At the freezing point, $K = \sim 1.5$ and $b_1 = \sim 0.07$ had been found. Assuming that these values are for the median temperature of the range studied (−5°C) and that $K = 4$ at 30°C, the heat and entropy of the dimerization reaction[5] can be calculated to be $\Delta H° = 4500$ cal and $\Delta S° = 17.5$ e.u.

UO_2F_2 in $NaClO_4$ Solutions. Two ultracentrifugations to equilibrium were carried out with uranyl fluoride (initial concentration 0.153 *M* and 0.526 *M*) in 1 *M* sodium perchlorate to test the assumption that the ionization of uranyl fluoride is negligible at the concentrations employed. If dissociation into ions were pronounced, it would be expected that the activity coefficients of uranyl fluoride would vary differently with concentration for the uranyl fluoride-water and uranyl fluoride-supporting electrolyte systems. The results are shown in Fig. 1 (dotted curves) with y^* in the sodium perchlorate system matched at one concentration with y^* in the water system. At a concentration of about 0.15 *M* uranyl fluoride the ratios of the activity coefficients are very close for the two systems, thereby supporting the assumption of low ionization. For the 0.5 *M* experiment, the ratios indicate a somewhat slower change of y^* with concentration for the sodium perchlorate system than for the water system. However, the

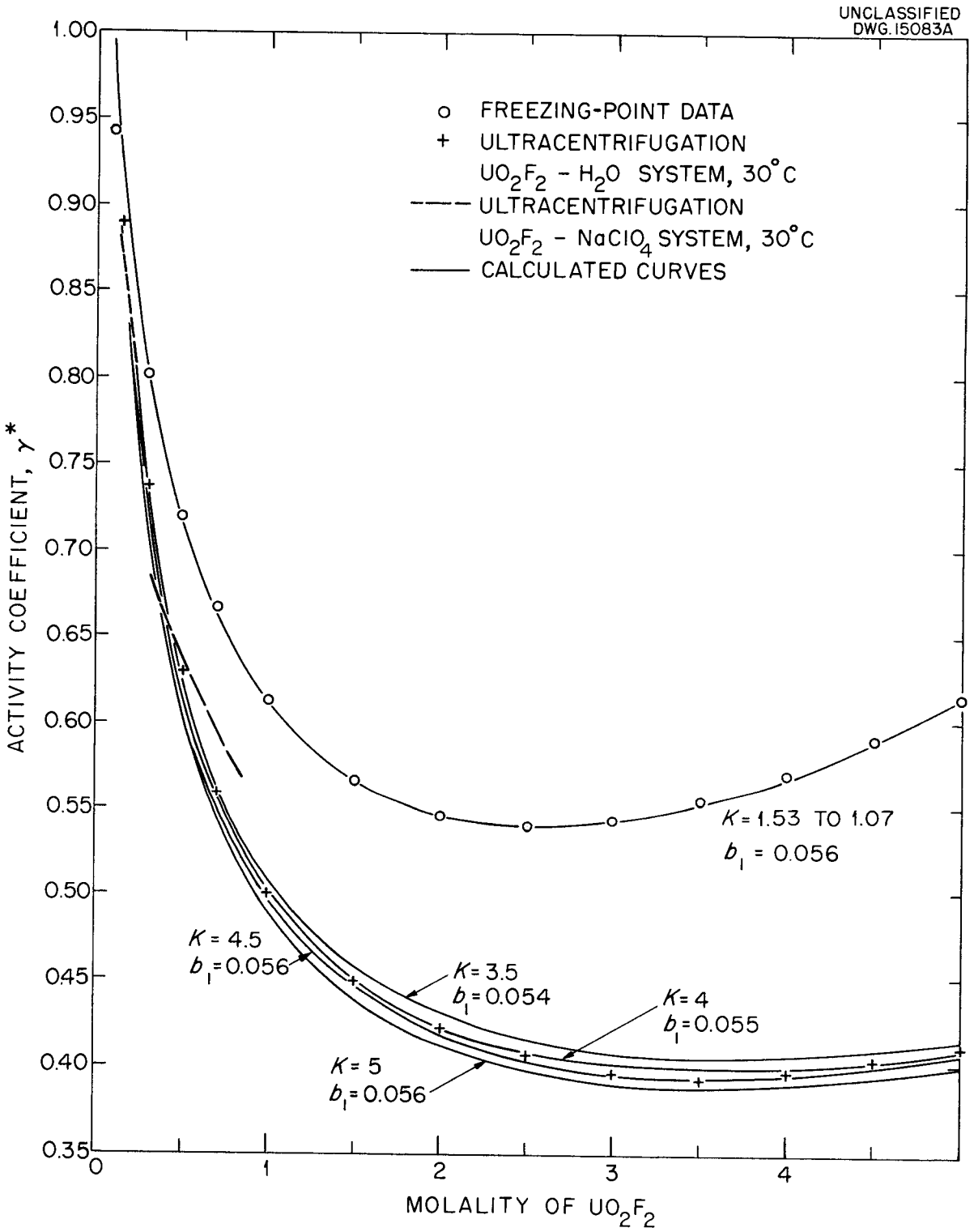

Fig. 1. Activity Coefficients of UO_2F_2.

uranyl fluoride concentration across the cell at equilibrium varies from 0.3 to 0.8 *M* in this case, and is comparable to the sodium perchlorate concentration. Therefore, it may have modified the activity coefficients of the sodium perchlorate in such a way that the background was not a true representation of its distribution.

Uranyl Fluoride in Potassium Fluoride Solutions. The effect of a strong complexing ion on the degree of polymerization of uranyl fluoride was investigated by means of two ultracentrifugations to equilibrium in potassium fluoride solutions (0.04 *M* UO_2F_2 in 0.73 *M* KF and 0.15 *M* UO_2F_2 in 1 *M* KF). In these systems, the activity coefficients of uranyl fluoride were essentially constant throughout the cell, thereby differing from the uranyl fluoride-water and uranyl fluoride-perchlorate solutions.

It was shown by Pedersen[5] that if the activity coefficients of the substance under study were practically constant for the concentrations covered, then

$$\frac{c_\beta}{c_\alpha} = \frac{\left(\frac{Z}{x}\right)_\beta}{\left(\frac{Z}{x}\right)_\alpha} . \qquad (7)$$

Thus by Eq. 1, a plot of log (Z/x) vs. x^2 should give a straight line, the slope of which multiplied by

$$\frac{2RT\ (2.303)}{(1 - v\rho)\omega^2}$$

gives the (apparent) molecular weight of the solute. As shown in Fig. 2, this plot indeed gives a straight line, which indicates that the activity coefficients are essentially constant. If v = 0.125 is assumed, the apparent molecular weights obtained are 610 and 580 for the 0.04 *M* and 0.15 *M* uranyl fluoride experiments. The (theoretical) molecular weight of uranyl fluoride is 308.1. It thus appears that uranyl fluoride exists predominantly as a dimeric species in potassium fluoride solutions. At the same concentrations it would be only slightly dimerized in water alone. Since this dimer in potassium fluoride solutions must contain some fluoride ions and hence carry a charge, the observed (apparent) molecular weights must be less than the actual molecular weights. These lower values stem from the incomplete suppression of the charge effect by the supporting electrolyte.[11] An estimate of the magnitude of this charge effect indicates that the observed apparent molecular weights are consistent with the assumption of a dimer of low negative charge, although the data are not sufficiently accurate to establish conclusively the magnitude of this charge.

HEAT AND ENTROPY OF HYDROLYSIS OF URANIUM(IV)

F. Nelson K. A. Kraus

It has been shown[12] that uranium(IV) hydrolyzes according to the reaction

$$U^{+4} + 2H_2O \longrightarrow U(OH)^{+3} + H_3O^+ . \quad (1)$$

By using the same spectrophotometric method as before, the temperature coefficient of this reaction was investigated by determining the equilibrium constant $K(IV)_1$ for Eq. 1 at 10.0, 25.0, and 43.0°C. Changes in the absorption spectrum of U^{+4} with temperature were taken into consideration. The temperature effect was confined, essentially, to a small decrease in the extinction coefficients. The following extinction

(11) O. Lamm, *Arkiv for Kemi, Mineralogi, och Geologi* **17A**, N:o 25 (1944).

(12) K. A. Kraus and F. Nelson, *J. Am. Chem. Soc.* **72**, 3901 (1950).

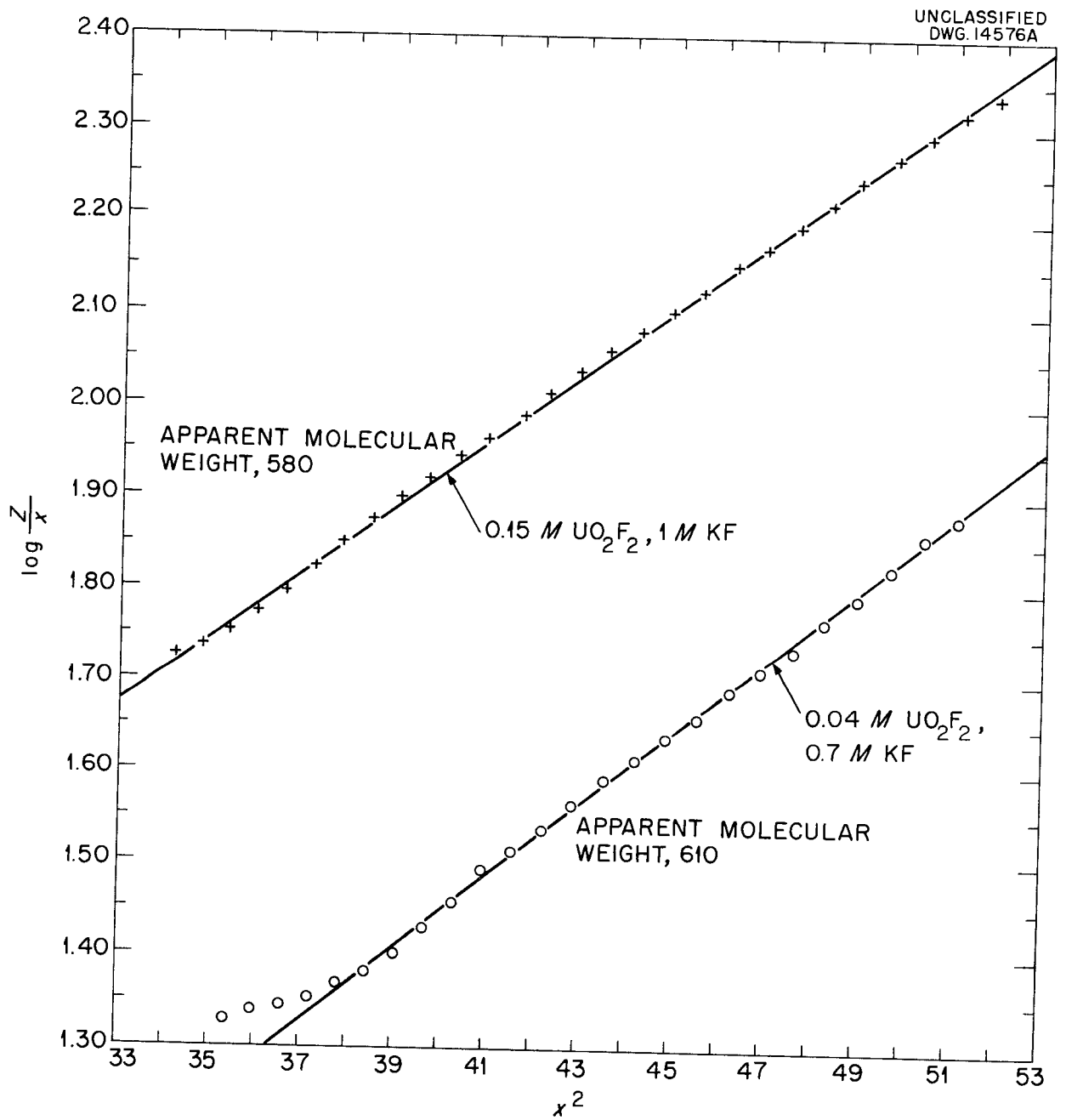

Fig. 2. Equilibrium Distribution in a Centrifugal Field (UO_2F_2-KF System).

coefficients were observed for the prominent 648 mμ band of U^{+4}: 10°C, 63.3; 25°C, 60.0; 43°C, 56.0.

It would appear from a preliminary interpretation of the data that the equilibrium constants $K(IV)_1$ for Eq. 1 are 0.012, 0.034, and 0.096 at 10, 25, and 43°C at an ionic strength of $\mu = 0.5$ in perchlorate solutions. The heat and entropy of hydrolysis were estimated to be $\Delta H = 11{,}000$ cal and $\Delta S = 30$ e.u.

It is interesting to note that if this heat of hydrolysis is constant from room temperature to 250°C, the acid constant of U^{+4} would be of the order of 10^5, for example, U^{+4} would be completely hydrolyzed even in strongly acidic solutions in the absence of complexing agents.

DETERMINATION OF THE STABILITY OF COMPLEX IONS WITH CATION EXCHANGE RESINS

R. A. Plane K. A. Kraus

Zinc. As mentioned in the previous report,[13] the preliminary data on the cation-exchange behavior of zinc in chloride and perchlorate solutions indicated that zinc is considerably complexed in 0.5 *M* HCl. However, Sillen and Liljeqvist,[14] on the basis of potentiometric measurements, suggested that there is no appreciable complexing under these conditions. In an attempt to discover whether the discrepancy is the result of a difference in methods, a series of cation-exchange equilibria of zinc vs. sodium ions were carried out using Dowex-50, both at room temperature and 80°C. The experiments indicated considerable complexing of zinc by chloride ions at low ionic strength, the same as with the earlier studies with zinc and hydrogen ions.

[13] R. A. Plane and K. A. Kraus, *op. cit.*, ORNL-1260, p. 10.

[14] L. G. Sillen and B. Liljequist, *Svensk. Kem. Tid.* **56**, 85-95 (1944).

Cobalt. By using a technique similar to that used for zinc and cadmium, cobalt(II) absorption by the cation-exchange resin Dowex-50 was studied at room temperature in chloride and perchlorate solutions at ionic strengths of 0.05 to 3. As with zinc and cadmium, cobalt is less strongly adsorbed from chloride solutions than from perchlorate solutions, which suggest that it forms a weak chloride complex. If all deviations in the adsorbability are attributed to the formation of the complex $CoCl^+$, according to the equation

$$Co^{++} + Cl^- \longrightarrow CoCl^+ ,$$

an equilibrium constant of about 0.7 can be estimated at $\mu = 0.5$.

At the present time it is not clear whether the differences in adsorbability of cobalt and zinc in chloride and perchlorate solutions are the result of complex formation at low ionic strength or whether they result from differences in the pertinent activity coefficient ratios for the adsorption equilibria. Similar experiments are now under way with alkaline earths in an attempt to resolve this question.

POLAROGRAPHY OF THALLIUM

G. W. Smith F. Nelson
K. A. Kraus

The polarography of thallium was investigated to determine whether the method could be used in the analytical determination of thallium(III). Thallium(III) is a relatively strong oxidizing agent with a standard potential E_{13} for the thallium (I)/(III) couple of approximately -1.25 volts.[15] Therefore it can be reduced easily at the dropping-mercury electrode under potentials producing oxidation of the mercury in chloride solutions. Thus the presence of thallium(III) can be

[15] W. M. Latimer, *The Oxidation States of the Elements and Their Potentials in Aqueous Solutions*, Prentice-Hall, New York, 1938.

detected polarographically only in the form of a cathodic current (Fig. 3) which, in the absence of other readily reducible substances, should be proportional to the concentration. The thallium (III)/(I) reduction wave should not be detectable with standard polarograms in chloride solutions.

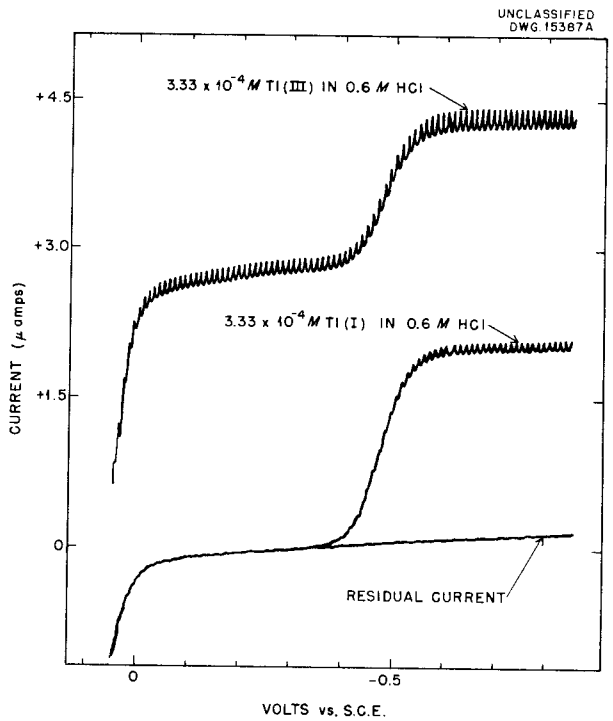

Fig. 3. Typical Polarograms of Thallium(I) and III.

It was found that the cathodic diffusion current of thallium(III) (corrected for residual current) is linear with concentration and could be used for the determination of thallium(III) (Fig. 4).

By using the Ilkovic equation $i_d = KC\ m^{2/3}\ t^{1/6}$ (where $K = 605\ n\ D^{1/2}$ and C, m, t, n, and D have the usual definitions[16]), the diffusion coefficient, D_3, of thallium(III) can be calculated from the observed diffusion currents and the characteristics of

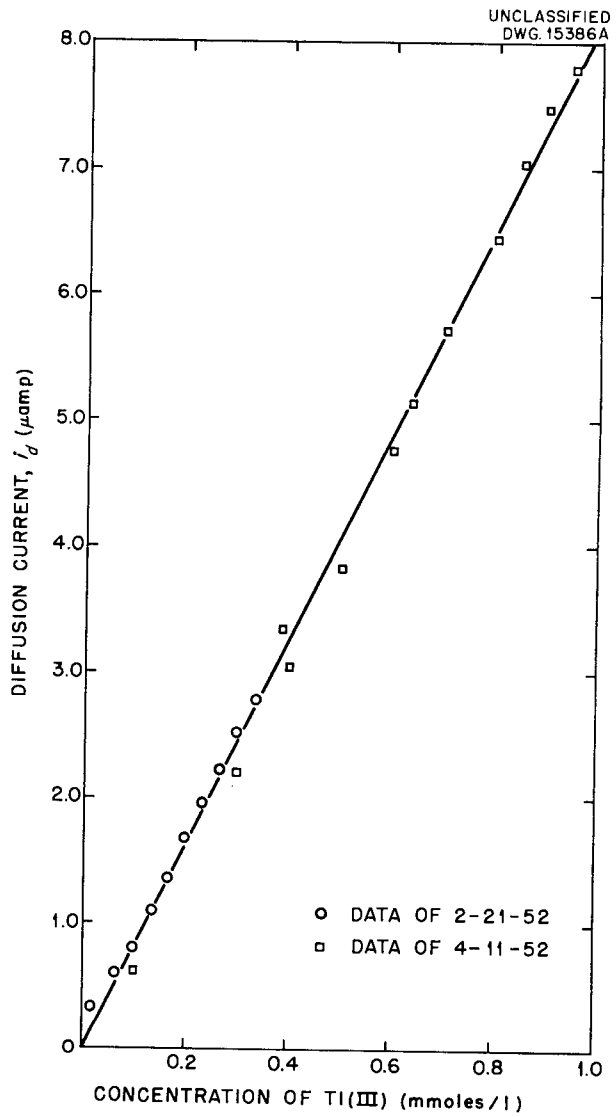

Fig. 4. Diffusion Current of Thallium(III) as a Function of Concentration.

the electrode ($m^{2/3}\ t^{1/6} = 2.173$, with m in milligrams and t in seconds, at an applied potential of −0.26 v vs. S.C.E.) by assuming n (the number of moles of electrons per mole of reduced ions) to be 2. The calculated diffusion coefficient D_3 was 1.00×10^{-5} $cm^2\ sec^{-1}$.

In addition to the cathodic current resulting from the reduction of

[16] I. N. Kolthoff and J. J. Lingane, *Polarography*, Interscience, New York, rev. 1946.

thallium(III) to thallium(I), thallium(III) shows the well-known[16] reduction wave for the reduction of thallium(I) to the metal (or amalgam) at an applied potential of approximately -0.5 v vs. S.C.E. It was found that the diffusion-current constant, K_1, of the thallium (I)/(O) wave varies linearly with the percentage of thallium(III) (Fig. 5), K_1 being approximately 2.67 in a (pure) thallium(I) solution and 1.93 in a (pure) thallium(III) solution. Using the relationship $K = 605\ nD^{1/2}$, the change in K_1 implies a change of D_1 from 1.95 to 1.02 as the percentage of thallium(III) increases from 0 to 100%. Thus D_1 in a pure thallium(III) solution is identical to D_3 within experimental error, which suggests that under such conditions the reduction of thallium(I) to the metal is controlled by the diffusion of thallium(III) to the electrode. In thallium(I) solutions, the reduction is controlled by the diffusion of thallium(I) to the electrode. Therefore the large change of K with changes in the percentage of thallium(III) can be correlated easily with the large differences in the diffusion coefficients of thallium(I) and thallium(III). Since the diffusion of thallium(I) and thallium(III) in mixtures should be essentially independent of the valence state, the observation that the diffusion-current constants vary linearly with the percentage of thallium(III) in the solution is not unexpected.

The reversibility of the thallium (I)/(O) wave apparently is independent of the thallium(I)-to-thallium(III) ratio as tested by the usual plot[16] of log $i/(i_d - i)$ vs. E, which yielded slopes of 0.059 ± 0.001 for both thallium(I) and thallium(III) solutions. It was also found unexpectedly that the half-wave potential of the thallium (I)/(O) wave is independent of the thallium(I)-to-thallium(III) ratio. In this case a change of

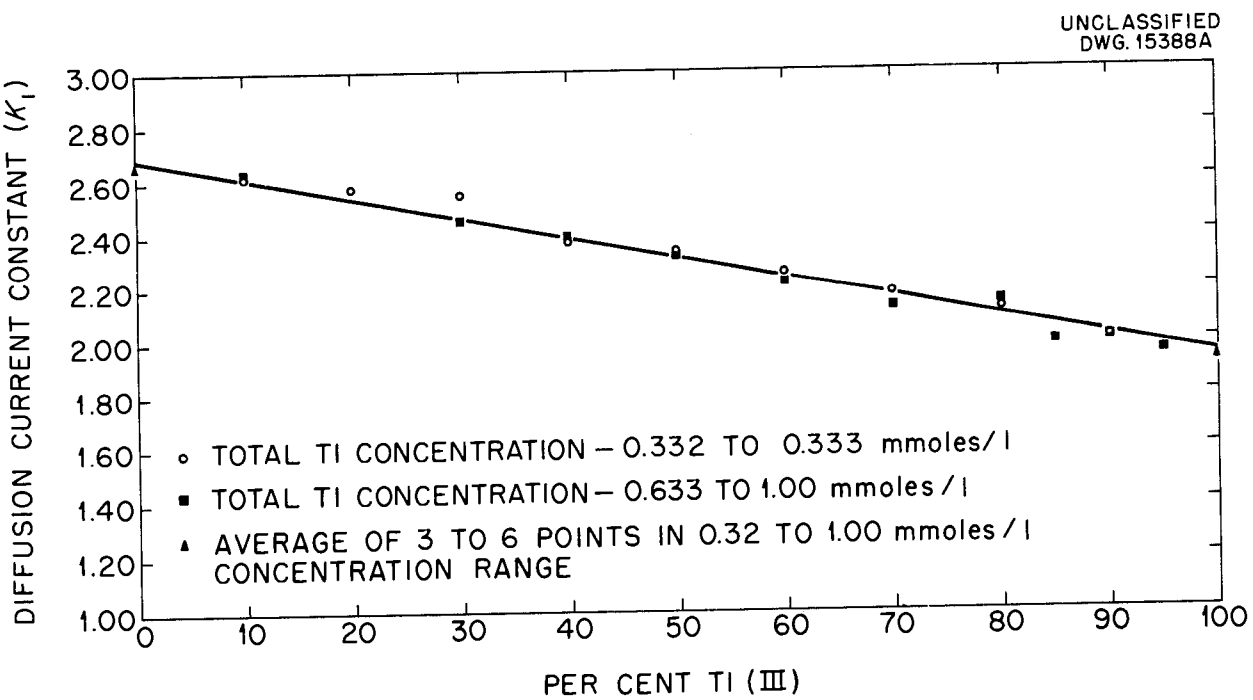

Fig. 5. Diffusion-Current Constant of Thallium(I) as a Function of Percentage of Thallium(III).

approximately 8.2 mv (0.059 log 0.72v) could have been expected, since the ratio of the diffusion current constants for the wave in thallium(III) and thallium(I) solutions is 0.72.

CHEMISTRY OF TECHNETIUM

J. W. Cobble G. E. Boyd W. T. Smith, Jr.

The Heat of Combustion of Technetium Metal. The heat of combustion of technetium in oxygen to give technetium heptoxide is a fundamental thermochemical measurement. The heats of formation, together with heats of solution and dilution, of technetium heptoxide and aqueous pertechnic acid can be calculated from such thermochemical measurements. Similar measurements have been made on rhenium by Roth and Becker,[17] who found it necessary to burn the metal with a paraffin oil accelerator, without which the combustion process would not proceed rapidly to completion. An identical procedure has been used successfully with technetium.

The calorimeter consisted of a 1-liter glass Dewar containing water as the calorimeter medium and fitted to receive a combustion bomb. The temperature rise was measured with a calibrated, glass-enclosed, platinum resistance thermometer. A cover plate containing a rubber "O" ring was bolted onto a flanged copper ring cemented to the Dewar to provide a water-tight seal. Three vertical copper tubes pierced the cover plate to allow the entrance of a resistance thermometer, a glass stirring rod, and the ignition wire into the calorimeter.

The combustion bomb, commercially available from the Parr Instrument Company, was of the semimicro type with an inlet-outlet valve and two ignition terminals. It was constructed of cobalt-nickel steel and the internal volume was 50 milliliters. The bomb was suspended in the calorimeter by strings attached to the cover plate.

The sample was placed in a small quartz cup held in a platinum wire ring suspended from the bomb head. The Dewar was filled with a weighed quantity of water. To ensure a constant heat leak from the calorimeter, a radiation shield, consisting of an inverted copper cup, was fitted snugly into the Dewar. Thus the heat leak was confined between two copper surfaces about 2 cm apart, in accordance with the recommendations of White.[18] The shield contained holes for the thermometer, stirrer, ignition wire, and strings. Hanging vertically from the shield were two copper fins that provided two sides of a stirring channel, and the bomb and Dewar formed the other two sides. A glass rod with a brass propeller was centered in the channel, and rotated at 1500 rpm by a synchronous motor to provide rapid mixing. The platinum resistance thermometer was immersed about 2 cm into the calorimeter medium to cover the sensitive volume.

The calorimeter assembly was submerged in a water thermostat bath at 25°C, regulated to ±0.002°C. The heat leak to the bath was about 25 microdeg sec^{-1} deg^{-1}. The stirrer introduced a constant heat input of about 25 microdeg sec^{-1}. The water accounted for 73.3% of the total heat capacity of the calorimeter.

The temperature rise was determined by measuring the change in resistance of the platinum resistance thermometer with a Mueller bridge. Resistances were read to ±0.00005 ohms, corresponding to about ±0.0005 degrees. The temperature rise of the calorimeter was determined by the Dickinson method[19] whereby the difference in

(17) W. A. Roth and G. Becker, *Z. Physik. Chem.* **A159**, 27 (1932).

(18) W. P. White, *The Modern Calorimeter*, p. 169, Chemical Catalog Co., New York, 1928.

(19) H. C. Dickinson, *Natl. Bur. Standards Bull.*, **11**, 189 (1914).

temperature between the two extrapolated flat portions of the temperature-time curve is taken at that time which corresponds to 0.6 of the total temperature rise. The average temperature of the combustion measurements was taken as the absolute temperature at the 0.6 time. Since the average temperature was within one-half degree of 25°C in all cases, the heats are referred to 25°C.

Up to 100 mg of technetium metal, prepared by the reduction of ammonium pertechnetate, was burned together with 50 mg of paraffin oil in oxygen at 30 atm pressure. The oil-metal combustion charge was ignited by a measured length of a cotton-thread fuse hung over a platinum wire. The pulse of current was not sufficient in itself to melt the wire, but the additional heat from the fuse did so in a fraction of a second (approx. 0.2 sec). The heat resulting from the ignition process was determined by separate experiments.

Nitric acid formed from traces of nitrogen in the oxygen amounted to 0.0131 meq and resulted in a temperature rise of 0.00016°C.[20] Because the amount of acid was independent of the oil charge, it was assumed that the same amount of acid was also formed in the oil-technetium combustion. The correction for the fuse and nitric acid was 0.0047 ± 0.0001°C. The heat of combustion of the oil was determined by a number of separate experiments (Table 2). The standard deviation reported for the values were calculated from the equation, $S = \Sigma(\Delta x)^2/n(n-1)$, where $\Sigma(\Delta x)^2$ represents the sum of the squares of the deviation of each determination from the average of n determinations. This error function has been recommended for calorimetry[21] and is in common

[20] E. W. Washburn, *J. Research Nat. Bur. Standards* **10**, 525 (1933).

[21] F. D. Rossini and W. E. Deming, *J. Wash. Acad. Sci.* **29**, 416 (1939).

Table 2

HEAT OF COMBUSTION OF PARAFFIN OIL ACCELERATOR

ΔR (ohm)	ΔT (deg)	$\Delta T_{corr.}$* (deg)	SAMPLE WEIGHT (mg)	TEMPERATURE RISE PER GRAM (deg g^{-1})
0.05840	0.5420	0.5373	68.66	7.826
0.05810	0.5400	0.5353	68.32	7.835
0.08829	0.8183	0.8136	103.00	7.996
0.12234	1.1381	1.1334	142.42	7.958
0.05163	0.4798	0.4751	59.89	7.933
0.06820	0.6344	0.6297	79.54	7.917
0.08334	0.7745	0.7698	97.65	7.884
0.07950	0.7395	0.7348	92.77	7.921
0.08941	0.8302	0.8255	104.20	7.922
			Average:**	7.910 ± 0.018

*Corrected for fuse ignition and nitric acid formation.

**This corresponds to a heat of combustion (not reduced to standard-state conditions) of 11.04 kcal g^{-1}.

use today. In order to obtain a precision of a few-hundredths of one per cent, it would have been necessary to correct each of the oil determinations by the Washburn corrections[20] to standard-state conditions. Since the maximum precision of this calorimeter was only about 0.2 per cent, because of its necessarily small design, these corrections were not significant.

The heat capacity of the calorimeter was determined by the combustion of samples of benzoic acid provided by the Bureau of Standards for this purpose (sample 39*f*). (Table 3.) In this case, the Washburn[20] corrections, although small, were made. Thus, the standard heat of combustion of the acid sample was quoted to be 26.4284 international kilojoules g^{-1}; corrected, this became 26.4279 international kj g^{-1}, or 6316.42 cal g^{-1}. Using 4.521 deg g^{-1}, the heat capacity of the calorimeter is estimated as 1397.1 cal deg^{-1} at 25°C.

In the case of the technetium-oil mixtures, two corrections (subtractions) were made: (1) the temperature rise caused by the ignition process (0.0047 deg); (2) the rise resulting from the combustion of the oil. As in the case of the combustion of pure oil alone, the Washburn corrections should also be applied for both the technetium and oil. Since the oil and technetium were burned under the same conditions as the oil alone, these corrections were negligible. The combustion data for technetium-oil mixtures and the resulting corrections to obtain the heat of combustion of technetium at constant volume are given in Table 4. These data are for the conditions existing in the bomb, therefore, corrections must be made to obtain the true standard-state enthalpy of combustion.

The technetium heptoxide from the combustion of technetium would have dissolved in the water resulting from the combustion of the oil to give a concentrated solution of pertechnic acid. Heat of dilution studies could not be made on these relatively concentrated solutions because of the limited quantities of technetium available, therefore, 2.00 additional ml of water was placed in the bomb so that the final product of the combustion was a more dilute solution of pertechnic acid. This solution was then used for the heat of dilution studies reported later.

Table 3

BENZOIC ACID COMBUSTION CALIBRATION

ΔR (ohm)	ΔT (deg)	$\Delta T_{corr.}$ (deg)*	SAMPLE WEIGHT (mg)	TEMPERATURE RISE PER GRAM (deg g^{-1})
0.06330	0.5891	0.5844	128.86	4.535
0.03632	0.3370	0.3324	73.72	4.509
0.05646	0.5237	0.5190	114.68	4.526
0.05914	0.5489	0.5442	120.53	4.515
			Average:	4.521 ± 0.006

*Corrected for fuse ignition and nitric acid formation.

Table 4

HEAT OF COMBUSTION OF TECHNETIUM METAL

ΔR (ohm)	ΔT (deg)	$\Delta T_{corr.}$ [a] (deg)	WEIGHT OF OIL (mg)	ΔT_{oil} (deg)	ΔT_{net} (deg)	WEIGHT OF TECHNETIUM [b] (mg)	TEMPERATURE RISE PER GRAM (deg g^{-1})
0.07150	0.6645	0.6598	79.56	0.6293	0.0305	31.01	0.983
0.08422	0.7834	0.7787	94.83	0.7501	0.0286	29.25	0.979
0.09801	0.9117	0.9070	107.44	0.8499	0.0572	56.39	1.014
0.12368	1.1526	1.1479	135.26	1.0699	0.0780	76.25	1.023
0.06718	0.6244	0.6197	72.78	0.5757	0.0440	45.38 [c]	0.969
0.13433	1.2492	1.2445	144.60	1.1438	0.1007	99.00 [c]	1.018
						Average:	0.998 ± 0.009

[a] Corrected for fuse ignition and nitric acid formation.

[b] Weight of technetium metal actually burned; this represents 80 to 90% of the initial charge.

[c] Samples had been degassed at 800°C for 2 to 3 hr in vacuum.

The bomb heat, from Table 4, is 0.998 deg g^{-1}. By using a heat capacity for the calorimeter of 1397.4 cal deg^{-1}, and an atomic weight for technetium of 98.91, the following is obtained for the actual bomb process:

$$2Tc_{(s)} + \tfrac{7}{2}O_{2(g,\ 30\ atm)} + H_2O_{(l)} + aq. = 2HTcO_4(0.3\ M)$$

$$\Delta E' = -276.0 \pm 2.8 \text{ kcal} . \quad (1)$$

The concentration of 0.3 *M* represents the average concentration for the six experiments given in Table 4. Since there was no noticeable trend in the heat of reaction with the amount of metal burned, it was concluded that the differences in concentration of pertechnic acid solutions formed did not contribute any significant error.

It was found that 80 to 90% of the technetium in the charge burned and that the residue in the ignition cup was pure technetium metal. This observation was checked by determining the actual amount of technetium present as pertechnic acid in the bomb solution. The average distribution of technetium was as follows: on the bomb head, 10%; on the bomb walls, 5%; in the bomb solution, 85%. Since most of the technetium was found in the bomb solution, the average concentration of this solution will be taken as the average concentration of the pertechnic acid formed in Eq. 1.

Two of the samples of technetium metal were thoroughly degassed at high temperatures in a vacuum. Since the heats of combustion of these two samples were, within the experimental error, the same as for the nondegassed samples, it may be concluded that technetium prepared by hydrogen reduction of ammonium pertechnetate does not contain appreciable amounts of hydrogen.

To correct Eq. 1 to standard-state conditions, a heat term for the change of pressure from 30 atm to unit fugacity must be added:

$$\tfrac{7}{2}O_{2(g,\ \text{unity fugacity})} = \tfrac{7}{2}O_{2(g,\ 30\ \text{atm})} \quad (2)$$

Taking $(\partial E/\partial P)_{25°C}$ equal to −6.5 joules atm^{-1} mole^{-1} for the compression,[22] 0.68 kilojoules or 0.16 kcal is obtained for Eq. 2. Hence:

$$2Tc_{(s)} + H_2O_{(l)} + \tfrac{7}{2}O_{2(g,\ \text{unit fugacity})} + \text{aq.} = 2HTcO_4(0.3\ M)$$

$$\Delta E = -276.2 \pm 2.8 \text{ kcal.} \quad (3)$$

The actual energy measured for the bomb process corresponds to a change in E, therefore, this must be added to the PV work done to obtain the enthalpy change:

$$\Delta H = \Delta E + \Delta nRT \quad (4)$$

Taking Δn as −7/2, ΔnRT has the value of −2.1 kcal. The heat of formation for the pertechnic acid solution then becomes:

$$2Tc_{(s)} + H_2O_{(l)} + \tfrac{7}{2}O_{2(g)} = 2HTcO_4(0.3\ M)$$

$$\Delta H = -278.3 \pm 2.8 \text{ kcal.} \quad (5)$$

Heat of Solution of Technetium Heptoxide. Oil was used to produce satisfactory combustion of technetium metal samples; consequently, the final state of the technetium was that of an aqueous solution of the oxide, that is, a solution of pertechnic acid. Before the heat of formation of the oxide can be determined it is necessary to know its heat of solution to give the same concentration of acid as that resulting from the combustion (0.3 M).

The solution calorimeter was constructed from a small, cylindrical Dewar 5 1/4 in. long and 1 1/2 in. in diameter. It was fitted with a standard-taper joint so that it could be fitted with a glass-stoppered top. Two glass tubes were sealed vertically into the top to provide inlets for a platinum resistance thermometer and a glass stirrer. The calorimeter was submerged in a thermostat bath controlled to ±0.002°C.

A sample of technetium heptoxide weighing 100 to 200 mg was sealed in a small, thin-walled, glass bulb which was cemented to the end of the platinum resistance thermometer. The bulb could then be broken against the bottom of the calorimeter by applying a slight pressure to the top of the thermometer. The stirrer was operated at 250 rpm by a synchronous motor. The calorimeter contained 32.0 ml of water, which served as both solvent and as a calorimeter medium. The resistance of the platinum resistance thermometer was measured as before, except that the individual measurements were determined to ±0.0001 ohms, or ±0.001°C. The temperature rise was about 0.3°C, so a precision of about 0.3% was possible. The total temperature rise was measured by taking the rise at the 0.6 time as in the combustion calorimetry.

The calorimeter was calibrated by the neutralization of an aqueous sodium hydroxide solution with a slight excess of hydrochloric acid. The sodium hydroxide solution was weighed into a small glass bulb which was subsequently broken under the hydrochloric acid solution. The heat data for sodium hydroxide, sodium chloride, and hydrochloric acid were taken from Harned and Owen.[23] Corrections were made for the heats of dilution. During the measurements

[22] F. D. Rossini and M. Frandsen, *J. Research Nat. Bur. Standards* **9**, 733 (1932).

[23] H. S. Harned and B. B. Owen, *The Physical Chemistry of Electrolytic Solutions*, Reinhold, New York, 1943.

the first calorimeter was accidentally broken and a second one had to be constructed. Therefore the agreement (Table 6) between values obtained from the two calorimeters was gratifying.

From the calibration data of Table 5 and the heat data from Table 6, the heat of solution of the oxide at 25°C was estimated:

$$H_2O_{(l)} + Tc_2O_{7(s)} + aq. = 2HTcO_4(0.04\ M)$$

$$\Delta H = -11.59 \pm 0.08 \text{ kcal.} \quad (6)$$

Because the solution was so dilute, it was assumed that the heat also represented the heat of solution of the oxide at infinite dilution.

Heat of Dilution of a Pertechnic Acid Solution. The pertechnic acid formed in the combustion bomb experiments was relatively concentrated, therefore, it was necessary to determine the heat of essentially infinite dilution. The heat-of-solution calorimeter previously described was used. Two ml of a 0.328 *M* pertechnic acid solution was sealed in a small glass bulb and broken in the calorimeter containing 30.00 ml of water to give a solution that was 0.0205 *M*. The heat change of −0.005°C corresponded to the absorption of 0.28 kcal mole^{-1} of acid. As before, it was assumed that the final concentration of pertechnic acid is essentially infinitely dilute.

Table 5

CALIBRATION OF SOLUTION CALORIMETER

CALORIMETER	LOADING (g of H_2O)	H_2O FORMED (meq.)	ΔH*	ΔT (deg)	$\bar{C}$ (cal deg^{-1} at 25°C)	$\bar{C}_{corr.}$** (cal deg^{-1})
I	32.00	0.994	−12,981	0.2037	39.7_7	39.7_7
I	31.97	0.971	−12,981	0.3184	39.5_7	39.6_0
					Average:	$39.6_9 \pm 0.09$
II	31.86	0.862	−13,000	0.2833	38.9_2	38.8_2

*Corrected for heats of dilution of NaOH, HCl, and NaCl.

**Adjusted to loading of 32.00 ml at 25°C.

Table 6

HEAT OF SOLUTION OF TECHNETIUM HEPTOXIDE

CALORIMETER	WEIGHT OF Tc_2O_7 (mg)	ΔT (deg)	CONCENTRATION OF RESULTING SOLUTION (moles/liter)	$-\Delta H_{soln.}$ (kcal mole^{-1})
I	215.6	0.2045	0.0448	11.67
II	182.0	0.1741	0.0368	11.51
		Average:	0.0408	11.59 ± 0.08

The heat of combustion of technetium to give anhydrous technetium heptoxide and pertechnic acid at infinite dilution ($HTcO_{4(aq)}$) can now be calculated.

From Eq. 5:

$$2Tc_{(s)} + \tfrac{7}{2}O_{2(g)} + H_2O_{(l)} + aq. = 2HTcO_4(0.3\ M)$$

$$\Delta H = -278.3 \pm 2.8 \text{ kcal} .$$

Adding to this

$$2HTcO_4(0.3\ M) + aq. = 2HTcO_{4(aq)}$$

$$\Delta H = +0.6 \text{ kcal} \qquad (7)$$

$$2Tc_{(s)} + \tfrac{7}{2}O_{2(g)} + H_2O_{(l)} + aq. = 2HTcO_{4(aq)}$$

$$\Delta H = -277.7 \pm 2.8 \text{ kcal} \qquad (8)$$

is obtained. Adding Eq. 6

$$2HTcO_{4(aq)} = Tc_2O_{7(s)} + H_2O_{(l)} + aq.$$

$$\Delta H = 11.6 \pm 0.1 \text{ kcal}$$

to Eq. 8 gives:

$$2Tc_{(s)} + \tfrac{7}{2}O_{2(g)} = Tc_2O_{7(s)}$$

$$\Delta H = -266.1 \pm 2.6 \text{ kcal} . \qquad (9)$$

Taking the value of 68,317.1 cal/mole^{-1} for the heat of formation of water[24] under standard conditions at 25°C and adding it to Eq. 8, the heat of formation of aqueous pertechnic acid from its elements is:

$$Tc_{(s)} + 2O_{2(g)} + \tfrac{1}{2}H_{2(g)} + aq. = HTcO_{4(aq)}$$

$$\Delta H = -173.0 \pm 1.7 \text{ kcal} . \qquad (10)$$

[24] *Selected Values of Chemical Thermodynamic Properties*, National Bureau of Standards, Washington, D. C., 1948, Series I.

MAGNETIC STUDIES ON TECHNETIUM COMPOUNDS

C. M. Nelson W. T. Smith, Jr.
G. E. Boyd

Several compounds containing technetium(IV) and rhenium(IV) were prepared for magnetic susceptibility measurements. The complex compounds of rhenium were made at the University of Tennessee with the exception of Ag_2ReCl_6, which was produced by double decomposition of K_2ReCl_6 with $AgNO_3$. The compound K_2TcCl_6 was prepared by the reduction of an aqueous NH_4TcO_4 solution with KI, in a manner similar to that used to make K_2ReCl_6. Although the $ReCl_6^=$ ion is quite stable, the corresponding $TcCl_6^=$ ion hydrolyzes easily, unless present in concentrated HCl solutions. Only a few $MnX_6^=$ ions have been prepared in aqueous solutions since they hydrolyze quite readily to give MnO_2. Apparently in this instance technetium is similar to manganese rather than to rhenium, as is the more usual case. All three elements form insoluble, black dioxides. The compound $TcO_2 \cdot 2H_2O$ was prepared by the reduction of NH_4TcO_4 in HCl solution with zinc.

The complex ions of Group VII B are very similar in their magnetic behavior. Magnetic moments are shown in Table 7 that correspond to values expected for three unpaired electrons. Since d^2sp^3 orbitals are available for bonding without doubling up the unpaired electrons, magnetic studies will not serve to differentiate between ionic and covalent bonding. The magnetic behavior of the dioxides (Table 8) is very interesting. It would be expected that the magnetic moment, μ, would be less than the theoretically predicted value owing to "magnetic concentration" effects. Actually, the susceptibilities of $TcO_2 \cdot 2H_2O$ and $ReO_2 \cdot 2H_2O$ are only about one-tenth that for $MnO_2 \cdot 0.48H_2O$, so that

Table 7

MAGNETIC MOMENTS FOR THE QUADRIVALENT STATES OF TECHNETIUM AND RHENIUM

	K_2ReCl_6	$K_2Re(SCN)_6$	Ag_2ReCl_6	$Ag_2Re(SCN)_6$	$Tc_2Re(SCN)_6$	K_2TcCl_6
μ	3.66	3.60	3.80	3.88	3.58	4.26
ΔT	57	149	120	212	41	87

Table 8

MAGNETIC MOMENTS FOR THE DIOXIDES OF TECHNETIUM AND RHENIUM

TEMPERATURE (°K)	MAGNETIC MOMENTS (μ)	
	For $ReO_2 \cdot 2H_2O$	For $TcO_2 \cdot 2H_2O$
78	0.4	0.6
400	0.6	0.9

a large change in the number of unpaired electrons must occur. A similar difference has been observed between metallic manganese and technetium (and rhenium) (Table 9).

Compounds of other valence states of technetium and rhenium have been difficult to prepare. A direct union of chlorine with technetium metal does not occur readily. Thermal decomposition was used to prepare some of the halides. If Ag_2ReCl_6 is heated to 400 to 600°C it decomposes to give $ReCl_3$ and $ReCl_5$. However, K_2TcCl_6 cannot be thermally decomposed except to give technetium metal, chlorine, and KCl. Efforts to prepare the technetium chlorides will continue, as will magnetic measurements on both rhenium and technetium compounds.

Br_2-BrO_3 EXCHANGE IN ACID MEDIA USING Br^{82} AS TRACER

O. E. Myers

The mathematical analysis outlined in the previous report[25] was found to be extremely difficult, therefore, new methods and the use of the REAC at Argonne National Laboratory are required. No results are available at this time.

Six runs in the $HBrO_3$-Br_2-$HClO_4$ system have been completed; these were designed to determine the rates of growth and destruction of HBrO. In

[25] O. E. Myers, *op. cit.*, ORNL-1260, p. 27.

Table 9

SUMMARY OF SUSCEPTIBILITIES FOR SEVERAL TECHNETIUM AND RHENIUM COMPOUNDS

TEMPERATURE (°K)	SUSCEPTIBILITIES, $\chi_M \times 10^6$							
	Re	Tc	$KReO_4$	NH_4ReO_4	NH_4TcO_4	Re_2O_7	Tc_2O_7	ReO_3
406	69	250	-30	-35	Decomposition	-16	-50	16
298	68	270	-26	-32	9	-15	-40	16
78	65	290	-18	-29	14	-10	-22	16

order to interpret the spectrophotometric curves, it is necessary to have accurate values of the extinction coefficients of the several species involved. The following information has been obtained.

Bromine. Thirty grams from a newly opened bottle of A.R. bromine were double vacuum-distilled in darkness; only the middle gram was retained. A solution, subsequently found to be 0.00621 *M* Br_2, in 1.58 *M* A.R. $HClO_4$ (using double-distilled H_2O) was prepared rapidly in diffuse light and placed immediately in the thermostated Beckman spectrophotometer at 25°C. Measurements were completed in the range of 450 to 230 mμ within 20 min of the time the frozen Br_2 had been removed from the vacuum line. In spite of the elaborate precautions, it was not possible to obtain an extinction coefficient curve free from the effects of Br_3^-. Unless the Br_3^- extinction coefficient at 265 mμ is considerably greater than 2×10^5, it must be concluded that it is impossible to prepare a pure bromine solution, with only an equilibrium amount of Br_3^-.

Tribromide. After one week in the dark, the bromine solution showed an increase in optical density of 0.725 at 265 mm (the peak of Br_3^- absorption as shown in Fig. 6). From this and other experiments in which HBr was added it is estimated that for Br_3^- in 1.58 *M* $HClO_4$, $4(10)^4 < \epsilon_{265} < 2(10)^5$. The rate of growth of Br_3^- is considerably enhanced by room light.

Hypobromous Acid. Seven grams of silver carbonate were dissolved in 150 ml of dilute H_3PO_4, and the solution was frozen over 8 g of solid bromine, placed on a light-tight vacuum line, and fractionated under

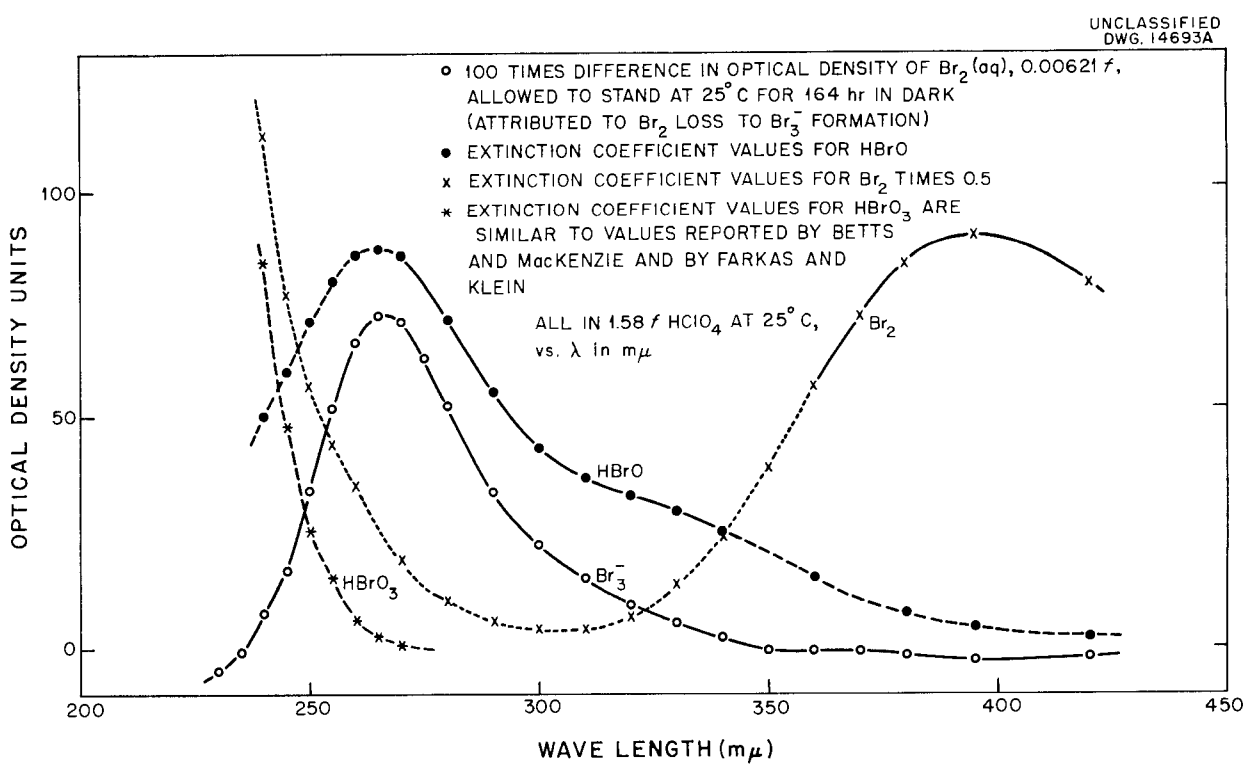

Fig. 6. Optical Density vs. Wavelength for Bromine-Water Solutions.

vacuum. From the product a solution approximately 0.05 *M* in HBrO, contaminated with less than 0.00005 *M* Br_2 or $HBrO_3$, was prepared. Accurate extinction coefficients have been obtained in the region 340 to 270 mμ, and it is hoped that still higher purity acid can be prepared so that the range of accurate measurement can be extended.

Bromic Acid. Concentrations and extinction coefficients of $HBrO_3$ involved in these experiments are so low that only crude determinations have been required.

It should be possible to obtain good values for the extinction coefficients of Br_2(aq) by subtracting accurately known effects of HBrO from a Br_2-HBrO mixture (where Br_3^- formation would be negligible). However, the effects of HBrO seem to be different for different mixtures – as though another species were absorbing light at short wavelengths. The effects seem to be greater at low bromine concentration, a hypothesis supported by material balance curves plotted against time. The decrease of material balances with reaction time during the early part of a run might also be explained by reaction with stopcock grease, and steps are being taken to eliminate this possibility in further experiments.

THERMODYNAMICS OF COMPLEX IONS

G. H. Cartledge

Further study has been devoted to the complexes formed by the manganese(III) ion with pentanedione. The equilibrium constant for the reaction between the bis- and tris-pentanedione complexes has been measured at different temperatures, in order to permit a calculation of the heat and entropy of the reaction. Also, a redetermination of the dissociation constant of pentanedione at different temperatures was required.

ENTROPIES OF AQUEOUS IONS

G. H. Cartledge

A theoretical study has been made of the correlation of the entropy of aqueous ions with the ionic potential (ratio of charge to radius). It appears that such a correlation may be used not only for empirical interpolation purposes, where unknown entropies are needed, but also to interpret the nature of the action of the ions upon their aqueous environment. Although the requisite data are not highly accurate, they seem to show that there is a discontinuity in the entropy-ionic potential curve at the point where numerous other properties of compounds show fairly abrupt change with increasing cationic potential.

CHEMISTRY OF FUSED SALTS

E. R. Van Artsdalen A. S. Dworkin

The new research program commenced during the present quarter has as its purpose the fundamental physical chemical investigation of the behavior of molten salts. Plans have been made for study of the electrical conductivity of certain pure salts and their mixtures, as well as attempts to measure ionic transport phenomena. It is believed that these investigations will prove fruitful in helping to elucidate complexes (ionic or molecular) that may exist in fused salt mixtures. Some equipment for these high-temperature studies has been designed and is in process of construction, whereas other apparatus has been assembled or ordered. A series of ceramics of potential use in construction of cells, crucibles, etc. has been tested at 800°C in various fused salts by F. Kertesz. The investigations are being

conducted in close collaboration with members of the ANP Reactor Chemistry section of the Materials Chemistry Division.

BOND STRENGTHS IN SILICON COMPOUNDS

E. R. Van Artsdalen

The heats of formation of a number of compounds containing carbon-to-silicon and oxygen-to-silicon bonds have been determined.[26,27] The results, combined with well-established thermal data and information on the heats of formation of the appropriate free radicals, have permitted the estimation that the sum of one Si-C bond plus one Si-O bond lies in the range of 160 to 180 kcal/mole in the case of a small series of compounds of varying type. An estimate, based on kinetic data,[28] indicates that the average Si-C bond strength in $Si(CH_3)_4$ is about 79 kcal/mole. Therefore it appears that the Si-O bond strength is of the order of 80 to 100 kcal/mole. More detailed investigation of silicon bond strengths will be attempted as soon as it is possible to determine heats of combustion and formation of several further key compounds.

(26) T. Tanaka, U. Takahashi, R. Okawara, and T. Watase, *J. Chem. Phys.* **19**, 1330 (1951).

(27) *Selected Values of Chemical Thermodynamic Properties*, National Bureau of Standards, 1949.

(28) D. Helm and E. Mack, Jr., *J. Am. Chem. Soc.* **59**, 60 (1937).

NUCLEAR CHEMISTRY

HALF LIFE AND MASS ASSIGNMENT OF ARGON-39

H. Zeldes B. H. Ketelle
A. R. Brosi[1]

An argon isotope that decays with an alpha type of forbidden beta spectrum and a half life greater than 15 y was tentatively assigned to mass number 39 in an earlier report.[2] The mass assignment has been confirmed and a definite half life has been established for A^{39}.

The argon produced in four samples of potassium chloride by bombardment in a nuclear reactor for about one year was released by dissolving the potassium chloride in water. After purification with hot calcium vapor, the volume of inert gas in three of the samples was measured. The bremsstrahlung radiation of the samples was compared with that of sample 4 in a high-pressure ionization chamber. The isotopic-abundance ratios in the three samples with known volumes, measured in a 60-deg-sector type of mass spectrometer, are given in Table 10.

The disintegration rate of sample 4 was determined by mounting it, in a thin-walled bulb, as a source in a magnetic-lens beta-ray spectrometer.

Table 10

ISOTOPIC-ABUNDANCE RATIOS OF ARGON FROM BOMBARDED POTASSIUM CHLORIDE

MASS NO.	ABUNDANCE (%)		
	Sample 1	Sample 2	Sample 3
36	0.24	0.16	0.092
38	85.96	85.76	84.65
39	5.35	5.43	5.32
40	8.38	8.57	9.84
(41)	0.077	0.066	0.10

(1) In cooperation with C. R. Fultz and R. F. Hibbs, Assay Laboratory, Y-12 Plant.

(2) A. R. Brosi, H. Zeldes, and B. H. Ketelle, *Phys. Rev.* **79**, 902 (1950).

The transmission of the spectrometer was determined by measuring the beta spectra of Na^{24}, P^{32}, Co^{60}, and Au^{198} sources having known disintegration rates. From the spectrometer transmission and the integral of the alpha-type of beta-energy distribution, sample 4 was found to have 6.8×10^6 disintegrations per second.

The disintegration rate and the number of atoms with masses 36, 38, 39, 40, and 41 are known for each of the three samples; therefore, a decay constant can be computed provided the activity can be assigned to a definite mass number. The argon isotopes with mass numbers 36, 38, and 40 are known to be stable with respect to beta decay and can be excluded from consideration. From a study of Cl^{39}, Haslam and co-workers[3] have concluded that A^{39} has a long half life. However, Zucker and Watson[4] have produced a 2-m activity by a deuteron bombardment of enriched A^{38}, which they assigned to A^{39}.

In the present experiments the amount of radioactivity correlates within 10% with the number of mass 39 atoms but only within a factor of 2 with the number of mass 41 atoms. In addition, if the observed activity is attributed to mass 41 instead of mass 39, the data yield a half life of about 4 y, whereas direct decay measurements now show that the half life is greater than 50 years. It is concluded therefore that the long-lived beta emitter observed in this work is associated with mass number 39, and the computations summarized in Table 11 have been made accordingly.

The data in Table 11 have been corrected for two sources of error. Air, containing approximately the same volume of argon as the A^{39} samples, was treated with hot calcium vapor to determine the vol % of inert gas. The results were reproducible but averaged 5% higher than the accepted value for the abundance of argon in air. Therefore the volumes recorded in Table 11 are 5% less than the measured volumes. It seems probable that hydrogen was not completely removed by the hot-calcium treatment. The disintegration rate of the beta-ray spectrometer source was corrected for absorption losses in the source container. This correction, which amounted to 6.5%, was determined by measuring a Au^{198} source with and without absorbers.

(3) R. N. H. Haslam, L. Katz, H. J. Moody, and H. M. Skarsgard, *Phys. Rev.* **80**, 318 (1950).

(4) A. Zucker and W. W. Watson, *Phys. Rev.* **80**, 966 (1950).

Table 11

A^{39} DECAY CONSTANT DATA

	SAMPLE 1	SAMPLE 2	SAMPLE 3
Vol (mm^3 at 0°C and 760 mm)	32.6	62.3	57.5
Abundance of mass 39 (%)	5.35	5.43	5.32
Atoms of mass 39	4.7×10^{16}	9.1×10^{16}	8.2×10^{16}
Activity relative to sample 4	0.628	1.11	0.903
Disintegrations per second	4.3×10^6	7.6×10^6	6.2×10^6
Decay constant (sec^{-1})	9.2×10^{-11}	8.3×10^{-11}	7.5×10^{-11}

On the basis of the measurements reported, it is concluded that A^{39} has a half life of 265 ± 30 years. The log (ft) value is 9.9 and the log $[(W_0^2 - 1)ft]$ value is 10.4. The latter falls within the range of values given by Mayer, Moszkowski, and Nordheim[5] for beta transitions, where $\Delta l = 1$ and $\Delta I = 2$.

A. F. Rupp furnished the samples of bombarded potassium chloride used in making the measurements.

NEUTRON CAPTURE CROSS SECTION OF PROTACTINIUM-233

J. Halperin R. W. Stoughton

The 27.4-d Pa^{233} is formed as an intermediate product in converter and breeder reactors in which the Th^{232} to U^{233} transformation is conducted. The reactions occurring are:

$$Th^{232}(n,2n)Th^{231} \xrightarrow[\beta^-]{25.5\ h} Pa^{231}(n,\gamma)Pa^{232} \xrightarrow[\beta^-]{1.32\ d} U^{232}\ ;$$

$$U^{233}(n,2n)U^{232} \text{ and/or } Pa^{233}(n,2n)Pa^{232} \xrightarrow[\beta^-]{1.32\ d} U^{232}$$

$$\begin{array}{ccccccc}
Th^{234} & \xrightarrow[\beta^-]{24.6\ d} & Pa^{234} & \xrightarrow[\beta^-]{1.1\ m;\ 6.7\ h} & U^{234} & \xrightarrow[\alpha]{2.35 \times 10^5\ y} & \\
\uparrow (n,\gamma) & & \uparrow (n,\gamma) & & \uparrow (n,\gamma) & & \\
Th^{233} & \xrightarrow[\beta^-]{23.5\ m} & Pa^{233} & \xrightarrow[\beta^-]{27.4\ d} & U^{233} & \xrightarrow[\alpha]{1.62 \times 10^5\ y} & \\
\uparrow (n,\gamma) & & & & & & \\
Th^{232} & & & & & &
\end{array}$$

The relatively long half life of Pa^{233} causes its concentration to remain high during irradiations of thorium. Losses in U^{233} production due to neutron capture by Pa^{233} depend, of course, upon the concentration and capture cross section, σ_{13}, of this nuclide. Hence it is necessary to know the value of σ_{13} to determine the magnitude of such losses and to design methods for decreasing the losses to an acceptable value.

Katzin and Hagemann,[6] at Argonne, have estimated the capture cross section of Pa^{233} by alpha-to-fission ratio measurements, and they report a value of 37 ± 14 barns. However, Stoughton[7] has shown that the alpha activity from 70-y U^{232} may make the validity of such measurements doubtful. U^{232} may be formed by:

Furthermore, mass spectrographic measurements on uranium separated from Hanford-irradiated thorium by the Chemical Technology Division[8] of ORNL are inconsistent with Katzin's value and may be interpreted as indicating a value of 100 to 200 barns for σ_{13}, on the assumption that the capture cross section of U^{233}, σ_{23}, is 50 barns for Hanford-reactor neutrons.

The high specific beta and gamma activity of Pa^{233} (approximately 23

(5) M. G. Mayer, S. A. Moszkowski, and L. W. Nordheim, *Rev. Mod. Phys.* **23**, 315 (1951).

(6) L. Katzin and F. Hageman, *Determination of Thermal Neutron Cross Section of Pa^{233}*, CF-3630 (Aug. 15, 1946).

(7) R. W. Stoughton, private communication, Feb. 12, 1947.

(8) D. E. Ferguson and E. L. Nicholson, *Summary Report for the 23 Pilot Plant Program*, ORNL-715 (July 27, 1950).

curies/mg) precludes a direct measurement of the total cross section by the "reactor oscillator" method. A transmission technique would also seem to be prohibited by the large amounts of activity that would be encountered in both the chemical separation and the actual measurements. An additional problem in either of these methods is the formidable time limitation imposed by the growth of the U^{233} daughter, with its 550-barn absorption cross section.

$$U^{233} \xrightarrow[\alpha]{1.62 \times 10^5 \text{ y}} Th^{229} \xrightarrow[\alpha]{7000 \text{ y}} ; \quad U^{234} \xrightarrow[\alpha]{2.35 \times 10^5 \text{ y}} Th^{230} \xrightarrow[\alpha]{30{,}000 \text{ y}} .$$

Other methods depend upon measuring the product of neutron capture by Pa^{233}, which is easily accomplished by irradiating Th^{232} with neutrons, separating the uranium formed, and analyzing for the amount of U^{234} in the U^{233}. It is evident that the U^{234} content of the uranium is principally determined by σ_{13}, σ_{23}, and the flux-time distribution. The contribution to the 234 chain by Th^{233} capture is relatively small owing to its short half life.[9] In irradiations of short duration, U^{234} is formed primarily via the $Pa^{233}(n,\gamma)Pa^{234}$ route, whereas long irradiations will produce U^{234} mainly through the U^{233} capture route. Thus, both σ_{13} and σ_{23} may be determined for reactor neutrons by measuring the amount of U^{234} in the U^{233} formed during neutron irradiations.

Since all other methods appear to be too insensitive, the measurement of small amounts (1:1000) of U^{234} in U^{233} is best performed by means of the mass spectrograph. The half lives of U^{233} and U^{234} are 1.62×10^5 years and 2.35×10^5 years. Thus, specific alpha activity methods must be considered unsatisfactory. The alpha decay energies are about 4.82 and 4.77 Mev. A difference of 50 kev is inadequate for separation with an alpha pulse analyzer; furthermore, the abundant isotope is the more energetic. U^{234} does not appear to possess gamma radiation of sufficient distinction to permit measurement in the presence of U^{233}. A comparison of the decay chains of these isotopes provides little hope of a sensitive analytical method based on this distinction, since both U^{233} and U^{234} decay to long-lived daughters:

The fissionability property of U^{233} is of little value in this instance since it is the abundant isotope. Excitation spectra also appear to be too insensitive for this purpose.

The experimental procedure begins with the irradiation of thorium slugs for varying periods of time. The samples are then cooled for a long period, and the U^{233}-U^{234} product, which is to be isotopically analyzed, is separated and isolated by chemical means. The chemical separations are conducted by D. E. Ferguson and other members of the Chemical Technology Division of ORNL. R. F. Hibbs of the Assay Laboratory Department at Y-12 will conduct the isotopic analyses, by means of which it may be possible to determine U^{234}-to-U^{233} ratios to within 10%, at the 1 part per 1000 U^{234} level, with 50-mg samples.

To date, 11 thorium slugs (approximately 1650 g per slug) have been irradiated for varying periods of time over a six-month period in the Low Intensity Test Reactor (LITR) of ORNL. The irradiation has been carried out in a vertical beryllium channel in the reactor assembly, in which four thorium slugs with cobalt monitors may be placed at any one time. The maximum slow-neutron flux available

[9] E. A. Hyde, R. J. Bruehlman, and W. M. Manning, *The Neutron Capture Cross-Section of the 23 Minute Isotope, Th^{233}*, ANL-4165 (June 25, 1948).

was found to be approximately 10^{13} neutrons/cm^2·sec for a reactor power level of 770 kw. Unfortunately, the reactor power fluctuated irregularly during the irradiation period, and therefore evaluation of the cross-section data is complicated.

Calculations giving the approximate U^{234}-to-U^{233} and U^{233}-to-Th ratios to be expected after various periods of irradiation are shown in Table 12. The third and fourth columns give the amounts of U^{234} resulting from neutron capture by Pa^{233} and U^{233}. Apparently it is entirely feasible to obtain reasonably good values for σ_{13} and σ_{23} from the changes in the values given in columns 3 and 4 with time of irradiation. The values represent the complete decay of Pa^{233} following irradiation. The minimum three-month cooling period being used in these experiments approximates the condition of complete decay. The calculations of Table 12 are based on σ_{13} equal to 50 barns; therefore the calculated values probably represent a minimal contribution to the 234 chain by the Pa^{233} route. Minor corrections to this calculation have been neglected. For example, neutron capture by Th^{233} will, in a 10-day irradiation, produce 10% of the total U^{234}, a quantity that diminishes at longer times. The destruction of the uranium isotopes has been neglected. This approximation is good for U^{234} ($\sigma_{24} \cong 70$ barns) but introduces an error of several per cent for U^{233} in a 100-day irradiation.

PREPARATION OF TECHNETIUM AND PROMETHIUM COMPOUNDS FOR EXHIBITION

G. W. Parker W. J. Martin

As requested by the American Academy of Arts and Sciences, a comparative display of some of the chemical forms of technetium and rhenium has been prepared for exhibition with samples of the other synthetic elements: neptunium, plutonium, americium, curium, etc. prepared at Argonne and Berkeley. The following samples, comprising a total of 150 mg of technetium compounds arranged in a display case, have been received at the Academy in Boston.

Table 12

PRODUCTION OF U^{233} AND U^{234} BY NEUTRON IRRADIATION OF Th^{232} ON THE BASIS OF FLUX = 10^{13} neutrons/cm^2·sec AND $\sigma_{13} = \sigma_{23} = 50$ BARNS

IRRADIATION TIME (*d*)	$\frac{U^{233}\ (mg)}{Th^{232}\ (kg)}$	$\frac{U^{234}\ \text{from}\ Pa^{233}}{U^{233}} \times 10^3$	$\frac{U^{234}\ \text{from}\ U^{233}}{U^{233}} \times 10^3$	$\frac{U^{234}}{U^{233}} \times 10^3$
3	18.2	0.063	0.0017	0.065
5	30.4	0.105	0.0044	0.109
10	60.8	0.195	0.017	0.212
20	121	0.371	0.064	0.435
30	182	0.514	0.136	0.650
50	304	0.743	0.342	1.08
70	425	0.913	0.606	1.52
100	608	1.09	1.08	2.17
150	911	1.27	1.97	3.26

σ_{02} = 7 barns $T_{1/2}(13)$ = 27.4 days Flux = 10^{13} neutrons/cm^2·sec

1. Technetium metal powder: by hydrogen reduction of Tc_2O_7; 10 mg.

2. Technetium dioxide: black, TcO_2; by thermal decomposition of NH_4TcO_4; 13 mg.

3*a*. Technetium trioxide: red, TcO_3; a tentatively described product of carbon monoxide reduction of Tc_2O_7 yet to be confirmed by x-ray diffraction; 1 to 2 mg.

b. Rhenium trioxide: red, ReO_3 (prepared by the University of Tennessee Department of Chemistry); 55 mg.

4. Technetium heptoxide: yellow, Tc_2O_7; 5 mg.

5. Ammonium pertechnetate: white, NH_4TcO_4; including a single crystal of 43 mg; 75 mg.

6. Potassium pertechnetate: white, $KTcO_4$; 27 mg.

7*a*. Potassium hexachloro-technetate(IV): yellow, K_2TcCl_4; 18 mg.

b. Potassium hexachloro-rhenate(IV): green, K_2ReCl_6 (prepared by Cecil Nelson of ORNL); 34 mg.

8*a*. Pertechnetic acid, $HTcO_4$: green, in 36 *N* H_2SO_4; ~ 0.1 mg.

b. Pertechnetic acid, $HTcO_4 \cdot XH_2O$: amber, in 36 *N* H_2SO_4; ~ 0.1 mg.

A display of milligram quantities of the oxalate, oxide, nitrate, and chloride salts of promethium is also being assembled.

A SPECIFIC SOLVENT EXTRACTION METHOD FOR TECHNETIUM

G. W. Parker

Among the fission products occurring in wastes separated from radiochemical extraction plants, at existing radiation intensities, it has been shown[10] that only technetium forms a compound of low solubility with the analytical reagent, tetraphenyl arsonium chloride. Because of its specificity for ions of the type XO_4^-, the precipitation of milligram quantities of the synthetic element with the aid of carrier perchlorate ion (ClO_4^-) had been readily accomplished.[10] The precipitation method (particularly the dissolution of organic perchlorates, etc.) has not been without disadvantages; therefore the development of a specific solvent extraction method promises to be of much greater significance.

An analytical method[11] for technetium in separated crude sulfuric-acid concentrate has been developed, taking full advantage of the selective properties of the reagent and the solubility of its compounds in chloroform, as reported by Tribalat.[12]

Fission-product wastes from radiochemical processes are usually in the form of nitrates (Redox) or nitric acid (Purex); therefore it was hoped that the solvent extraction of tetraphenyl arsonium pertechnetate, over a wide range of nitric acid concentrations, might be possible.

[10] G. W. Parker and W. J. Martin, *Chemistry Division Quarterly Progress Report for Period Ending September 30, 1950*, ORNL-870, p. 47.

[11] E. I. Wyatt, *Analytical Chemistry Division Quarterly Progress Report for Period Ending June 26, 1951*, ORNL-1113, p. 52.

[12] S. Tribalat, *Anal. Chim. Acta.* **3**, 113 (1949).

Accordingly, a series of trial extractions of pure tracer $Tc^{99}O_4^-$ (pertechnetate) was designed and completed. In 0.1 *M* HNO_3, the distribution coefficient between chloroform and the aqueous phase was found to be 90 to 95 compared with at least 99 in distilled water. The ratio diminished rapidly to 40 to 70 at 1.0 *M* and to 3 to 20 at 4.0 *M*. This degree of extraction is that observed over a tenfold concentration of tetraphenyl arsonium chloride: from 5 to 50 milligrams per milliliter. Repeated extractions resulted in nearly quantitative yields from less than 2 *M* HNO_3. The number of extractions required ranges from 2 to 10 over the range investigated.

A large number of extractions was performed in 25-ml glass separatory funnels fitted with Teflon plugcocks to avoid the use of grease. The first step was to add a 75-μl aliquot portion of tracer TcO_4^-, which gave 510 cps at 4% end-window geometry, to 10 ml of each of the various nitric acid solutions. Next, 0.1 or 1.0 ml of tetraphenyl arsonium chloride, equal to 5 or 50 mg in 5% water solution was added and allowed to react. A substantial precipitate formed when 50 mg was added to the sample (1/20 mg) of technetium. Exactly 1 ml of chloroform was then added and shaken in the funnel for 5 min, followed by 30-min settling. Samples were then taken from either or both phases and counted. Chloroform removes the tetraphenyl reagent; therefore it was necessary to add an equal number of portions if more than one extraction was made. The results of the extractions are summarized in Fig. 7.

Tests will be made on the intermediate-level pilot plant Purex wastes that have accumulated in storage to establish the practical yields in the presence of radiation. A further analysis of the effect of technetium concentration will be advisable since it can be controlled by the preliminary evaporation for acid reduction. Normal Purex wastes are excessively high (above 2 *M*) in HNO_3. The next step toward a production process will involve the experimental adaptation of multiple-unit countercurrent contactors such as the standard, short, pulse column.

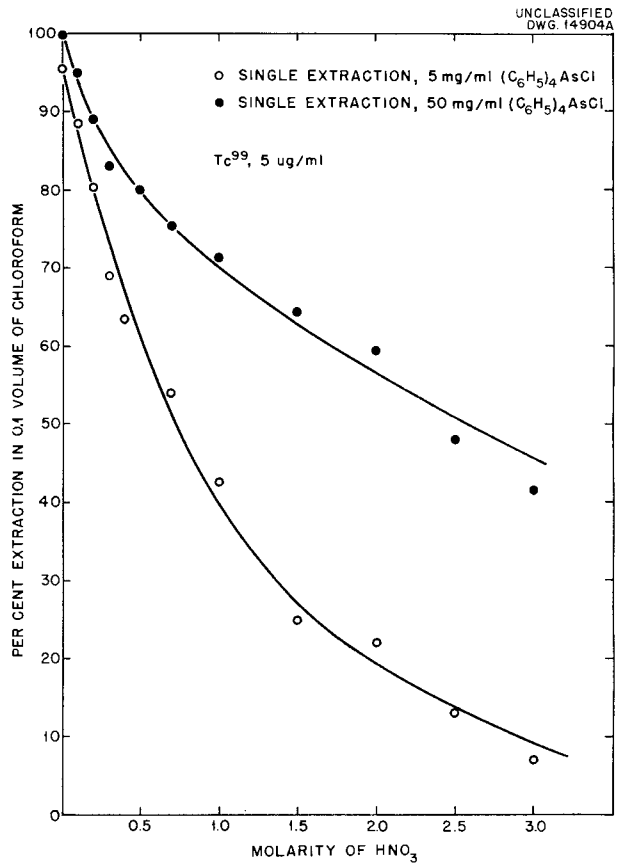

Fig. 7. Extraction of TcO_4^- with Tetraphenyl Arsonium Chloride and Chloroform vs. HNO_3 Concentration.

A simple steam distillation and filtration should suffice for recovery of the technetium as solid tetraphenyl arsonium pertechnetate, as well as for the recovery and recycle of the chloroform and tetraphenyl reagent.

GAMMA RADIATIONS FROM 36.5-h RHODIUM-105

G. E. Boyd

There has been occasion to examine the radiations from 36.5-h Rh^{105} in the continuing investigations of the radioactivities in technetium. Recently, there has been some question as to whether gamma radiations are emitted during the decay of this radionuclide. Duffield and Langer[13] have reported a magnetic-lens-spectrometer study in which only one beta group of 570-kev maximum energy was found. Neither conversion electrons, in the neighborhood of 300 kev, nor any gamma radiations were observed. On the other hand, Mandeville and Shapiro,[14] have obtained absorption and beta-gamma coincidence rate data that indicate a 0.3-Mev gamma ray in approximately 8% of the disintegrations.

Purified RuO_2 was irradiated with slow neutrons for 11 hr in the ORNL graphite reactor. One milligram of rhodium carrier was added, and the ruthenium was separated by distillation with perchloric acid. Two additional distillations were made after adding inactive ruthenium; the residue was then taken up in HCl and the rhodium isolated by reduction to the metal with magnesium. Gamma-ray spectra (Fig. 8) from this source at various times showed photolines at 322 ± 5, 157 ± 5 (very weak), and possibly at 80 ± 5 kev, which decayed with a 36-h half life. Measurements were made with a scintillation-counter spectrometer consisting of a 1 by 2 in. cylindrical, thallium-activated, sodium iodide crystal (hermetically packed in powdered MgO), together with a selected RCA 5819 photomultiplier, an A-1 linear pulse amplifier, and a sliding-channel differential discriminator.[15] The resolution at 661 kev was about 10% with a peak-to-valley ratio exceeding 30 to 1.

Energy-dependent beta-gamma coincidences were also observed (Fig. 9), suggesting that the beta spectrum was complex. A mica end-window beta-proportional counter and a 1 by 1 in., thallium-activated, sodium iodide crystal for gamma rays, together with a coincidence detector[16] set at a resolving time of 1.6 μsec, were employed for these measurements. Absorption of the coincidences in aluminum gave a range of 63 mg of Al per square centimeter, corresponding to a maximum beta energy of approximately 260 kev. This energy, when added to that of the coincident gamma ray (320 kev), gives 580 kev, which is in satisfactory agreement with the energy of the main beta transition. A comparison of the normalized coincidence rate, extrapolated to zero total absorber, with the rate for 2.69-d Au^{198} counted in the same geometry indicated that 10 ± 2% of the 36.5-h Rh^{105g} disintegrations go through the 320-kev gamma ray, assuming that the latter is not appreciably delayed or converted.

Log *ft* values for the 570- and 250-kev beta groups are 5.7 and 5.6, respectively, so that both transitions are empirically allowed. Recently, spin values of 5/2 (most probable) and 3/2 (possible) for Pd^{105g} have been reported.[17] Therefore if Pd^{105g} is $d^{+}_{5/2}$, then Rh^{105g} should be $(7/2)^{+}$ and the 320-kev level may be $g^{+}_{7/2}$. It is of interest to note that

(13) R. B. Duffield and L. M. Langer, *Phys. Rev.* **81**, 203 (1951).

(14) C. E. Mandeville and E. Shapiro, *J. Frank. Inst.* **253**, 145 (1952).

(15) E. Fairstein, *Rev. Sci. Inst.* **22**, 761 (1951).

(16) R. A. Dandl, *Chemistry Division Quarterly Progress Report for Period Ending June 30, 1949*, ORNL-286, p. 206.

(17) P. Brix and A. Steudel, *Naturwiss.* **38**, 431 (1951).

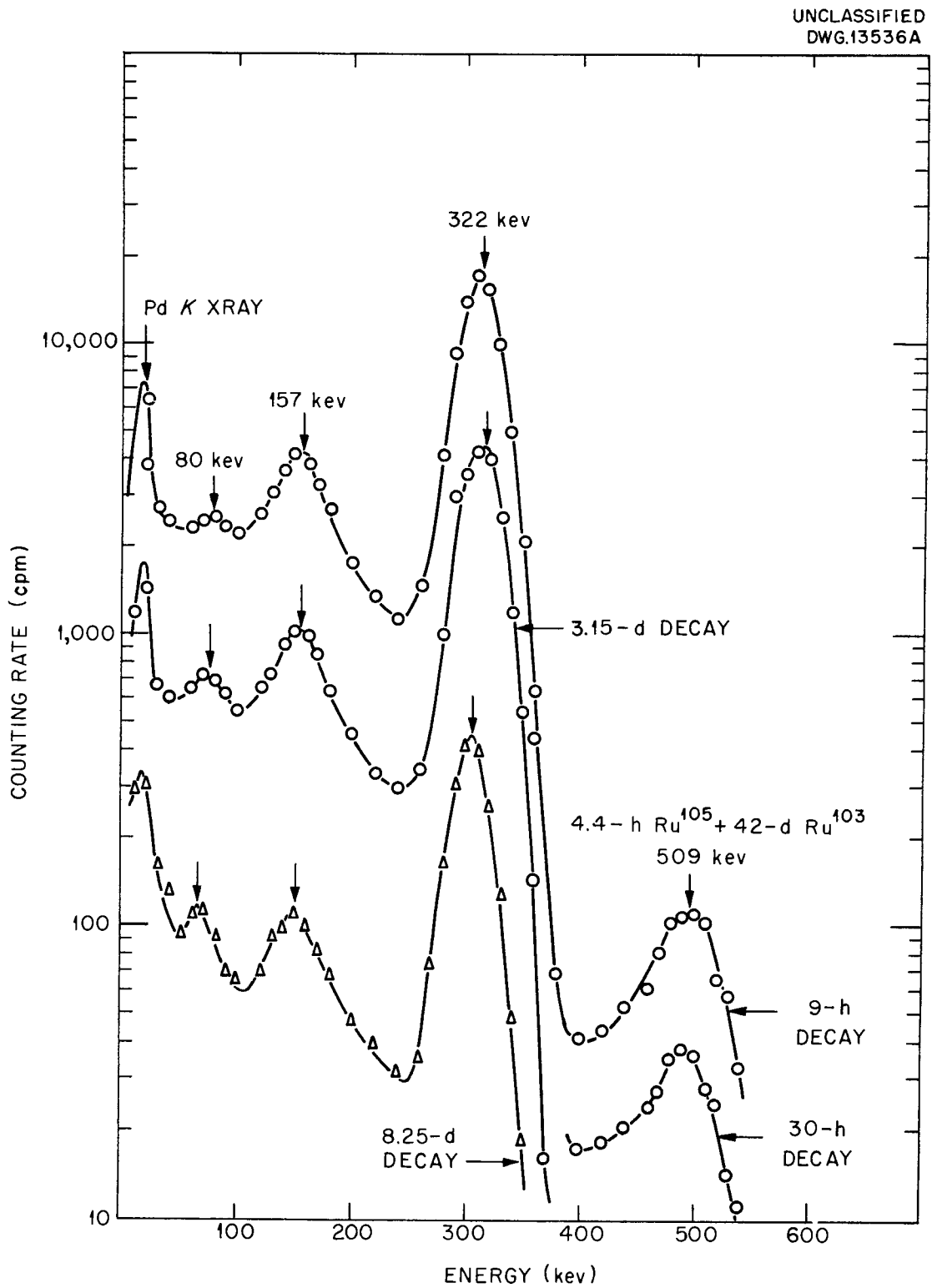

Fig. 8. Gamma-Ray Spectrum of 36-h Rh^{105}(g) Obtained with a Thallium-Activated, Sodium Iodide Scintillation-Counter Spectrometer.

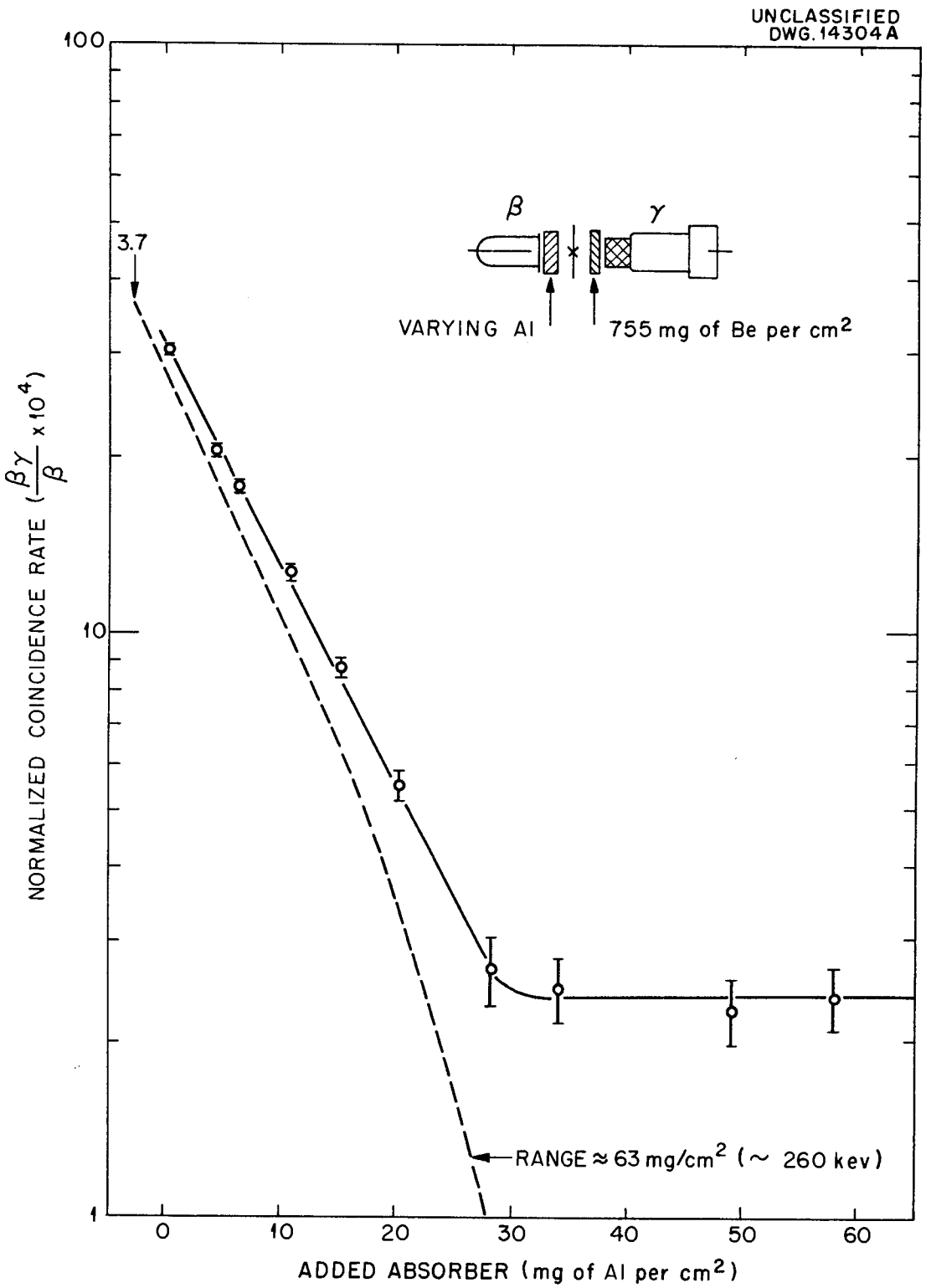

Fig. 9. Coincidence-Rate Absorption Measurements Taken on 36-h Rh^{105}(g) After 57-h Decay.

other levels in Pd^{105} have been observed[18] in the decay of 45-d Ag^{105}.

HALF LIFE AND RADIATIONS OF TECHNETIUM-100

G. E. Boyd Q. V. Larson
G. W. Parker

A preliminary report[19] on a material with an 80 ± 10-sec activity and chemical properties that parallel technetium was made several years ago. Subsequent G. E. Boyd conducted 14-Mev-deuteron and 7-Mev-proton bombardments of 90.2% Mo^{100} and showed the half life to be 70 ± 2 sec with a charged particle energy of 2.1 ± 0.2 Mev. Magnetic deflection measurements indicated that the particles were positrons. Although positron emission in Tc^{100} was unexpected, the possibility of its occurrence could not be excluded since this radionuclide is isobaric with stable Mo^{100} as well as with Ru^{100}. Additional chemical tests were made, since the half life and radiations of the ostensible technetium activity were very similar to those reported for F^{17} ($T_{½}$ = 69 s; 2.1-Mev positrons). The rapid-volatility procedure, employed earlier to separate technetium from irradiated Mo^{100} metal, was modified to include a separation of HF. The 70-sec period was then found only in the fluoride fractions. The 70-s F^{17} activity, previously confused with technetium, presumably resulted from $(d,2n)$ and (d,n) reactions on very small amounts of oxygen remaining in the probe target after the reduction of $Mo^{100}O_3$ to molybdenum metal with hydrogen.

Additional proton and deuteron irradiations of Mo^{100} were made in a careful search for Tc^{100}. After the chemical tests were made, no new technetium activities were observed with a Geiger counter, from which it was concluded that the half life of Tc^{100} was either less than 30 sec or greater than several years. Because of the time required for the chemical tests, it was not possible to decide whether a reported[20] 18-sec beta-emitting activity produced in natural molybdenum by 7-Mev protons should be assigned to technetium. The availability of fractional gram amounts of long-lived, fission-product Tc^{99g} has recently made it possible to prepare Tc^{100} without the need for ultrarapid chemical separations. Milligram amounts of purified Tc metal[21] and TcO_2 were irradiated with thermal neutrons for 20- to 30-sec periods in the ORNL graphite reactor. The decay of the induced activity was measured through varying thicknesses of aluminum and lead by using a mica end-window beta-proportional counter as a detector that records on a strip-chart. A typical decay curve of the gamma radiations is shown in Fig. 10, and a rough aluminum-absorption curve taken from an isochrone is given in Fig. 11. It has been concluded that Tc^{100} decays with a 15.8 ± 0.2-sec half life and that beta rays of 2.8 ± 0.2-Mev maximum energy are emitted together with gamma radiations. The beta and gamma spectrum of Tc^{100} is believed to be complex.[22] Numerous levels in Ru^{100} have been seen in the decay of 20-h Rh^{100}, although the log ft value for 15.8-s Tc^{100} is only 4.45 when it is assumed that no beta rays

(18) R. W. Hayward, *Bull. Am. Phys. Soc.* **26**, 12 (1951).

(19) E. E. Motta and G. E. Boyd, *Phys. Rev.* **73**, 1470 (1948).

(20) G. T. Seaborg, *Rev. Mod. Phys.* **16**, 14 (1944).

(21) J. W. Cobble, C. M. Nelson, G. W. Parker, W. T. Smith, Jr., and G. E. Boyd, *J. Am. Chem. Soc.* **74**, 1852 (1952).

(22) R. A. House, R. L. Colligan, D. N. Kundu, and M. L. Pool, *Bull. Am. Phys. Soc.* **27**, 21 (1952).

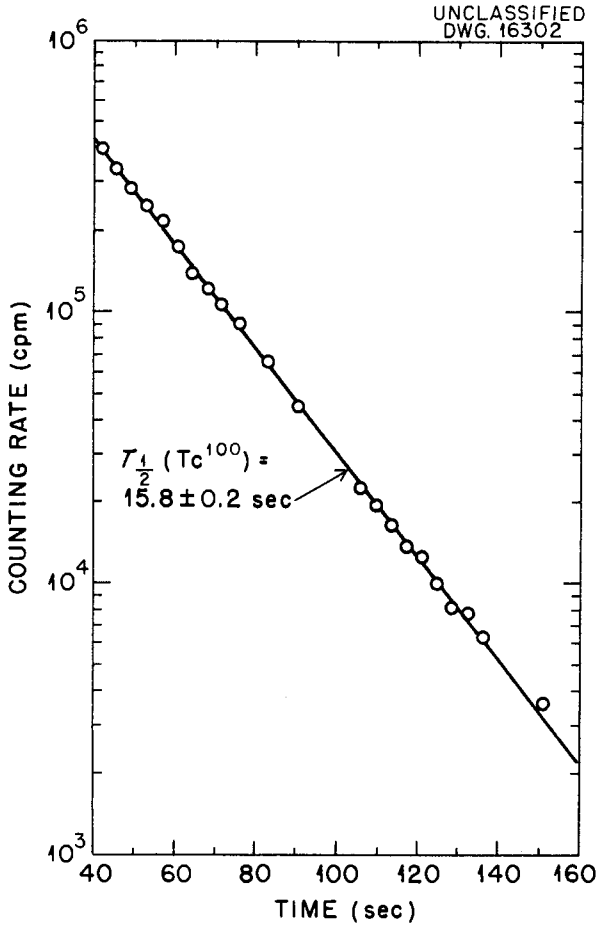

Fig. 10. Decay of Gamma Radiation from Tc^{100} Measured Through 1.96 g of Pb per cm^2.

other than the 2.8-Mev group occur in the decay. Quantitative measurements of the radiations of Tc^{100} are in progress.

A search was made for a possible long-lived isomeric state of Tc^{100}, the results were negative. Ten milligrams of technetium metal was

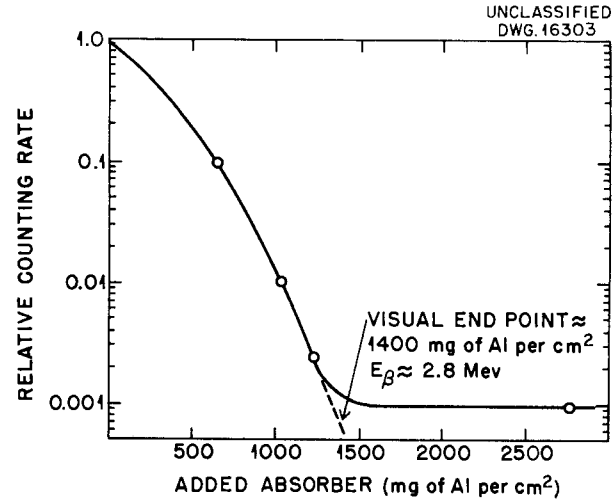

Fig. 11. Aluminum Absorption Curve for 15.8-s Tc^{100} Constructed from Isochrone on Decays Through Varying Thicknesses of Aluminum.

irradiated with slow neutrons until an integrated flux, *nvt* of 1.8×10^{18} neutrons/cm^2, was accumulated. The irradiated metal was converted to the pertechnetate, and the latter was purified by anion-exchange chromatography. Sources were prepared and examined within 32 hr after bombardment by using a thallium-activated, sodium iodide scintillation spectrometer and a krypton-filled, beta-proportional spectrometer. No quantum radiations other than those that could be attributed to very small amounts of 92.8-h Re^{186} and 26.8-h As^{76} impurity were seen. The finding appears to be consistent with the absence of Tc^{100} in mass-spectrographically analyzed fission-product Tc^{99}.[23]

[23] M. G. Inghram, D. C. Hess, Jr., and R. J. Hayden, *Phys. Rev.* 72, 1269 (1947).

RADIO-ORGANIC CHEMISTRY

RADIATION CHEMISTRY

E. J. Dowling A. R. Jones
W. J. Skraba

Design, Construction, and Calibration of a New Cobalt-60 Source. The investigation of reactions induced by the gamma-radiation of organic compounds in aqueous solution has continued. Experimental procedures were developed, and a Co^{60} source, together with its accessories, was constructed and calibrated. The source and its shield are similar to that used by Ghormley and Hochanadel.[1]

The source contains approximately 1000 curies of Co^{60} in the form of cylinders 1 cm in diameter and of various heights that were loaded into six peripheral holes of a hollow, brass cylinder so that a uniform intensity distribution was obtained over a 10-cm length along the vertical axis. Thus, a space 35 mm in diameter and 10 cm long inside the cylinder is furnished with an average gamma intensity of 17,000 r/min, leaving 29 mm below and 78 mm above the active length. The cylinder is slotted its entire length to permit lowering the source over containers with protruding arms.

Water samples irradiated inside the source cylinder were heated from room temperature to approximately 40 °C. The resulting hydrostatic pressure caused the breakage of samples in sealed tubes with insufficient vapor space. Therefore one cavity of the shield is cooled by circulating cold water through a square helix of copper tubing around the sides. A centrifugal blower, mounted under the sample-positioning table, circulates the air in the cavity over the coils, past the sample, and through the source cylinder. The other cavity contains a sample-positioning table that can be rotated by means of a 10-rpm gear-reduction motor.

The sample holders are brass cylinders (some slotted to accommodate containers with side arms) open at one end, with a 1/4-in. stud projecting from the closed end. The sample container is slipped into one of the holders, which is then placed on the sample-positioning table with its stud in one of a number of socket holes.

The intensity of radiation at three different positions was determined by irradiating aqueous acidic solutions of ferrous sulfate:

1. inside the source holder - 17,300 r/min,
2. in the sample cup immediately outside the source holder - 6600 r/min,
3. in the sample cup at the outer edge of the rotating table - 3630 r/min.

Irradiation Experiments. The principal results of the irradiation of aqueous aliphatic acid solutions with gamma rays from Co^{60} have been shown to be decarboxylation and alpha-coupling. Data have been obtained in answer to a number of questions:

1. What are the quantitative yields (*G* values) of the products and in what way are they dependent upon the conditions? What conditions affect the reactions?

Since all the carbon dioxide was not removed by sweeping the irradiated

[1] J. A. Ghormley and C. J. Hochanadel, *A Cobalt Gamma-Ray Source for Studies in Radiation Chemistry*, ORNL-897 (Feb. 6, 1951).

solutions with oxygen and the precipitation of barium carbonate in the range of 1 to 5 mg was not reproducible, a constant-volume, monometric, gas-analysis system was constructed and calibrated. In using the system, the irradiated solutions are degassed in a vacuum. The gas condensed by liquid nitrogen but not by dry ice is forced into a fine capillary by mercury.

It was found that extraction of the nonvolatile material from irradiated aqueous acetic acid solutions with organic solvents was incomplete and lowered the melting point of the residue. Thus, more significant data was obtained by evaporating the water solutions to dryness. Inorganic materials, such as sulfuric acid, in the solutions were removed by partition chromatography. Table 13 illustrates the effect of dissolved gas on the system.

2. What is the fate of the CH_3 group that was originally attached to the COOH group of irradiated acetic acid?

A second proof of the absence of higher homologs of acetic acid in the volatile fraction from the irradiation of aqueous acetic solutions was obtained. Fifteen milliequivalents of such a fraction was titrated with sodium hydroxide solution. The dry sodium salts were converted to the free acids on a celite-0.5 *N* H_2SO_4-benzene column, and several hundred milliliters of benzene was run through. Aliphatic acids of longer chain length than that of acetic are rapidly eluted from such a column by benzene. The 1.5 meq. of eluted acidic material (this 10% would have contained any higher homologs of acetic acid) was titrated, and then the free acidic substance was chromatographed on paper with butanol-water-diethylamine. Only one spot was obtained, and that was acetic acid.

3. What substances other than succinic acid are present in the nonvolatile acidic product?

It is evident that the material is largely succinic acid. When the nonvolatile material is subjected to paper chromatography in a small amount so that the paper is not flooded, only one spot is formed and that spot is succinic acid. In chromatographic separations, the latitude of the paper is small compared with that of a column. Therefore, after a number of blank-partition chromatograms had been run with various solvents, the nonvolatile acidic product from the irradiation of aqueous acetic acid with about 10^6 r was chromatographed on celite-0.5 *N* H_2SO_4 columns. The use of chloroform-butanol mixtures of continually increasing polarity, by the technique of Donaldson, Tulane, and Marshall,[2] separated the material into three components; the last band was broad and possibly consisted of several substances. Ether separated the nonvolatile acidic material into five fractions. The main component was chromatographed side by side with a known mixture of acids, containing succinic acid, by using an ether-acetic acid-water mixture. The unknown gave only one spot, and, as suspected, it was succinic acid.

4. How does the amount of decarboxylation depend upon the structure of the acid?

The gas analysis apparatus does not as yet have the precision necessary to yield data on the decarboxylation of unlabeled acids. Therefore results are reported only for 0.05 *M* solutions of acetic (G = 8.37), butyric (G = 2.71), and valeric (G = 1.89) acids when irradiated under identical conditions with 6.3×10^6 roentgens.

---

[2] K. O. Donaldson, V. J. Tulane, and L. M. Marshall, *Anal. Chem.* **24**, 185 (1952).

Table 13

EFFECT OF DISSOLVED GASES ON PRODUCTION OF NONVOLATILE ACIDIC MATERIAL BY GAMMA IRRADIATION OF AQUEOUS ACETIC ACID

ACID CONCENTRATION (*M*)	SAMPLE (mmoles)	DOSE ($r \times 10^6$)	NONVOLATILE PRODUCT (mg)	MELTING POINT (°C)	CONDITIONS
0.25	7.38	5.5	29	*	Presaturated with hydrogen
0.25	7.40	5.5	28	*	Open to atmosphere
0.25	7.94	6.0	30	165	Continuous hydrogen saturation during irradiation
0.25	7.52	3.6	22	160	Continuous hydrogen saturation during irradiation
0.25	7.42	5.5	28	173	Continuous hydrogen saturation during irradiation
0.25	7.36	5.5	29	165	Continuous hydrogen saturation during irradiation
0.29	5.31	5.3	16	*	Presaturated with hydrogen
0.29	5.68	63.7	94	150	Long-time irradiation; stock solution irradiated in sealed cell with no presaturation
0.25	7.36	5.5	8	*	Continuous oxygen saturation during irradiation
0.29	4.07	6.2	15	*	Presaturated with hydrogen; solution also 0.95 *N* in sulfuric acid; irradiated solution saturated with sodium chloride and continuously ether extracted to obtain nonvolatile product upon evaporation
0.25	6.86	6.0	10	*	Continuous saturation with hydrogen and oxygen during irradiation

*Melting point not taken.

5. Since the decarboxylation reaction decreases with increasing chain length of the aliphatic acid, does alpha-coupling or some other reaction take its place – or are the more complex molecules simply more stable?

Although it was shown that the nonvolatile acidic substance produced by the action of gamma rays on aqueous butyric acid was largely α,β-diethylsuccinic acid, the radiolysis of aqueous caproic acid apparently yields a nonvolatile acidic substance different from α,β-dibutylsuccinic acid.

6. What is the agent that causes the alpha-coupling reaction to occur? Is the action of hydroxyl radicals on aqueous solutions of an aliphatic acid the same regardless of the source of these radicals?

The agent suspected of causing the alpha-coupling reaction of acetic acid is the hydroxyl radical. The radical can also be produced in aqueous solution by Fenton's reagent or the irradiation of aqueous hydrogen peroxide by ultraviolet light. The former produces no succinic acid, which may be interpreted as meaning that the hydroxyl radical preferentially reacts with ferrous ion. The ultraviolet-peroxide treatment produces only a small amount of succinic acid with a greatly depressed melting point. Because it appears that some peroxide compound or complex is formed which decomposes when the solution is evaporated to dryness, further work may show that a greater amount of the substance is actually produced. In both experiments, large amounts of carbon dioxide are formed; however, labeled acid has not been used and it is not known whether the carbon dioxide represents oxidation or decarboxylation.

7. Since good evidence of beta oxidation has been obtained with Fenton's reagent, does it also occur with gamma irradiation?

Data are not available for answering this question.

Some exploratory experiments on the irradiation of other types of compounds have been made.

Methanol. A 0.0495 *M* aqueous solution containing 1.02 mmole (20.4 μc) of methanol-C^{14} was irradiated in a sealed ampoule with 4.8×10^6 r of gamma rays. Analysis of the product showed that 0.82 μc (4.0% of the alcohol) was converted to carbon dioxide, 0.21 μc (0.98%) to noncondensable gas ($CO+CH_4$)-(?), and 0.18 μc (0.88%) to formaldehyde. Qualitative tests showed that ethylene glycol was one of the nonvolatile products.

Oxalic Acid. A 0.25 *M* aqueous solution containing 5.28 mmoles was irradiated with 5.5×10^6 r of gamma rays. Carbon dioxide (0.71 mmoles was formed. Only a trace of noncondensable gas (CO)-(?) was formed.

Succinic Acid. A 0.25 *M* aqueous solution containing 5.32 mmoles was irradiated with 5.5×10^6 r of gamma rays. The solution was then evaporated to dryness. A 3% loss in weight had occurred and the residue melted at 182°C, whereas the starting material had a m.p. of 189°C.

ISOTOPE EFFECT STUDIES

Comparison[3] of the Isotope Effects in the Decarboxylation of Malonic-1-C^{14} Acid and Malonic-2-C^{14} Acid at 154°C (G. A. Ropp and V. F. Raaen). Work

[3] G. A. Ropp and V. F. Raaen, *Chemistry Division Quarterly Progress Report for Period Ending December 31, 1951*, ORNL-1260, p. 43.

on the comparison of the isotope effects in the decarboxylation of carboxyl-labeled and methylene-labeled malonic acids is now complete. The rate constants evaluated are defined by the four equations:

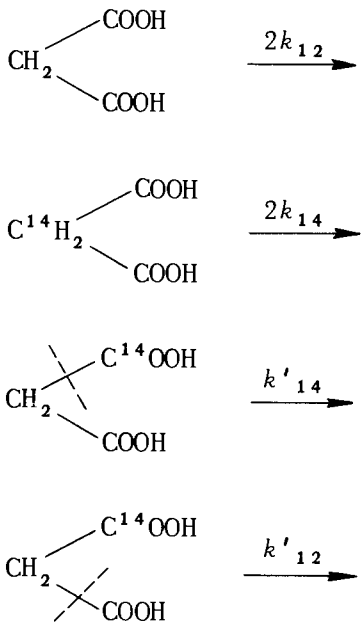

(1)

(2)

(3)

(4)

The equations define the rate constants so that k_{12} and k'_{12} refer to the breaking of single C^{12}-to-C^{12} bonds, and k_{14} and k'_{14} refer to the breaking of single C^{14}-to-C^{12} bonds. Therefore the comparison desired was between k_{14} and k'_{14}.

Derivation of the Equation Used to Evaluate the Isotope Effect for Decarboxylation of Malonic-2-C^{14} Acid. For Eq. 2 let

n^{14} = number of moles of malonic-2-C^{14} acid left unreacted at time t,

n_0^{14} = number of moles of malonic-2-C^{14} acid at time $t = 0$.

Since the reaction is first order,

$$n^{14} = n_0^{14}\ e^{-2k_{14}t}\ .$$

Similarly for Eq. 1

$$n^{12} = n_0^{12}\ e^{-2k_{12}t}\ ,$$

therefore

$$\frac{n^{14}}{n^{12}} = \frac{n_0^{14}}{n_0^{12}}\ e^{2(k_{12}-k_{14})t}\ ,$$

and

$$2.303\ \ln\frac{n^{14}}{n^{12}} = 2.303\ \ln\frac{n_0^{14}}{n_0^{12}} + 2\ (k_{12} - k_{14})\ t\ .$$

Since at tracer level (n^{14}/n^{12}) is proportional to the specific activity of the malonic acid remaining at time, t, $2(k_{12} - k_{14})$ may be obtained from the slope of a plot of log specific activity of remaining malonic acid vs. time. Dividing by $2k_{12}$, the experimentally measured first-order kinetic rate constant, gives a value of $2(k_{12} - k_{14})/2k_{12}$ from which the ratio k_{14}/k_{12} is calculated.

Evaluation of the Isotope Effect for the Decarboxylation of Malonic-1-C^{14} Acid. For Eqs. 3 and 4 let

N^{14} = the number of moles of malonic-1-C^{14} acid left unreacted at time t,

and

N_0^{14} = the number of moles of malonic-1-C^{14} acid at time $t = 0$.

then

$$N^{14} = N_0^{14}\ e^{-(k'_{12}+k'_{14})t}.$$

Since Roe and Hellman[4] have shown that the ratio k'_{12} to k'_{14} has the value 1.06, the previous equation may be rewritten:

$$N^{14} = N_0^{14}\ e^{-2.06\ k'_{14}t}.$$

Dividing by the corresponding relation from Eq. 1 gives

$$\frac{N^{14}}{n^{12}} = \frac{N_0^{14}\ e^{-2.06\ k'_{14}t}}{n_0^{12}\ e^{-2k'_{12}t}} = \frac{N_0^{14}}{n_0^{12}}\ e^{2(k_{12}-1.03k'_{14})t},$$

therefore

$$2.303\ \ln\frac{N^{14}}{n^{12}} = 2.303\ \ln\frac{N_0^{14}}{n_0^{12}} + 2(k_{12}-1.03\ k_{14})t.$$

Thus at tracer level the slope of the plot of log specific activity of the unreacted malonic acid vs. time determines $2(k_{12} - 1.03\ k'_{14})$. Division by the kinetic rate constant established the relations: slope divided by the measured rate constant is

$$\frac{2(k_{12} - 1.03\ k'_{14})}{2\ k_{12}} = 1 - 1.03\ \frac{k'_{14}}{k_{12}},$$

therefore k'_{14}/k_{12} = [1 − (slope divided by measured rate constant)]/1.03.

Use of the Flow Method of Evaluation of the Isotope Effect in the Decarboxylation of Malonic-1-C^{14} Acid. Since decarboxylation of malonic-1-C^{14} acid produces the labeled gas, carbon-C^{14} dioxide, the isotope effect was further checked by application of the flow method previously used for studying the dehydration of formic-C^{14} acid.[5]

The equation was slightly more complex than in the case of formic acid because the malonic-1-C^{14} acid decomposes by two paths represented by Eqs. 3 and 4, instead of one path as in the case of formic acid. The relation becomes:

$$2.303\ \ln S = 2.303\ \ln\left[\frac{k'_{14}\ N_0^{14}}{2k_{12}n_0^{12}}\right] + 2(k_{12} - 1.03\ k'_{14})\ t.$$

Here S refers to the instantaneous specific activity of the carbon-C^{14} dioxide produced at time t. Therefore, at tracer level the relationship of k'_{14}/k_{12} to the slope of the plot of log of the instantaneous specific activity of the carbon dioxide vs. time is the same as that derived previously. The difference is that the specific activity of malonic-1-C^{14} acid remaining is replaced by the instantaneous specific activity of the carbon dioxide.

(4) A. Roe and M. Hellman, *J. Chem. Phys.* **19**, 660 (1951).

(5) G. A. Ropp, A. J. Weinberger, and O. K. Neville, *J. Am. Chem. Soc.* **73**, 5573 (1951).

Experimentally Measured First-Order Rate Constants. The values of $2k_{12}$ at 154°C are, in $min^{-1} \times 10^2$, 6.13, 6.72, 6.10, 6.44, and 6.86. The mean value is 6.45 ± 0.31 (95%-confidence interval).

Isotope Effect for Decarboxylation of Malonic-2-C^{14} Acid at 154°C. The specific activity values were:

TIME (min)	SPECIFIC ACTIVITY ($\mu c/mg \times 10^2$)
8	1.995
12	2.021
16	2.085
20	2.097
24	2.165
28	2.178
32	2.207

The rate constant values were: $2(k_{12} - k_{14})$ = 2.303 × slope = 0.00455 (Fig. 12); $(k_{12} - k_{14})/k_{12}$ = 0.0706; k_{14}/k_{12} = 0.929.

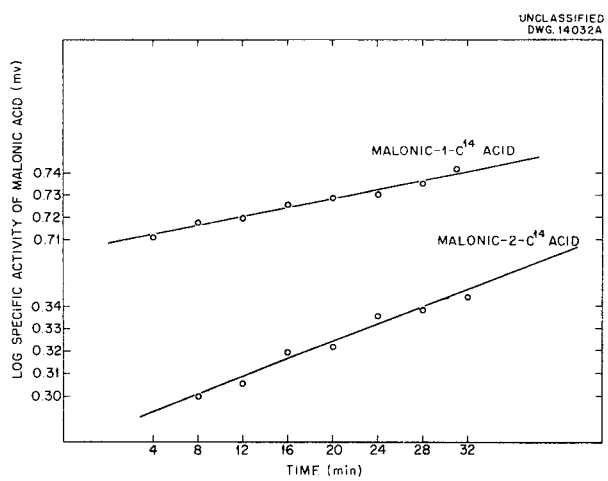

Fig. 12. Relation of Specific Activity of Malonic Acid to Time of Sampling in the First-Order Decarboxylation at 154°C.

Isotope Effect for Decarboxylation of Malonic-1-C^{14} Acid at 154°C. Following the variation of the specific activity of the remaining malonic-1-C^{14} acid the specific activity values were:

TIME (min)	SPECIFIC ACTIVITY ($\mu c/mg \times 10^3$)
4	5.14
8	5.22
12	5.24
16	5.31
20	5.35
24	5.37
28	5.43
31.5	5.52

The rate constant values were: 2.303 × slope = 0.00225 (Fig. 12); 1.03 k'_{14}/k_{12} = (1 − 0.00225/0.0645) = 0.965; k'_{14}/k_{12} = 0.937.

By following the variation of specific activity of carbon-C^{14} dioxide evolved by the flow system, in the first run the millivolt readings taken from Brown Recorder Chart at regular intervals were:

TIME (min)	MILLIVOLTS (proportional to specific activity)
0	287
3	290
6	292
9	293
12	294
15	295
18	297
21	298.5
24	301.5
27	304

The rate constant determined simultaneously = 0.0610 min^{-1}; 2.303 × slope = 0.00194 (curve *a* of Fig. 13); 1.03 k'_{14}/k_{12} = (1 − 0.00194/0.0610) = 0.968; k'_{14}/k_{12} = 0.940.

In the second run the values were:

TIME (min)	MILLIVOLTS (proportional to specific activity)
0	289
3	293
6	294
9	296
12	298
15	297.5
18	300
21	302.5
24	304
27	307.5

The rate constant determined simultaneously = 0.0644 min^{-1}; 2.303 × slope = 0.00214 (curve *b* of Fig. 13); 1.03 k'_{14}/k_{12} = (1 − 0.00214/0.0644) = 0.967; k'_{14}/k_{12} = 0.939.

SUMMARY OF RESULTS

	$\frac{k'_{14}}{k_{12}}$	$\frac{k_{14}}{k_{12}}$	$\frac{k'_{14}}{k_{14}}$
	0.937		
	0.940		
	0.939		
Avg.	0.939	0.929	1.01

The 1% difference between k'_{14} and k_{14} is probably not significant in view of the broad interval (1.06 ± 0.02) reported[4] for the value, 1.06, of k'_{12}/k'_{14}. The conclusion therefore is that only a very slight increase, if any, in the isotope effect results from moving the C^{14} label from the carboxyl group to the methylene group. It is worthy of note that the isotope effects calculated here are not in agreement with certain previously reported values.[6] A further approximate calculation may be made to demonstrate that k'_{12} is essentially equal to k_{12}:

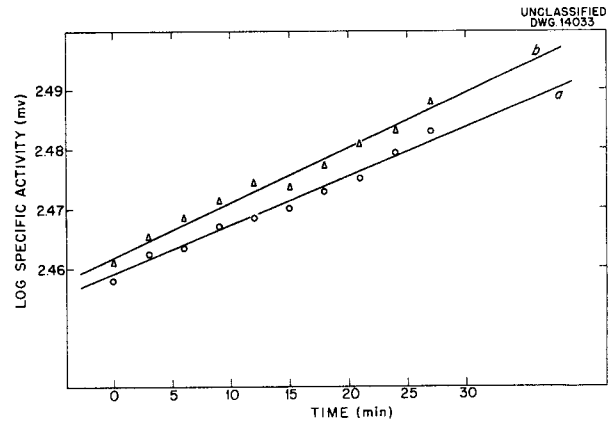

Fig. 13. Use of the Flow System in Following the Relation of Specific Activity of $C^{14}O_2$ to Time in the Decarboxylation of Malonic-1-C^{14} Acid.

$$\frac{k'_{12}}{k_{12}} = \frac{\frac{k'_{12}}{k'_{14}}}{\frac{k_{12}}{k'_{14}}} = \frac{1.06}{\frac{1}{0.039}} = 0.995 .$$

As would have been predicted, the second-order effect of the C^{14} isotope on the rate of breakage of an adjacent C^{12}-to-C^{12} bond amounts to less than 1%.

Synthesis of Malonic-2-C^{14} Acid and Malonic-1-C^{14} Acid. Malonic-2-C^{14} acid was prepared by the reaction of chloroacetic-2-C^{14} acid with potassium cyanide, followed by hydrolysis of the resulting cyanoacetic-2-C^{14} acid. Malonic-1-C^{14} acid was prepared from a corresponding series of reactions beginning with chloroacetic acid and potassium cyanide-C^{14}. Both acids

(6) P. E. Yankwich and M. Calvin, *J. Chem. Phys.* **17**, 109 (1949).

were carefully purified by crystallizations from ether and acetone to remove radioactive impurities. The malonic-1-C^{14} acid was also sublimed at 90 to 100°C at a pressure of less than 1 millimeter.

Determination of the First-Order Rate Constant for the Decarboxylation of Malonic Acid at 154°C. Decarboxylations of 4-g samples of molten malonic acid were carried out in a 7-ml glass vessel heated by the vapors of refluxing anisole. The carbon dioxide evolved was passed through a small U-tube cooled with dry ice to remove entrained acetic acid. The carbon dioxide was collected over 85% phosphoric acid and its volume was noted at regular time intervals. The calculated first-order rate constants were in fair agreement with the values estimated at 153.2°C by Hinshelwood.[7]

Decarboxylation of Malonic-2-C^{14} Acid at 154°C. The reaction vessel described was used to decompose 2 g of malonic-2-C^{14} acid at the temperature of refluxing anisole. No attempt was made to collect the carbon dioxide or to prevent escape of acetic acid. At 4-min intervals small samples were drawn from the reaction mixture with a pipet and quenched in cold ligroin. The ligroin and acetic acid were allowed to evaporate, and the malonic acid samples were purified by sublimation at 90 to 100°C at less than 1 mm Hg pressure. A weighed portion of each sample was burned,[8] using Van Slyke solution, and the resulting carbon dioxide was swept into an ion chamber and assayed by using the vibrating-reed electrometer.[8]

Decarboxylation of Malonic-1-C^{14} Acid at 154°C. The specific activity of the remaining malonic-1-C^{14} acid was followed using eight 500-mg samples. The samples, in test tubes prepared from 3-in. lengths of 7-mm tube, were bathed in the vapors of refluxing anisole in an all-glass apparatus designed to ensure the same rate of heating of all eight tubes. Carbon-C^{14} dioxide and acetic-1-C^{14} acid escaped at will. At the end of each 4-min interval, one tube was withdrawn and quenched by cooling in liquid nitrogen. The malonic-1-C^{14} acid was recovered from each tube, purified, and assayed as previously described.

The flow system was also used to follow the decomposition of malonic-1-C^{14} acid. Four grams of the acid was decomposed by heating with refluxing anisole. The evolved carbon-C^{14} dioxide was first passed through a small U-tube cooled with dry ice and then through a 9-in. length of 7-mm copper tube to ensure equilibration with the temperature of the room. The gas then passed through the 10-ml stainless steel ion chamber[3] where its instantaneous specific activity was measured and plotted on the chart of a Brown recorder as a function of time. Gas leaving the ion chamber was collected over 85% phosphoric acid to permit simultaneous measurement of the first-order rate constant. Specific activities (mv) were taken at 3-min intervals from the Brown recorder plot. Logarithms of these values were plotted as shown in Fig. 13.

Dehydration of Formic-C^{14} Acid (O. K. Neville, A. J. Weinberger, G. A. Ropp). The work[5] on isotope fractionation, in the sulfuric acid dehydration of C^{14}-labeled formic acid, is being extended to include studies of the effect of changing the sulfuric acid concentration. To improve the accuracy of determining the isotope effect, the method has been modified as follows:

(7) C. N. Hinshelwood, *J. Chem. Soc.* **117**, 156 (1920).

(8) O. K. Neville, *J. Am. Chem. Soc.* **70**, 3501 (1948).

1. The C^{14}-activity level has been raised by a factor of 10 to give much more precisely defined plots of logarithm of specific activity of carbon monoxide vs. time.

2. The apparatus has been refined (Fig. 14) in several ways and operation is now automatic, so that runs lasting 15 to 24 hr can continue unattended. The carbon-C^{14} monoxide evolved is collected in a 2-liter thermostated glass bulb. The number of moles of gas accumulated is recorded at intervals on a Brown recorder that is activated by a mercury-filled manometer having mercury-tungsten contacts at 12-mm intervals. As the mercury rises with increasing pressure in the 2-liter bulb, the resistors are progressively shorted out. The potential indicated on the Brown recorder varies in a stepwise manner as the successive resistors are shorted. Thus the kinetic data needed in calculating the isotope effect may be obtained from the time-potential record of the Brown recorder.

Two further modifications of the apparatus make it possible to maintain a constant temperature and constant pressure of carbon-C^{14} monoxide (a constant number of millimoles of of $C^{14}O$) in the 10-ml stainless steel flow chamber. The chamber temperature is kept at 25 °C by the passage of air through a thermostated copper tube

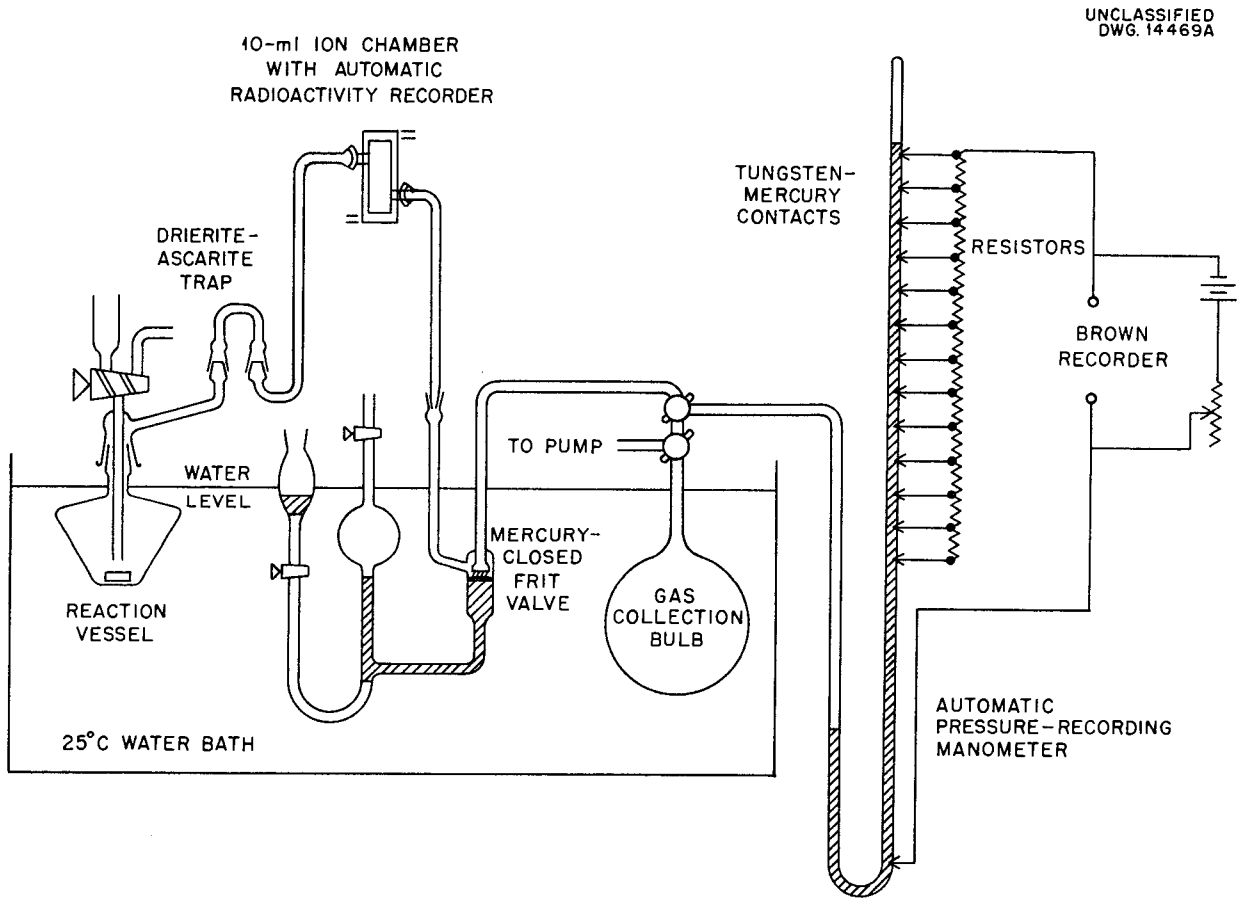

Fig. 14. Apparatus Used in Automatically Following the Isotope Fractionation in the Dehydration of Formic-C^{14} Acid.

and thence through a Lucite jacket surrounding the chamber. The pressure in the flow chamber is kept constant by allowing the gas produced in the dehydration to pass through the chamber and escape (into the 2-liter collection bulb) through a mercury-closed frit valve. The valve is set in such a way that a definite pressure (about 740 mm) is required for opening. The opening of the valve does not vary with atmospheric pressure but is governed by adjusting the air pressure in a closed, thermostated bulb at the top of the mercury leg opposite the frit.

By using the modified apparatus, a single determination has been made of the isotope effect in the dehydration of formic-C^{14} acid in 86% sulfuric acid at 25°C. The measured value $100(k_{12} - k_{14})/k_{12}$ was 10.9. Under these conditions the value of the kinetic rate constant, k_{12}, was 0.00262 per minute.

Alkaline Hydrolyses of *meta*- and *para*-Substituted Ethyl Benzoates Labeled with Carbon-14 in the Carboxyl Groups (V. F. Raaen and G. A. Ropp). The effects of the carbon-14 isotope have been evaluated[9] for the saponification of a series of ring-substituted ethyl benzoates labeled in the carboxyl groups at 25°C and for the saponification of ethyl benzoate-7-C^{14} at two temperatures. The method of evaluating the extent of isotope fractionation in each case has been previously discussed.[9] Data collected to date are presented in Table 14. In Table 15 the corresponding values of E, the Arrhenius activation energy,[10] σ, the Hammett

[9] G. A. Ropp and V. F. Raaen, *Chemistry Division Quarterly Progress Report for Period Ending September 30, 1951*, ORNL-1153, p. 43, and *Chemistry Division Quarterly Progress Report for Period Ending December 31, 1951*, ORNL-1260, p. 47.

[10] C. K. Ingold and W. S. Nathan, *J. Chem. Soc.* **1936**, 222; D. P. Evans, J. J. Gordon, and H. B. Watson, *ibid.*, **1937**, 1430; *ibid.*, **1938**, 1439.

Table 14

EFFECT OF *meta*- AND *para*-SUBSTITUENTS ON THE EXTENT OF ISOTOPE FRACTIONATION IN THE SAPONIFICATION OF ETHYL BENZOATES LABELED WITH CARBON-14 IN THE CARBOXYL GROUPS

SUBSTITUENT	TEMPERATURE (°C)	SPECIFIC ACTIVITIES* (μc/mg)			$\frac{S_3}{S_{100}} = \frac{k_{14}}{k_{12}}$	
		$S_3 \times 10^4$	$S_6 \times 10^4$	$S_{100} \times 10^4$		
m-NO_2	25	144.0	145.0	153.7		0.937
p-Cl	25	648	649	702		0.922
-H (*a*)**	25	731	729	788	0.928	0.929
(*b*)	25	709	713	763	0.930	
p-CH_3	25	587	591	640		0.917
p-OCH_3	25	129.3	130.1	141.3		0.915
-H (*a*)	0	698	703	763	0.915	0.918
(*b*)	0	724	733	786	0.921	

*Note that each value of S reported here is the average of nine assays. The complete data for the *para*-methoxy ester were reported earlier.[9]

**Samples marked (*a*) and (*b*) are repeat runs on the same ester at slightly different activity levels.

Table 15

TREND OF THE ISOTOPE EFFECTS AS COMPARED WITH RATE CONSTANTS, ARRHENIUS ACTIVATION ENERGIES, AND HAMMETT'S SUBSTITUENT CONSTANTS IN THE SAPONIFICATION OF *meta*- AND *para*-SUBSTITUTED ETHYL BENZOATES LABELED WITH CARBON-14 IN THE CARBOXYL GROUPS

SUBSTITUENT	σ	$k^*_{25°} \times 10^4$	E^* (cal/mole)	$\frac{k_{14}}{k_{12}}$ (25°C)
m-NO_2	+0.710	567	14,500	0.937
p-Cl	+0.227	23.7	16,800	0.922
p-H	0	5.5	17,700	0.929
p-CH_3	-0.170	2.5	18,200	0.917
p-OCH_3	-0.268	1.2	18,650	0.915

*These constants were measured by Ingold and Nathan[10] and apply to *para* substituents only. The values for the *meta* nitroester are similar to the *para* nitroester but are not listed here.

substituent constant,[11] and k, the specific rate constant,[10] are listed with the values of the isotope effect at 25°C.

Effect of the Ring Substituents on the Isotope Effect at 25°C. Table 15 reveals that the isotope effect becomes greater (k_{14}/k_{12} differs more from unity) as the activation energy increases, or in terms of Hammett's equation, as the value of σ decreases. The value of the isotope effect for the C^{14}-labeled ethyl p-chlorobenzoate, k_{14}/k_{12} = 0.922, is an exception to the trend, and further experiments are in progress in an attempt to check the value. The apparent increase in the isotope effect in proceeding from the faster to the slower reactions of this ester series is in accord with previous work. It has been shown that the more active members of a series of free radicals appeared to give greater isotope selectivity in extracting hydrogen from deutero-organic compounds.[12]

Variation with Temperature of k_{14}/k_{12} for the Saponification of Carboxyl-Labeled Ethyl Benzoate. By using the values of the isotope effect reported in Table 14 for saponification of ethyl benzoate at 0 and 25°C, the difference between the activation energies for the reaction of the two isotopic species was calculated[5] to be:

$$E_{14} - E_{12} = 77 \text{ cal per mole .}$$

The calculation depends upon the assumption that A_{14}/A_{12} (where A is the frequency factor from the Arrhenius equation) is not dependent upon temperature.

Substitution of this value of $E_{14} - E_{12}$ into the ratio of the

[11] L. P. Hammett, *Physical Organic Chemistry; Reaction Rates, Equilibria, and Mechanisms*, McGraw-Hill, New York, 1940, p. 188.

[12] W. H. Urry, *Reports of the Organic Division Symposium, Denver, Colorado, June, 1951*, p. 30.

Arrhenius equations for the two isotopic species at 25°C gives:

$$\frac{k_{14}}{k_{12}} = \frac{A_{14}}{A_{12}} e^{-(E_{14}-E_{12})/298.2R}$$

$$\frac{A_{14}}{A_{12}} e^{-77/1.987 \times 298.2} = 0.929$$

from which, $A_{14}/A_{12} = 1.058$, indicating a 6% greater frequency factor in the reaction of the heavier isotopic compound. Since, according to the theory of absolute reaction rates,[13]

$$A = \frac{k'T}{h} e^{\Delta S^{\ddagger}/R}$$

where

k' = the Boltzman constant,

h = Plancks constant,

$\Delta S^{\ddagger}$ = entropy of activation,

and

$$\frac{A_{14}}{A_{12}} = \frac{e^{\Delta S^{\ddagger}_{14}/R}}{e^{\Delta S^{\ddagger}_{12}/R}} = 1.058,$$

$$\Delta S^{\ddagger}_{14} - \Delta S^{\ddagger}_{12} = 0.12 \text{ e.u.}$$

From the data of Ingold and Nathan[2] the entropy of activation of the normal molecule is,

$$A_{12} = 5.32 \times 10^{9}$$

and

$$\Delta S^{\ddagger}_{12} = -14 \text{ e.u.}$$

[13] E. G. Foster, A. C. Cope, and F. Daniels, *J. Am. Chem. Soc.* **69**, 1895 (1947).

Decomposition of Hydrogen Peroxide (A. J. Weinberger, G. A. Ropp, O. K. Neville). The potassium iodide-catalyzed decomposition of neutral, aqueous hydrogen peroxide to oxygen and water is known to be of the first order, kinetically, with respect to hydrogen peroxide concentration.[14] The reaction, which is homogeneous under those conditions, apparently involves the intermediate formation of hypoidite ion:

$$H_2O_2 + I^- \longrightarrow H_2O + IO^-.$$

Preliminary experiments are under way to determine the O^{18} isotope effect and its dependence on the conditions of the reaction.

Hydrogen peroxide, enriched in O^{18}, was prepared by passing water vapor (enriched seven times in O^{18}) through a silent discharge tube at 0.3 mm and collecting the product in a liquid-nitrogen-cooled trap.[15] The resultant 56% aqueous hydrogen peroxide solution was diluted with normal water to a concentration of 6%.

In the experimental decomposition, with apparatus previously described,[16] 25 ml of 6% hydrogen peroxide solution was added to 140 ml of 0.05 *M* potassium iodide solution. Successive 50-ml volumes of evolved oxygen were collected for mass spectrophotometric determinations of O^{18}-to-O^{16} ratios. The kinetics, determined simultaneously, revealed a first-order dependence on hydrogen peroxide. A rate constant of 0.0682 min^{-1} was found at this potassium iodide concentration. The value of the isotope effect, calculated from the O^{18}-to-O^{16} ratios, will be reported subsequently.

[14] F. O. Rice and O. M. Reiff, *J. Phys. Chem.* **31**, 1352 (1927).

[15] J. Halperin and H. Taube, *J. Am. Chem. Soc.* **74**, 380 (1952).

[16] A. J. Weinberger, G. A. Ropp, and O. K. Neville, *Chemistry Division Quarterly Progress Report for Period Ending December 31, 1951*, ORNL-1260, p. 41.

Isotope Effect in the Carbonation of Organometallic Compounds (B. M. Benjamin,[17] C. J. Collins). The experiments of Pearson, Hess, and Collins[18] on the isotope effect during the carbonation of 1-methyl-9-fluorenesodium have been re-examined under conditions that eliminate errors arising from contamination during reaction by atmospheric carbon dioxide and errors arising from possible impurities in the reagents. Thus, the carbonations were carried out in an apparatus arranged so that the same reagents could be used in all phases of the experiment and so that all the experiment could be completed in a closed system. No time was allowed to elapse between completing one phase and starting the next. Carbon-C^{14} dioxide for all the experiments was stored in a common reservoir; likewise, triphenylmethylsodium was drawn from a common reservoir.

In the first experiment, a 2.22-mmole sample of 1-methylfluorene was metalated with 1.60 mmole of triphenylmethysodium, and the 1-methyl-9-fluorenesodium produced was carbonated with 0.88 mmole of carbon-C^{14} dioxide. The mixture was hydrolyzed with carbon dioxide-free water and hydrochloric acid. The resulting 1-methyl-9-fluorenecarboxylic-C^{14} acid (I) (0.806 mmole, 92.5% yield based on carbon-C^{14} dioxide), was purified by several crystallizations from benzene. The data for the millimolar radioactivity of (I), which represents the specific activity of the carbon-C^{14} dioxide in the reservoir, follows:

2.395 μc/mmole
2.413
2.456
2.424
2.428

Mean 2.423 ± 0.010 (standard deviation)

In the second experiment, 1.2 mmole of 1-methyl-9-fluorenesodium was carbonated with 2.27 mmole of carbon-C^{14} dioxide by adding the metalated compound to a solution of the carbon-C^{14} dioxide in ether at dry ice temperature. When the reaction was complete, as evidenced by the color change, all the ether and the excess carbon-C^{14} dioxide were distilled, under high vacuum, into a separate flask where the remaining carbon-C^{14} dioxide reacted with an excess of 1-methyl-9-fluorenesodium.

The specific activity of the 1-methyl-9-fluorenecarboxylic-C^{14} acid (II) (0.694 mmole) obtained when an excess of carbon-C^{14} dioxide was used, follows:

2.372 μc/mmole
2.341
2.393
2.373
2.397
2.284
2.321

Mean 2.340 ± 0.019 (standard deviation)

The specific activity of the 1-methyl-9-fluorenecarboxylic-C^{14} acid (III) (1.190 mmole) derived from the carbon-C^{14} dioxide left over from (II) follows:

2.463 μc/mmole
2.471
2.413
2.469
2.447

Mean 2.453 ± 0.012 (standard deviation)

[17] Oak Ridge Institute of Nuclear Studies Graduate Fellow From the University of Florida, Gainesville, Florida.

[18] D. E. Pearson, D. N. Hess, and C. J. Collins, *Chemistry Division Quarterly Progress Report for Period Ending September 30, 1951*, ORNL-1153, p. 24.

The combined acids (II) and (III) (1.884 mmole) represent an 83.1% yield [36.8% in (II) and 63.2% in (III)] based on the original 2.27 mmole of carbon-C^{14} dioxide.

It is clear from the data that the specific activity of acid (II) is 4.82% lower than the specific activity of acid (III), and 3.55% lower than the specific activity of the original carbon-C^{14} dioxide. The total activity of acids (II) and (III), 4.539 μc [36% of which is in (II) and 64% in (III)] is equal, within the experimental error, to the activity of an equimolar quantity of acid (I) or the original carbon-C^{14} dioxide, 4.560 microcuries.

The data are conclusive evidence for an isotope effect in the carbonation of organometallic compounds.

Migration Ratios in the Rearrangement of 2,2-Diarylethanols (L. S. Cieresko, J. G. Burr, Jr.). The rearrangements of six more substituted 2,2-diarylethanols-1-C^{14} have been investigated, by employing the synthetic and degradative procedures previously[19] outlined. The additional experimental data are summarized in Tables 16, 17, and 18.

The compounds used in the new examples (Table 16) were all prepared from the same batch of cuprous cyanide-C^{14}. The base level of activity used for the calculation of the migration ratios was the average of 29 determinations, taken on 13 intermediates from 6 different series of rearrangements. Its value was 1.69, equivalent to 0.05 μc of C^{14} per millimole. This is also the base level of activity for reference in Table 19. The value of 66.4 (0.95% average deviation) for the migration ratio of 2-phenyl-2-(*p*-tolyl)ethanol-1-C^{14} listed in Table 16 is the average obtained from six separate rearrangements.

Table 16

REARRANGEMENT OF DIARYLETHANOLS

SERIES	MIGRATION OF Ar (%)	MIGRATION RATIO Ar:C_6H_5
p-Xenyl	57.2	1.34
m-Tolyl	61.3	1.58
p-(2-Propyl)-phenyl	64.5	1.82
3,4-Dimethylphenyl	65.6	1.91
p-Tolyl	66.4 ± 0.95	1.98
p-Ethylphenyl	68.6	2.18
p-(*t*-Butyl)-phenyl	76.3	3.22
p-Methoxphenyl	95.5	21.2
α-Naphthyl	51.5	1.06
β-Naphthyl	56.6	1.30

In carrying out the rearrangements described above, it was apparent, in most cases, that the rearrangement was probably complete at some temperature below the boiling point of the xylene. Since the temperature of the rearrangement was thus indeterminate and possibly significant, a series of rearrangements were carried out under a wide variety of experimental conditions on one of the cases, 2-phenyl-2-(*p*-tolyl)ethanol-1-C^{14}. The results are summarized in Table 19. It is evident that the migration ratio of *p*-tolyl vs. phenyl is, within a very few per cent, insensitive to these variations in the conditions of rearrangement.

Thermal Stabilities of Organic Compounds (R. W. Johnson, D. N. Hess). An apparatus has been constructed and tested prior to its use in determining thermal stabilities of organic compounds. No significant results have yet been obtained.

[19] L. S. Cireszko and J. G. Burr, Jr., *Chemistry Division Quarterly Progress Report for Period Ending December 31, 1951*, ORNL-1260, p. 53.

Table 17

COMPOUNDS AND DERIVATIVES PREPARED

SERIES	CHLORIDE		NITRILE		ACID		CARBINOL		STILBENE	
	MELTING POINT (°C)	YIELD (%)	MELTING POINT (°C)	YIELD (%)	MELTING POINT (°C)	YIELD (%)	MELTING POINT (°C)	YIELD (%)	MELTING POINT (°C)	YIELD[ff] (%)
p-Tolyl	Oil	84	60 to 61[a]	64	110 to 112[b]	89	43 to 44[c]	93	120[d]	100
α-Naphthyl	50		95 to 96		140 to 141		91 to 92		699	100
p-Ethylphenyl	Oil		Oil	90	78[e]	65	Oil[f]	95	82[g]	100
β-Naphthyl			85 to 86		128 to 130		63 to 64		147	100
p-(2-Propyl)-phenyl	Oil		Oil	86	Oil[h]	54	Oil	92	80[i]	100
p-(*t*-Butyl)-phenyl	Oil		98[j]	76	139[k]	57	82[l]	100	96[m]	100
3,4-Dimethylphenyl	Oil	79	54[n]	70	124[o]	70	Oil[p]	90	78[q]	100
m-Tolyl	b.p. 136[r]		26[s]	80	122[t]	93	Oil[u]	92	49 to 50[v]	100
p-Xenyl	62[w]	72	131 to 132[x]	70	143 to 144[y]	88	100 to 101[z]	88	222[aa]	100
p-Methoxylphenyl	61[bb]	55	130[cc]	71	96[dd]	68	Oil	93	135[ee]	100

[a] Lit. 61°C, Michael and Petre, *Ber.* **25**, 1676 (1892).

[b] Lit. 115°C, McKenzie and Widdows, *J. Am. Chem. Soc.* **107**, 713 (1915).

[c] Lit. 45 to 46°C, Remart and Amagat, *Compt. Rend.* **179**, 713 (1915).

[d] Lit. 120°C, Anschutz, *Ber.* **18**, 1946 (1888).

[e] Calcd. for $C_{16}H_{16}O_2$: C, 79.2; H, 6.64. Found: C, 79.2; H, 6.84.

[f] α-Naphthyl urethane, m.p. 92°C, calcd. for CH O N: N, 3.54. Found: N, 3.43.

[g] Calcd. for $C_{16}H_{16}$: C, 92.2; H, 7.74. Found: C, 92.1; H, 7.85.

[h] Amide, m.p. 97°C, calcd. for $C_{17}H_{19}ON$: N, 5.52. Found: N, 5.62. Analide, m.p. 211°C, calcd. for $C_{23}H_{23}ON$: N, 4.25. Found: N, 4.16.

[i] Calcd. for $C_{17}H_{18}$: C, 90.8; H, 8.18. Found: C, 91.0; H, 8.09. Dibromide, m.p. 228°C, calcd. for $C_{17}H_{18}Br_2$: Br, 41.6. Found: 41.7.

[j] Calcd. for $C_{18}H_{19}N$: N, 5.61. Found: N, 5.61.

[k] Calcd. for $C_{18}H_2O_2$: C, 80.6; H, 7.53. Found: C, 80.5; H, 7.64.

[l] Calcd. for $C_{18}H_{22}O$: C, 85.0; H, 8.72. Found: C, 84.8; H, 8.83.

[m] Calcd. for $C_{18}H_{20}$: C, 91.5; H, 8.54. Found: C, 91.54; H, 8.54. Dibromide, m.p. 230°C, calcd. for $C_{18}H_{21}Br_2$: Br, 40.4. Found: Br, 40.6.

[n] Calcd. for $C_{16}H_{14}N$: N, 6.35. Found: N, 6.36.

[o] Calcd. for $C_{16}H_{16}O_2$: C, 80.1; H, 6.70. Found: C, 80.0; H, 6.61.

[p] α-Naphthyl urethane, m.p. 149°C, calcd. for $C_{27}H_{25}O_2N$: N, 3.54. Found: N, 3.54.

[q] Calcd. for $C_{16}H_{16}$: C, 92.2; H, 7.74. Found: C, 92.1; H, 7.66.

[r] n_D^{25} 1.5850, d_4^{25} 1.109 MR_D calcd. 65.14. Found: 65.48.

[s] n_D^{25} 1.5670.

[t] Calcd. for $C_{15}H_{14}O_2$: C, 79.6; H, 6.24. Found: C, 79.9; H, 6.36.

[u] α-Naphthyl urethane, m.p. 118°C, calcd. for $C_{26}H_{23}O_2N$: N, 3.67. Found: N, 3.67. Found: N, 3.80.

[v] Lit. 48°C, Bergmann and Schapiro, *J. Org. Chem.* **12**, 57 (1947). Dibromide 178°C, Lit. *ibid*, 176°C.

[w] Lit. 62.5°C, Wittig and Petri, *Ann.* **513**, 26 (1934).

[x] Lit. 130 to 131°C, *ibid.*

[y] Lit. 141 to 142°C, Blicke and Grier, *J. Am. Chem. Soc.* **65**, 1725 (1943).

[z] Calcd. for $C_{20}H_{18}O$: C, 87.5; H, 6.57. Found: C, 87.4; H, 6.60.

[aa] Lit. 221°C, Bergmann and Weymann, *J. Org. Chem.* **9**, 415 (1944).

[bb] Calcd. for $C_{14}H_{13}OCl$: Cl, 15.2. Found: Cl, 15.3.

[cc] Calcd. for $C_{15}H_{13}ON$: N, 6.27. Found: N, 6.30.

[dd] Lit. 100°C, Poincet, *Compt. Rend.* **148**, 419 (1909).

[ee] Lit. 135 to 136°C, Van Duin, *Rec. Trav. Chim.* **45**, 347 (1926).

[ff] Although the yields of purified stilbenes usually were less than 100%, the residual material was very high boiling and was presumably polymeric stilbene.

Table 18

OXIDATION PRODUCTS

ARYL SERIES	OXIDATION CONDITIONS	OXIDATION PRODUCT
p-Xenyl	Neutral $KMnO_4$ in aqueous acetone	*p*-Phenylbenzoic acid
m-Tolyl	Alkaline $KMnO_4$	Isophthalic acid
p-(2-Propyl)-phenyl	Alkaline $KMnO_4$	Terephthalic acid
3,4-Dimethylphenyl	Alkaline $KMnO_4$	Trimellitic acid
p-Tolyl	Alkaline $KMnO_4$	Terephthalic acid
p-Ethylphenyl	Alkaline $KMnO_4$ in water	Terephthalic acid
p-(*t*-Butyl)-phenyl	CrO_3HAc	*t*-Butylbenzoic acid
p-Methoxphenyl	Neutral $KMnO_4$ in aqueous acetone	Hydroxybenzoic acid
α-Naphthyl	Neutral $KMnO_4$ in aqueous acetone	α-Naphthoic acid
β-Naphthyl	Neutral $KMnO_4$ in aqueous acetone	β-Naphthoic acid

Table 19

REARRANGEMENT OF 2-PHENYL-2-(*p*-TOLYL)ETHANOL-1-C^{14}

REAGENT	SOLVENT	TEMPERATURE (°C)	TEREPHTHALIC ACID (μc of C^{14} per mmole)
P_2O_5	Xylene	90	1.15
P_2O_5	Xylene	139	1.14
P_2O_5	None	200	1.13
$KHSO_4$	None	200	1.10
$ZnCl_2$	None	200	1.13

SEPARATIONS PROCESSES

ORGANIC CHEMISTRY OF SOLVENTS

W. H. Baldwin C. E. Higgins

Organo-Phosphorus Compounds. It has been shown[1] that organo-phosphorus compounds, in which the ester linkage (C-O-P) had been replaced by carbon-to-phosphorus linkages, extracted more uranium than did the tri-ester. The improvement varied according to the number of C-P bonds in the molecule. A few of the compounds have been examined by Kosolapoff,[2] who measured the molar heat of mixing with chloroform and used this as a measure of the hydrogen-bonding ability. Comparison of Kosolapoff's results with uranium extraction data shows a direct relationship, as was to be expected.

Tests on the extraction of other cations from aqueous solution into CCl_4 containing 0.75 *M* phosphorus compound show that tributyl phosphine oxide extracted 20% of the Fe(III) from 0.1 *M* $FeCl_3$, no detectable Na(I) from 0.1 *M* $NaNO_3$, 5% Al(III) from 0.1 *M* $Al(NO_3)_3$, 8% Ba(II) from 0.1 *M* $Ba(NO_3)_2$, and 62% La(III) from 0.1 *M* $La(NO_3)_3$. The phosphine oxide does not show the high selectivity in extraction exhibited by solvents that do not extract so completely. It is believed that selectivity can be varied by the structure of the organic molecule and by the anionic character of the aqueous solution from which extraction is made.

The various types of phosphorus compounds studied should have many applications to solvent extraction of other than source and fissionable materials. The extraction data and the fact that tributyl phosphine oxide in CCl_4 will extract more than 20% of acetic acid, citric acid, tartaric acid, or nitric acid from 1 *M* aqueous solutions give an indication of the possibilities. Samples of tributyl phosphine oxide, butyl dibutylphosphinate, and dibutyl butylphosphonate will be made available to other research and development groups interested in testing them.

Estimation of the Equivalent Weight of Salts. It has frequently been necessary, during the current program, to identify organic-acid salts that have no melting point. Wet combustion with estimation of the evolved CO_2 has proved useful. A suggestion made by Lipkin[3] has also proved very helpful. Salts of organic or inorganic acids are dissolved in water or an aqueous organic solvent, passed over a small bed of cation-exchange resin in the hydrogen form (such as Amberlite IR-100H, Dowex 50, Nalcite HCR), and then washed with more solvent. The acid in the column effluent (resulting from exchange of H^+ from resin with cation of salt) can be successfully titrated with standard alkali. The determination of equivalent weight was made by using about 10 equivalents of resin per equivalent of salt. For the determination, 1 meq of the salt was weighed on an analytical balance; on a smaller scale, a microbalance was used to weigh about 0.05 meq of the salt. Lipkin claimed a precision of 1% for the method, and this has been readily reproduced. Attempts are being made to extend the method to use anion-exchange resins.

PROTIUM-DEUTERIUM EXCHANGE IN ION-EXCHANGE RESINS

P. Agron J. Halperin

Work on protium-deuterium exchange in ion-exchange resins has been temporarily discontinued because other problems now require more attention.

(1) W. H. Baldwin and C. E. Higgins, *Chemistry Division Quarterly Progress Report for Period Ending December 31, 1951*, ORNL-1260, p. 67.

(2) G. M. Kosolapoff and J. F. McCullough, *J. Am. Chem. Soc.* **73**, 5392 (1951).

(3) D. Lipkin, *The Isolation and Identification of Alkylated Phosphoric Acids*, AECD-2234 (Aug. 23, 1948).

CHEMICAL PHYSICS

NEUTRON DIFFRACTION STUDIES

H. A. Levy S. W. Peterson

Crystal Structures of Tetragonal and High-Temperature Cubic Ammonium Bromide. Deutero-ammonium bromide crystallizes in four distinct phases with temperatures of stability at normal pressure as follows:

Phase IV (cubic, CsCl type)

$\xrightarrow{-104^\circ}$ phase III (tetragonal)

$\xrightarrow{-58.4^\circ}$ phase II (cubic, CsCl type)

$\xrightarrow{\sim 125^\circ}$ phase I (cubic, NaCl type) .

The behavior of ordinary ammonium bromide is similar, with somewhat different transition temperatures, except that the transition corresponding to that at -104°C in ND_4Br has never been observed; the phase III structure persists to very low temperatures. The detailed crystal structures of ND_4Br in phases IV and II have been investigated by neutron diffraction and reported earlier.[1] The neutron diffraction studies of ND_4Br in phases III (tetragonal) and I (high-temperature cubic) have now been completed.

Tetragonal ammonium bromide was studied by x-ray diffraction by Ketelaar[2] and by Weigle and Saini;[3] their data lead to the space-group assignment $D_{4h}^7 - P\,4/nmn$.[4] The authors reported nonconcordant results for the unit cell dimensions. In view of the discrepancy, Borie has made precision determinations[5] of the unit-cell dimensions of NH_4Br at -145, -124, and -100°C with the results shown in Table 20, which are in substantial agreement with those of Weigle and Saini at -145 and -71.5°C.

Table 20

UNIT-CELL DIMENSIONS OF NH_4BR

TEMPERATURE (°C)	a (Å)	c (Å)	c/a
-100	5.711	4.054	1/1.409
-124	5.703	4.048	1/1.409
-145	5.695	4.043	1/1.409

These values are based on the old wave-length scale, Cu K_α = 1.539 Å. Borie's value for cubic a_0 at room temperature is 4.054 Å (same scale), as compared with the literature value of 4.047 Å.

In this structure, the unit cell is bimolecular with N in positions[4] (a) 000, ½½0 and Br in positions (c) 0½u, ½0$\bar{u}$. According to Ketelaar[2] the value of u is 0.53 (or 0.47); thus the arrangement is a slight distortion of the CsCl structure, for which u would be ½ and c/a would be $1/\sqrt{2}$. Ketelaar's value for u was assumed in the following analysis of the neutron data.

The hydrogen atoms would logically be placed in positions (i) $0xz$; $x0\bar{z}$; $\frac{1}{2},\frac{1}{2}+x,\bar{z}$; $\frac{1}{2}+x,\frac{1}{2},z$; $0\bar{x}z$; $\bar{x}0\bar{z}$; $\frac{1}{2},\frac{1}{2}-x,\bar{z}$; $\frac{1}{2}-x,\frac{1}{2},z$. If the ammonium ion is tetrahedral, the values of z and x will be nearly equal. With these hydrogen positions, the N-D arms of

(1) H. A. Levy and S. W. Peterson, *Phys. Rev.* **83**, 1270 (1951); *Chemistry Division Quarterly Progress Report for Period Ending March 31, 1951*, ORNL-1053, p. 93.

(2) J. A. A. Ketelaar, *Nature* **134**, 250 (1934).

(3) J. Weigle and H. Saini, *Helv. Phys. Acta.* **9**, 515 (1936).

(4) The notation is that of the *International Tables for the Determination of Crystal Structures*, Gebrüder Borntraeger, Berlin (1935), and Edwards Bros., Ann Arbor, Michigan (1944).

(5) B. S. Borie, Jr., and R. M. Steele, *Metallurgy Division Quarterly Progress Report for Period Ending January 31, 1952*, ORNL-1267, p. 123.

the ammonium ions are directed essentially toward four of the eight surrounding bromide ions; however, unlike the phase IV structure, the arrangement of close-hydrogen atoms around Br is not tetrahedral, but square, and the bromide ion lies some distance out of the plane of the square along the fourfold axis. If the values of x and z are taken to be positive, the displacement of Br from the ideal CsCl location is toward the approaching hydrogen atoms for $u = 0.47$ and away for $u = 0.53$.

Neutron diffraction data were obtained from ND_4Br powder at -78°C. The size of the unit cell is such that only a limited number of Bragg reflections can be satisfactorily resolved by this method. Because of the limitations of the data, a complete, systematic variation of all parameters was not feasible; hence the following assumptions were made through most of the search for a model satisfying the neutron data:

1. The ammonium ion is tetrahedral ($x = z$).

2. The N-D distance is that found in phases IV and II, 1.03 Å; thus $x = z = 0.147$.

3. The value of the bromide parameter u is 0.47 or 0.53.

These assumptions completely fix the structure, except for temperature displacements of the various atoms. For describing temperature motion, separate temperature factors exp $-B_i(\sin\theta/\lambda)^2$ were applied to N, D, and Br amplitudes. In addition, an asymmetric displacement of D in the plane normal to the N-D link with characteristic half-angle at the nitrogen atom of α was tested; this asymmetric motion is similar to that found in phase II.[1]

Within the framework of the above assumptions, the following model gave satisfactory agreement with the neutron data:

$$\alpha = 10°, \qquad B_{Br} = 0.4\ A^2,$$
$$B_D = 3.7\ A^2, \qquad B_N = 1.2\ A^2,$$
$$u = 0.47.$$

The value $u = 0.53$ was completely unsatisfactory, since it indicated that the displacement of Br is toward the approaching hydrogens. Of the other parameters, α and B_D were the most sensitive in achieving a fit and received the most attention during the investigation. In addition, a limited number of trial structures departing from the above assumptions was investigated. Small rotations of the ammonium ions around the c axis (space group C_{4h}^3) and flattened ND_4^+ groups ($x > z$) were studied. None of the structures gave any indication of being in accord with the data. A comparison of observed structure factors with those calculated from the final model is shown in Table 21. The structure is illustrated in Fig. 15.

The structure found for tetragonal ND_4Br was anticipated by Nagamiya[6] in his theoretical treatment of second-order phase transitions in the ammonium halides and by Wagner and Hornig[7] in their interpretation of the infrared spectrum of this material.

High-temperature cubic ND_4Br, in common with several other ammonium halides, has been shown by x-ray diffraction[8] to have the NaCl structure, with the x-ray space group O_h^5, and the unit cell dimension

(6) T. Nagamiya, *Proc. Phys. Math. Soc. Japan* **25**, 540 (1943).

(7) E. L. Wagner and D. F. Horning, *J. Chem. Phys.* **18**, 305 (1950).

(8) R. W. G. Wyckoff, *Crystal Structures*, Interscience, New York (1951), Vol. I, Table III, p. 2.

a = 6.90 Å. This unit is tetramolecular, with ND_4^+ centered at (a) 000, face centered, and Br at (b) ½½0, face centered.[4]

Neutron diffraction data were obtained from ND_4Br powder at 200 and 250°C; similar patterns were obtained at the two temperatures. The patterns show rather severe attenuation of intensity with scattering angle, as was expected because of the augmented temperature motion; this feature limits the number and precision of the data obtained.

TABLE 21

CALCULATED AND OBSERVED NEUTRON INTENSITIES FOR TETRAGONAL ND_4Br

hkl	I_{calc}	I_{obs}*
001, 110	1616	1600
101	109	129
111, 200	3292	3285
201	116	129
211	122	157
002, 220	168	143
102	2	0
112, 221, 310	4	0
301	280	276
202, 311	667	533
212	215	260
321	58	57
222, 400	333	365
302	110	84
003, 330	114	151
103, 411	90	132

*Incompletely resolved maxima.

A large number of models with both static and rotating ammonium ions was examined for agreement with the neutron data. In all models, the ND_4^+ group was assumed substantially tetrahedral, with the N-D distance close to 1.03 Å as found in phases II and IV. The models tried included the following:

1. 16 D placed at random in 32-fold positions (f) of O_h^5, with and without rotatory oscillation,
2. 16 D at random in 96-fold positions (k),
3. freely rotating ND_4^+ ions,
4. ND_4^+ ions rotating about a twofold axis, with this axis set at random parallel to the three-crystal fourfold axes,
5. ND_4^+ ions rotating about a threefold axis, with this axis set at random along the eight threefold directions of the crystal,
6. ND_4^+ ions rotating about a threefold axis, with this axis set at random along the six fourfold directions of the crystal.

Of these models, only the last one (6) gave reasonably satisfactory agreement with the data. In this model, 12 D atoms are distributed around 24 circles that subtend a half-angle of 70°32′ at the four (a) positions[4] and whose axes are the six directions [001], etc. The remaining 4 D atoms are placed at random in the 24-fold positions (e) $x00$, etc. The expression giving the contribution of D to the

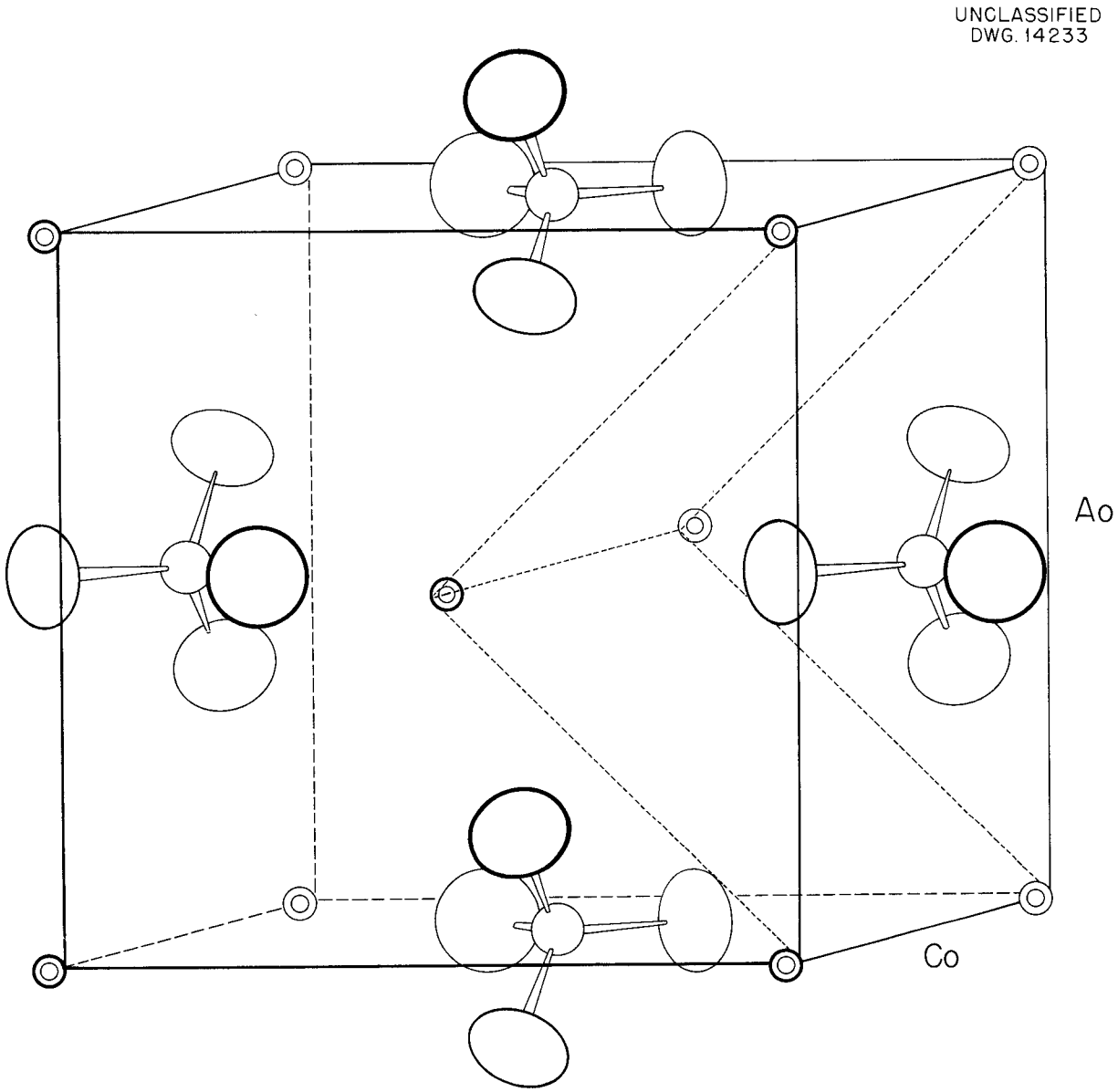

Fig. 15. Unit Cell of Tetragonal ND_4Br. The small circles represent Br, the large ellipses D, and the intermediate circles N. The sizes are roughly indicative of the extent of temperature motion of the nuclei. The dotted lines outline a monomolecular pseudocell showing the relation of the structure to the CsCl arrangement and to the structures of phase IV and phase II.

structure factors is a simple adaptation of that used to describe the rotatory oscillation of ND_4^+ ions in previous studies,[1] with $\alpha = 70°32'$ and $(x_0 y_0 z_0) = \pm (x00), \pm (0x0)$, and $\pm (00x)$, and sets equivalent by the face-centering operation, at random.

Table 22 shows a comparison of observed and calculated structure factors for this model and for several that proved unsatisfactory. Although the chosen model does not give ideal agreement with the data, it does give a reasonable approach to agreement. However, further refinement of the model does not seem worthwhile.

The final model incorporates the following position and temperature parameters:

$$B_D = 4.0\ A^2\ , \qquad B_N = 3.0\ A^2\ ,$$

$$B_{Br} = 3.0\ A^2\ , \qquad x = 0.15\ .$$

The N-D bond distance is 1.03 Å. A drawing of a portion of the structure is shown in Fig. 16.

RADIO-FREQUENCY SPECTROSCOPY

R. Livingston H. Zeldes

Instrumentation for Pure Quadrupole Spectra. An effort has been made to improve the spectrometer performance by utilizing a narrow-band amplifier and phase-sensitive detector. In order to utilize such equipment effectively, a better radio-frequency oscillator and detector circuit has been needed. A number of published circuits and new circuits developed by E. Fairstein have been built and tested. The work is still in progress. A narrow-band amplifier, phase-sensitive detector, audio oscillator, and vacuum-tube-voltmeter level indicator have been built in final form and appear to be operating satisfactorily.

Alkyl Chlorides (R. Livingston). The quadrupole resonances for chlorine have been observed in a variety of substituted ethanes and related compounds. The coupling values are consistent with those reported for

Table 22

CALCULATED AND OBSERVED STRUCTURE FACTORS FOR HIGH-TEMPERATURE CUBIC ND_4Br

hkl	CALCULATED |*F*|					OBSERVED |*F*|
	Model 1[a]	Model 1[b]	Model 3[c]	Model 3[d]	Model 6 (final)	
111	6.77		6.64	6.86	6.69	6.68
200	10.14	10.33	10.48	10.75	10.82	11.1
220	7.35		6.86	7.17	7.00	6.80
311	0.41		0.72	0.99	0.91	0.70
222	6.03		4.68	5.00	4.49	4.0
400	0.76	2.53	3.75	3.91	4.88	5.02
331	0.85		0.61	0.52	0.93	1.0
420	2.96		3.28	3.35	3.67	3.76
422	3.67		3.11	3.09	2.69	2.89
620					3.82	3.05

[a] Without rotatory oscillation.

[b] With rotatory oscillation, $\alpha = 20°$.

[c] N-D = 1.05 Å.

[d] N-D = 1.015 Å.

UNCLASSIFIED
DWG. 14232

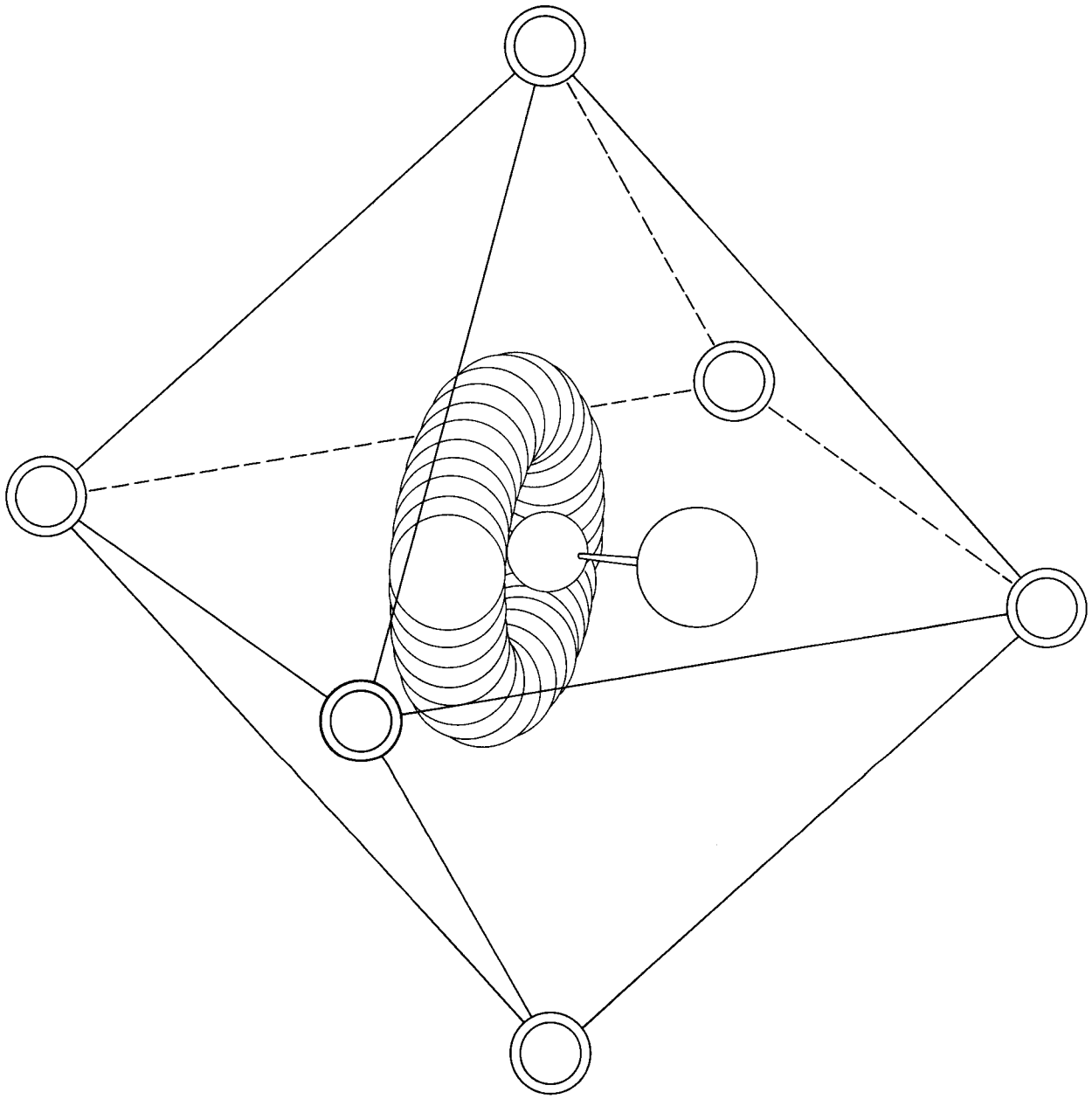

Fig. 16. A Portion of the Structure of High-Temperature Cubic ND_4Br. The rotating ammonium ion is shown in one orientation of the six occupied at random.

chloromethane[9] and can be explained by variations in ionic character in the carbon-chlorine bond as a function of chemical composition. The details are being prepared for publication.

Chlorates (R. Livingston and H. Zeldes). The quadrupole resonances for chlorine have been observed in the following: $NaClO_3$, $KClO_3$, $AgClO_3$, $Ba(ClO_3)_2 \cdot H_2O$, $Cu(ClO_3)_2 \cdot 6H_2O$, and $Ni(ClO_3)_2 \cdot 6H_2O$. A single Cl^{35} line was observed in each substance and the values centered near 30 megacycles with an approximate 6% spread. Models of the $NaClO_3$ and $KClO_3$ lattice have been constructed, and calculations are under way to determine whether the variation in frequency from one compound to another is due to e/r^3 terms from the environment of a chlorate ion in the lattice or from a distortion of the chlorate ion itself by other type of lattice interactions.

$NaClO_3$ gives the sharpest and strongest resonance of any substance observed. The copper and nickel salts are paramagnetic. Since a single line was observed for Cl^{35} in each salt at about 30 megacycles, there is essentially no perturbing magnetic field at the Cl positions in the lattice, and the paramagnetic ions must have a random orientation. If the substances, or similar ones, could be made antiferromagnetic, the magnetic field at the chlorine nucleus might be strong enough to permit the observation of an internal Zeeman effect. The intensity and direction of the internal magnetic field might then be evaluated by experiments with an externally applied homogeneous magnetic field on a single crystal of the antiferromagnetic substance.

(9) R. Livingston, *J. Chem. Phys.* **19**, 1434 (1951).

RADIATION CHEMISTRY

PEROXIDE PRODUCTION IN REACTOR-IRRADIATED URANYL SULFATE SOLUTION

A. C. Stewart J. A. Ghormley

The method for determining peroxide in the presence of uranyl ion reported earlier[1] was used to analyze reactor-irradiated uranyl sulfate solutions containing 44 g of uranyl sulfate per liter. After eight minutes of irradiation in hole 12 ($T = 30°C$), the samples were immediately immersed in liquid nitrogen to inhibit decomposition of peroxide during the period allowed for the decay of radioactivity in the samples. At the end of 24 hr the samples were removed from the liquid nitrogen and rapidly warmed to room temperature. Two identical portions were withdrawn from each of two samples. One portion from each sample was analyzed immediately after reaching room temperature and gave a peroxide yield of 0.97 molecules per 100 ev. The second portion of each sample, allowed to remain at room temperature for 1 hr before analysis, gave peroxide yields of 0.83 molecules per 100 ev. The results support the conclusion that the lower yields of peroxide calculated from gas analysis are due to peroxide decomposition in the presence of uranyl ion. The H_2 yield in a solution containing 44 g of UO_2SO_4 per liter, determined by gas analysis, is 0.98 molecules per 100 ev.[1] Since the yield of peroxide is 0.97 molecules per 100 ev where decomposition is retarded, it would appear that most of the initial products are H_2 and H_2O_2 rather than H_2 and O_2.

Peroxide is formed in uranyl sulfate solutions irradiated at liquid nitrogen

(1) J. W. Boyle *et al.*, *Chemistry Division Quarterly Progress Report for Period Ending December 31, 1951*, ORNL-1260, p. 89.

temperature. The peroxide observed does not represent a true yield since measurements were made at the end of a period in which decomposition could occur (24 hr at room temperature). At the time of analysis, decomposition was slow and identical portions of two separate samples analyzed 1 hr apart gave the same yield, 0.31 molecules per 100 ev.

PEROXIDE PRODUCTION IN GAMMA-IRRADIATED ICE

A. C. Stewart J. A. Ghormley

An investigation of the production of hydrogen peroxide in ice made from oxygen-saturated water has been reported by Bonet-Maury and LeFort[2] who found peroxide was produced at a rate that decreased with decreasing temperature and that none formed at temperatures below -116 °C. Gunther and Holzapfel[3] reported no hydrogen production in x-ray irradiated ice at -180 °C. However, in this laboratory[4] work on the decomposition of tritium-water by its own radiation has shown the production of gas in tritium ice at -196 °C, in apparent disagreement with the published work. Another apparent inconsistency is found in work on the effects of alpha particles on ice. Duane and Scheuer[5] have reported production of hydrogen and oxygen in equivalent amounts, whereas Bonet-Maury and LeFort observed a constant yield of hydrogen peroxide that is independent of temperature.

A study of the effects of ionizing radiation on ice to determine reasons for the discrepancies in previously reported work was therefore desirable. Results of some exploratory experiments are given in Table 23. Ice in sealed ampoules was prepared by rapidly freezing water or hydrogen peroxide solution, outgassed or saturated with the appropriate gas, in liquid nitrogen. The ice was then gamma-irradiated in liquid nitrogen, solid CO_2, or ice-salt mixture. After irradiation, the samples were brought to room temperature, and the hydrogen peroxide and other oxidants present were determined by oxidation of iodide followed by spectrophotometric measurement of triiodide produced.[6]

(2) P. Bonet-Maury and M. LeFort, *Nature* **162**, 381 (1948).

(3) P. Gunther and L. Z. Holzapfel, *Physik. Chem.* **B44**, 374 (1939).

(4) J. A. Ghormley and A. O. Allen, *Decomposition of Tritium Oxide Under its Own Radiation*, ORNL-128 (Sept. 1, 1948).

(5) W. Duane and O. Scheuer, *Compt. Rend.* **156**, 466 (1913).

(6) A. O. Allen *et al.*, *Decomposition of Water and Aqueous Solutions Under Pile Radiations*, ORNL-130, p. 9.

Table 23

PEROXIDE PRODUCTION IN WATER AND ICE GAMMA-IRRADIATED 16 HR AT 1000 r/min

SAMPLE	FINAL CONCENTRATION H_2O_2 (mmole/l)			
	At 0 °C	At ~ -5 °C	At -78 °C	At -196 °C
O_2-saturated	472	84.4	32.3	73.8
Degassed water	31.2	5.8	8.5	73.5
He-saturated water	24.6	20.9	6.19	54.8
H_2-saturated water	0	3.7	2.5	53.6
53 mmole/l of H_2O_2, H_2 saturated	0	3.5	0	72.6

Figure 17 shows peroxide production in ice prepared from oxygen-saturated water and exposed to cobalt-60 gamma rays for periods of 5 or 10 minutes. Temperatures down to -176 °C were obtained by placing the sample in a Dewar vessel and adding cold nitrogen gas from a flask containing liquid nitrogen that was boiled at a controlled rate by an immersed heater. Samples irradiated at -196 °C were immersed in liquid nitrogen. In both cases the source was lowered over the vessel containing the test samples.

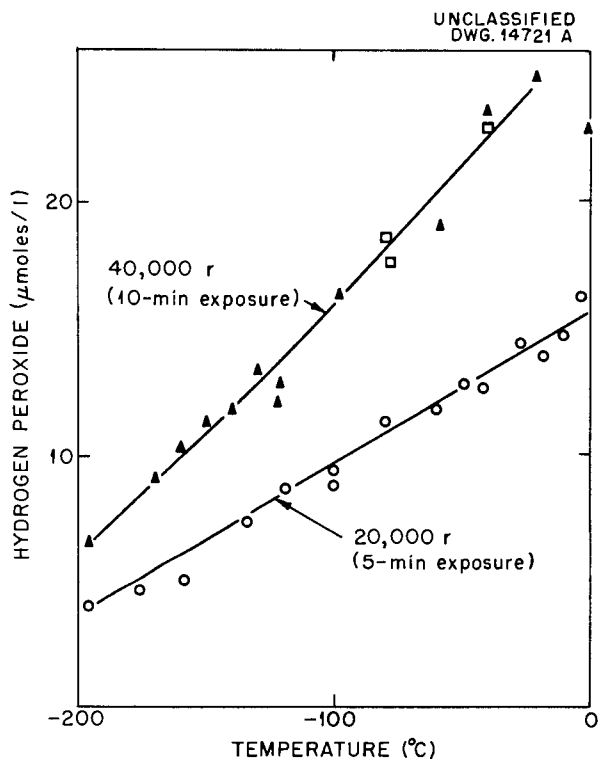

Fig. 17. Hydrogen Peroxide Production in Ice Prepared from Oxygen-Saturated Water Irradiated with Co^{60} Gamma Rays at Various Temperatures.

The results of the experiments seem to indicate that, although the initial rate of production of hydrogen peroxide decreases continuously with decreasing temperature (at least when oxygen is present), the tendency toward recombination of the products decreases even more rapidly, giving a higher steady-state concentration of hydrogen peroxide at low temperatures. At -196 °C the presence of oxygen or hydrogen has very little influence on the production of peroxide, whereas at higher temperatures the steady-state concentration is low in the absence of oxygen and even lower in the presence of hydrogen.

The peroxide concentrations shown in Table 23 for oxygen-free water are higher than usually reported. The difference may be attributed to the high H_2O_2-to-H_2 ratio in the liquid phase that results from H_2 diffusing into the gas phase more rapidly than O_2.

SOME EFFECTS OF COBALT GAMMA RAYS IN 0.8 *N* SULFURIC ACID SOLUTIONS

T. J. Sworski

Sulfuric Acid (0.8 *N*) as a Solvent. A linear production rate, with a yield of 0.38 molecules of hydrogen peroxide per 100 ev absorbed, is observed in helium-saturated 0.8 *N* sulfuric acid (Fig. 18). The rate is equal to that of hydrogen production by the forward reaction

$$2H_2O \rightsquigarrow H_2 + H_2O_2$$

in air-saturated, 0.8 *N* sulfuric acid, ferrous sulfate solution as reported by Hochanadel.[7] The conclusion is that 0.8 *N* sulfuric acid behaves as a radical remover and permits the linear production of forward reaction products by preventing the back reactions. Therefore caution must be exercised in using 0.8 *N* sulfuric acid as a solvent in radiation studies, since the solvent may compete with the solute for the radicals produced by ionizing radiations.

[7] C. J. Hochanadel, *J. Phys. Chem.* (to be published).

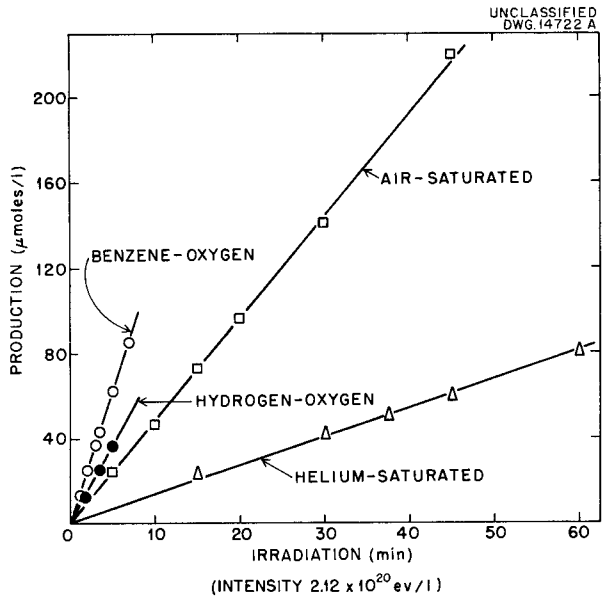

Fig. 18. H_2O_2 Production in 0.8 *N* H_2SO_4 Solutions.

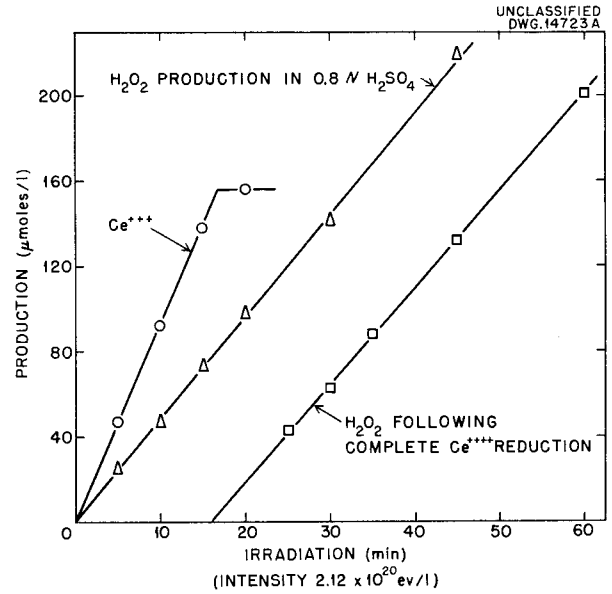

Fig. 19. Ce^{+++} and H_2O_2 Production in Air-Saturated 0.8 *N* H_2SO_4 Containing 156 μmoles/l Ce^{+++}.

Solutions of Benzene in 0.8 *N* Sulfuric Acid. The yield of hydrogen peroxide in 0.8 *N* sulfuric acid in the presence of benzene is 3.44 molecules per 100 ev absorbed (Fig. 18), an increase over the yield in unbuffered aqueous benzene solutions of 2.91 molecules per 100 ev.[8] The dependency of hydrogen peroxide and phenol formation on the pH of aqueous benzene solutions is under investigation.

Solutions of Ceric Sulfate in 0.8 *N* Sulfuric Acid. Following the complete reduction of ceric sulfate in air-saturated 0.8 *N* sulfuric acid solution, the yield for hydrogen peroxide formation (Fig. 19) is identical to that observed in air-saturated 0.8 *N* sulfuric acid and stoichiometrically equivalent to the yield for ceric reduction. The stoichiometry is in disagreement with the results of Clark and Coe.[9] The mechanism of ceric reduction will be investigated.

[8] T. J. Sworski, *Chemistry Division Quarterly Progress Report for Period Ending June 30, 1951*, ORNL-1116, p. 75.

[9] G. S. Clark and W. S. Coe, *J. Chem. Soc.* **5**, 97 (1937).

Benzene increases the yield for ceric reduction in helium-saturated 0.8 *N* sulfuric acid from 2.46 to approximately 17 ions per 100 ev absorbed. There is no oxygen effect in the benzene-enhanced ceric reduction. The increase may result partly from the reduction of ceric ion by phenol produced by the oxidation of benzene. Studies of this mixture will be continued.

Solutions of Ferrous Sulfate in 0.8 *N* Sulfuric Acid. The yield for hydrogen peroxide production is identical to that observed in pure solvent, following the complete oxidation of ferrous sulfate in air-saturated 0.8 *N* sulfuric acid (Fig. 20). The sum of ferric ion and hydrogen peroxide present after complete oxidation of ferrous sulfate differs for solutions given interrupted irradiation periods before complete oxidation and solutions completely oxidized in a continuous dose. This is due to the slow reaction between ferrous ion and hydrogen peroxide.

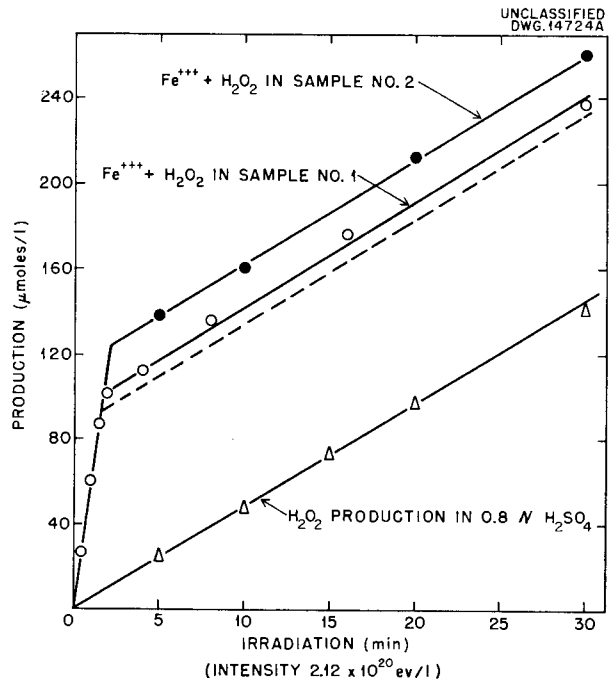

Fig. 20. Fe^{+++} and H_2O_2 Production in Air-Saturated 0.8 N H_2SO_4 Containing 93 μmoles/l Fe^{++}.

The slow reaction makes the error of Fricke and Morse[10] understandable. They concluded that the hydrogen peroxide yield after complete ferrous oxidation is stoichiometrically equivalent, initially, to the rate of ferrous oxidation. The analyses were made on aliquots removed from the samples between irradiation periods. The dotted line in Fig. 20 corresponds to the results expected if the reaction between ferrous ion and hydrogen peroxide is rapid or if the irradiation of a sample is halted at the time necessary for complete oxidation of ferrous sulfate with no excess hydrogen peroxide produced.

SOME EFFECTS OF COBALT GAMMA RAYS ON UO_2SO_4 SOLUTIONS

T. J. Sworski C. Hochanadel

Effect of UO_2SO_4 on the Yield of Gas in Gamma-Irradiated Solutions. Dilute aqueous solutions of a number of oxidizing and reducing agents give the same initial yield of molecular hydrogen upon exposure to x rays or gamma rays. During the decomposition of water by ionizing radiations two reactions are considered to occur simultaneously:

$$(F) \quad 2H_2O \rightsquigarrow H_2 + H_2O_2 \text{ (or } H_2 + \tfrac{1}{2}O_2 + H_2O)$$

$$(R) \quad H_2O \rightsquigarrow H + OH \,.$$

The final molecular products are presumed to be formed by recombination of radicals in regions of high radical concentration (hot spots). The remaining radicals (R) are assumed to be responsible for most of the reactions with solutes in irradiated solutions. Adding a reactive solute such as Br^- practically prevents recombination of H_2 and H_2O_2 (through reactions with H and OH) and allows the yield in (F) to be measured.

For solutions in 0.8 N H_2SO_4, the yield from reaction (F) was shown to be about 18% lower than that for unbuffered solutions.[11,12] Present studies show that UO_2SO_4 is also very effective in reducing the yield for reaction (F). The hydrogen yields for gamma-irradiated UO_2SO_4-KBr solutions are plotted in Fig. 21. The same effect was observed[13] for reactor-irradiated UO_2SO_4 solutions where it was shown that the hydrogen yield decreased continuously with increasing UO_2SO_4 concentration.

The mechanism by which UO_2SO_4 lowers the molecular yield is not understood. It may act to prevent formation of products or it may sensitize the recombination of products, making measurement impossible.

(10) H. Fricke and S. Morse, *Am. J. Roentgenol. and Radium Therapy* **18**, 430 (1927).

(11) C. J. Hochanadel, *J. Phys. Chem.* **56**, 587 (1952).

(12) A. O. Allen and E. Johnson, Paper Submitted to *J. Am. Chem. Soc.* (1952).

(13) J. W. Boyle *et al.*, *op. cit.*, ORNL-1260, p. 89.

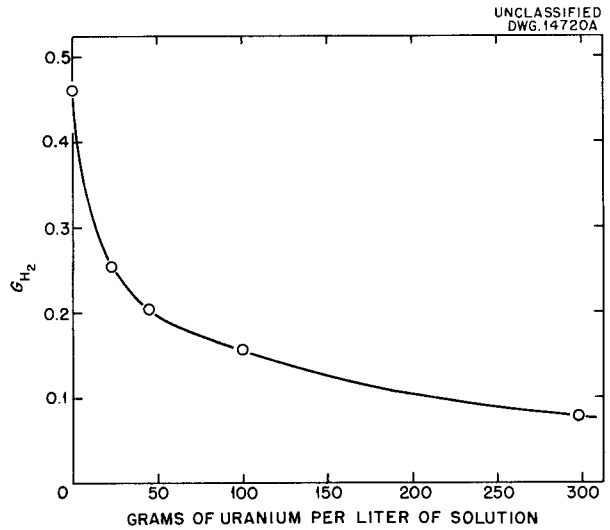

Fig. 21. Effect of UO_2SO_4 Concentration on Hydrogen Yield from Gamma Irradiation of UO_2SO_4-KBr Solutions.

Effect of UO_2SO_4 on Radical Yield (*R*). The yield of H and OH in reaction (*R*) has been estimated[11] by measuring H_2O_2 formation when water containing both H_2 and O_2 is irradiated. It was proposed that each pair of radicals produced in (*R*) is converted into one H_2O_2. For pure water containing H_2 and O_2, the initial H_2O_2 yield was 3.2 molecules per 100 ev, and for sulfuric acid solutions the yield was independent of pH from 2 to 7. However, in 0.8 *N* H_2SO_4 (pH 0.4) the H_2O_2 yield dropped to 2.1 molecules per 100 ev.

When UO_2SO_4 was added to give a concentration of 22 g of uranium per liter to the solution containing H_2 and O_2, the initial peroxide yield was 2.9 as compared with 3.2 for pure water. Subtracting the contribution of peroxide from reaction (*F*), the radical yields in pure water and UO_2SO_4 solution are about the same (about 2.7 H and OH per 100 ev).

Reaction of UO_2SO_4 with H and OH. The reactivity of UO_2SO_4 with H and OH was studied by several methods.

1. Steady-state gas pressures were only a few centimeters of Hg for solutions containing UO_2SO_4 at a concentration of 40 g of uranium per liter irradiated with gamma rays at 15,000 r/min. Since the low steady-state results from rapid recombination of molecular products brought about by reactions with radicals, this would indicate that UO_2SO_4 does not compete effectively for these radicals.

2. A direct study of the recombination of H_2 and H_2O_2 induced by radiation showed that on adding UO_2SO_4 at a concentration of 40 g of uranium per liter the rate of recombination was not greatly retarded. Solutions prepared with UO_2SO_4 from different sources behaved differently, indicating that impurities had some effect.

3. The radiation-induced decomposition of peroxide also proceeds through reactions with free radicals. The initial yield for peroxide decomposition was lowered from 3.6 H_2O_2 per 100 ev with no added UO_2SO_4 to about 0.4 H_2O_2 per 100 ev with UO_2SO_4 at a concentration of 22 g of uranium per liter. However, in this case the effect on the yield may be that of pH, since H_2O_2 in H_2SO_4 solutions and H_2O_2 in UO_2SO_4 solution, both at the same pH (about 3), decomposes at about the same rate on irradiation.

SOME EFFECTS OF COBALT GAMMA RAYS ON CCl_4-H_2O SYSTEM

J. Ghormley C. Hochanadel

The possible use of CCl_4 in the Purex process has created some interest in Cl^--formation in the CCl_4-H_2O system

under irradiation. It is well known that organic halide-H_2O systems yield the halogen acids on irradiation.[14,15] Some preliminary measurements were made on the increase in conductivity during irradiation of water saturated with CCl_4 (Baker and Adamson cp) with gamma rays at 4000 r/min. In oxygen-saturated solutions the conductivity increased linearly with time, whereas in helium-saturated solutions an initial lag was observed before the linear increase. Also, in helium-saturated solutions a precipitate was always observed (perhaps C_2Cl_6), whereas none occurred in oxygen-saturated solutions. The slopes of the linear portions of the curves were approximately the same for all solutions. Assuming all of the conductance to be by HCl (there is probably HOCl formed also), the yields calculated from conductance measurements were G = 9 to 12 HCl per 100 ev. Yields calculated from the measured pH were approximately the same.

GAMMA-RAY DOSIMETRY

J. Ghormley C. Hochanadel

Further measurements on the absolute yield for ferrous oxidation by cobalt gamma radiation have been completed. The possibility that the discrepancy between the value of $G_{Fe^{+3}}$ = 15.6 and that of Miller and of Hardwick, $G_{Fe^{+3}}$ = 20.6, represents an effect of radiation intensity was checked by making measurements at 0.2, 1.2, 4.1, 22, and 65 r/sec. The two lower intensities were obtained by means of lead shielding. Energy absorption was based on measurements with the polystyrene-cavity ion chamber previously described.[16] At first, the results indicated an increase in yield with decrease in intensity. Then it was noted that, whereas the unirradiated blank experiment for ferrous solutions stored in pyrex vessels showed negligible change during the course of exposure, the unirradiated solution in the polystyrene vessel oxidized appreciably upon standing. Also, after a solution was allowed to stand for several hours in the polystyrene vessel and then irradiated at the high intensity for a short time, a higher yield was always observed, thus indicating that some material dissolves, which raises the yield for ferrous oxidation. It is known that many organic materials increase the yield for ferrous oxidation.

Other measurements were made by substituting Baker's-analyzed-reagent 20% fuming sulfuric acid for Baker and Adamson's cp H_2SO_4. The same rate of ferrous oxidation was obtained for both acids except for an initial lag observed for the Baker's analyzed fuming acid. The low initial rate was traced to the presence of SO_2.

The conclusion is that the observed yield of 15.6 ferrous ions oxidized per 100 ev is independent of intensity over a wide range. The reagents used are not believed to be a source of impurities that would affect the yield.

PREPARATION OF ALPHA-RAY DEUTERIO-CUPRENE

S. C. Lind P. S. Rudolph

Approximately 2 g of alpha-ray deuterio-cuprene is being prepared in order to study its structure by neutron

(14) G. V. Taplin and C. H. Douglas, *A Colorimetric Dosimeter for Qualitative Measurement of Penetrating Radiations*, UCLA-58 (Jan. 31, 1950); and *The Chloroform-Alcohol-Dye System*, UCLA-192 (April 2, 1952).

(15) H. L. Andrews and P. A. Shore, *J. Chem. Phys.* **18**, 1165 (1950).

(16) C. J. Hochanadel and J. A. Ghormley, *op. cit.*, ORNL-1116, p. 74.

diffraction methods. The cuprene is being made in gram quantities by the homogeneous irradiation of deuterio-acetylene with radon[17] in a reaction vessel especially designed to meet the following requirements:

1. rechargeable with radon,
2. directly connected to an automatic deuterio-acetylene generator capable of maintaining a constant pressure,
3. of a sufficiently large diameter so that the alpha-rays expend most of their energy in the gas,
4. amenable to adequate shielding so as to offer no radiation hazard,
5. safe from explosions or excessive pressure.

An all-glass apparatus that fulfilled these requirements was designed, fabricated, and tested, then a final apparatus, somewhat modified, was constructed from glass and metal.

Special purity calcium carbide (92.7%) was furnished by the National Carbide Company. The acetylene generated from this carbide had the following analysis: PH_3, 0.0162%; H_2S, 0.174%; NH_3, 0.043%. The deuterium-oxide (99.8%) was procured from the Isotope Packing and Shipping Department of ORNL.

Radon and laboratory facilities were made available by the Works Laboratory at the K-25 plant. The radon is procured from the Radon Collection Station[18] established at the Works Laboratory.

A sample of the deuterio-acetylene was analyzed mass spectrographically by the Works Laboratory, and a preliminary report of this analysis indicates the following components in the gas: C_2D_2, 79.2%; C_2HD, 14.3%; C_2H_2, 6.1%; A, 0.4%. Production of cuprene has been initiated and is progressing satisfactorily.

[17] S. C. Lind, J. C. Jungers, and C. H. Schiflett, *J. Am. Chem. Soc.* 57, 1032 (1935).

[18] C. H. Schiflett, M. E. Steidlitz, and W. Davis, Jr., *Rev. Sci. Inst.* **21**, 842 (1950).

CHEMISTRY OF THE SOLID STATE

HIGH-TEMPERATURE X-RAY DIFFRACTION

M. A. Bredig

Various attempts to increase the operating temperature of the specimen above 2100°C by changing the design of the carbon heating element of the high-temperature x-ray-diffraction apparatus have been unsuccessful. The rapid failure of the heating elements was probably the result of the high rate of evaporation of carbon in vacuum at temperatures above 2300°C. A change-over to high-frequency induction heating is being considered for measurements in the temperature range above 2000°C, and a water-cooled induction coil is being fabricated.

REMOTE-CONTROL X-RAY DIFFRACTION SPECTROMETER

M. A. Bredig

B. S. Borie, Jr.,
Metallurgy Division

G. E. Klein F. A. Sherrill
Solid State Division

The difficulties in the operation of the G-E x-ray tube with the Norelco high-voltage equipment recently received and installed are being overcome.

EFFECTS OF RADIATION ON CRYSTAL STRUCTURE

M. A. Bredig

A check has been made on the possibility that the transformation of yellow lead oxide into the red form on irradiation in the Chalk River reactor was caused by a rise in the temperature of the specimen through gamma-ray absorption rather than by neutron collisions. A sample of the yellow high-temperature form of lead oxide was heated in an evacuated glass capsule for two months at 390°C, that is, approximately 100°C below the transition point. The x-ray pattern showed roughly 50% transformation into the red form which, in combination with the absence of such transformation in the irradiation in the LITR,[1] is a strong indication that the transformation observed in the Chalk River experiment resulted from heating rather than from neutron collisions. Possibly the neutron bombardment resulted in a lowering of the temperature at which transformation can take place at a finite rate. Further experiments on the problem are planned.

METAL-METAL HALIDE SYSTEMS

M. A. Bredig H. R. Bronstein
J. W. Johnson W. T. Smith, Jr.[2]

Alkaline Earth-Metal Halide Systems. The work described in the preceding progress report indicated the need for better technique. Some improvement has been achieved through careful purification of the salts used by steps such as removal of heavy metals as sulfides, recrystallization from aqueous solution, and especially more thorough dehydration by heating at 275°C in a current of gaseous HCl followed by fusion in an evacuated quartz tube. Materials thus obtained were handled in a dry box. The crimped and welded capsules used for heating the salt-metal mixtures were cut open under benzene or hexane. The alkalinity of the salts after fusion, but before addition of metal, amounted to 0.23 and 0.01 mole % in two tests with calcium dichloride and to only a trace in the case of barium dichloride, indicating that the dehydration procedure was successful.

A mixture of 50 mole % each of $BaCl_2$ (29 g) and barium metal (18 g) in an evacuated type 304 stainless steel capsule that was heated for 4 hr at 1000 ± 15°C and quenched in water yielded a dark-grey salt phase of rather uniform appearance. Analysis of the grey salt by hydrogen evolution and alkalinity gave an excess of 23 ± 1 mole % for barium over $BaCl_2$, which is considered good agreement. It compares with 24 and 28 mole % for two tests at this temperature by Cubiciotti and Thurmond,[3] who apparently used only chlorine analysis. An x-ray diffraction pattern of the salt phase was compared with ASTM standard patterns and interpreted to be a mixture of all three known crystal modifications of $BaCl_2$, namely, the monoclinic, orthorhombic, and cubic. Three weak or very weak additional lines with spacings 3.15, 295, and 2.69 Å remained unidentified. Except for the weak lines, the x-ray results seem to indicate the absence of a subchloride such as BaCl in the solid. Twenty-three mole per cent of barium in excess of $BaCl_2$, as found by chemical analysis, would correspond to 46 mole % of subchloride BaCl, an amount that must be expected to give rise to strong diffraction lines if present as a separate solid phase.

(1) M. A. Bredig, *Chemistry Division Quarterly Progress Report for Period Ending December 31, 1951*, ORNL-1260, p. 107.

(2) Professor of Chemistry, University of Tennessee, ORNL consultant.

(3) D. D. Cubiciotti and C. D. Thurmond, *J. Am. Chem. Soc.* 71, 2149 (1949).

On the other hand, if the subchloride were present in solid solution in the dichloride and produced, for instance, lattice distortion and vacancies in the chlorine positions, the diffraction pattern of the dichloride should show some, although possibly only slight, modifications. Unfortunately, the rather poor quality of the x-ray pattern caused by properties of the substance under investigation does not permit finding or excluding such slight structural modifications.

If the excess barium were present as a separate metal phase, it should also be detectable in the x-ray pattern; cadmium metal, for instance, can be detected in considerably smaller amounts in solidified melts with cadmium chloride. Unless the absence of barium metal lines in the x-ray pattern can be shown in other ways to be the result of the formation of a subchloride in solid solution with $BaCl_2$, there is the possibility that it results from the conversion of the metal on the surface of the crystal grains to colloidal products by oxidation and hydration. The non-crystalline products are not detectable by x-ray diffraction. Therefore it is evident that further efforts are required to determine the chemical and physical state in which the large excess of barium over $BaCl_2$, found analytically, is present in these solids.

Two similar tests in the calcium-calcium dichloride system led to values for the amount of excess calcium that differed according to the analytical method used. They also differed from those reported by Cubiciotti and Thurmond, who reported the amount to be 16 mole % on the basis of chloride determination, whereas the data developed at ORNL on the same basis yielded approximately half this figure, or 8.3 mole %. From hydrogen evolution even smaller figures were obtained, 6.1 and 6.2, which compare with 9.7 and 9.8 mole % for measurements of alkalinity. The latter discrepancy seems to indicate the presence of calcium oxide or the as yet unexplained failure to exclude water completely. X-ray patterns give evidence of the difficulty of preventing the formation of considerable quantities, up to 20 mole %, of the dihydrate $CaCl_2 \cdot 2H_2O$ on even short exposure to the atmosphere. Further work might lead to more satisfactory agreement. X-ray diffraction was also used to search for a subhalide to separate a phase different from $CaCl_2$ by treatment with various mixtures of ethyl iodide and bromoform, in attempts similar to those by Wohler and Rodewald.[4] No significant differences were observed in fractions thus separated by specific weight.

Although the results reported here are admittedly fragmentary, it now seems possible to state that the early work by Wohler and Rodewald[4] and by Guntz and Benoit[5] on the alleged preparation of solid alkali subhalides of the formula CaCl, or BaCl, has not been found to be reproducible. On the other hand, the more recent work of a California group indicates an appreciable solubility in the molten state, which although greatly below that corresponding to 100% subhalide formation is being confirmed to a large extent. Results on alkali metal-chloride systems that may have an interesting bearing on the "octahedral hole" theory, proposed by Harker and Cubiciotti,[6] of the atomic and electronic structure of these molten metal-salt solutions will be presented in the next quarterly report.

---

(4) L. Wöhler and G. Rodewald, *Z. anorg. u allgem. Chem.* **61**, 54 (1909).

(5) Guntz and Benoit, *Bull. Soc. Chim. France* **35**, 709 (1924).

(6) D. D. Cubiciotti, *J. Am. Chem. Soc.* (to be published).

Alkali Metal-Alkali Metal Fluoride Systems. As a short-cut to possibly important applications of the solutions of metals in molten salts for reactor fuel and coolant systems as suggested previously,[7] an investigation of alkali metal-fluoride systems to parallel that of other halides was started. Although consideration is being given to the (slight) possibility of increased electric and thermal conductivity, the main emphasis is on the prevention or reduction of corrosion, including that under fission radiation.

From thermodynamic data[8] equilibrium constants of reactions such as $Fe + 2KF \longleftrightarrow FeF_2 + 2K$ can be calculated by using the equation $\log K = -\Delta F/4.575\ T$. Although ΔF is found to have comparatively large, positive values, it can be shown that the order of magnitude of K permits the formation of concentrations of transition metal fluoride and alkali metal dissolved in the molten fluoride sufficient to explain the mass transfer from a hot (1500°F ≈ 815°C ≈ 1090°K) to a cold (1200°F ≈ 650°C ≈ 920°K) leg of a thermal convection loop, as observed in operations for the ANP project. Thus, for the above reaction at 1100°K (1500°F), estimated equilibrium concentrations of higher than 10^{-6} moles of FeF_2 per mole of KF are obtained from the calculation:

$$\log K_{1100°K} = \frac{-\Delta F}{4.575\ T} = \frac{-84,000}{4.575 \times 1,100} = -16.7$$

$$K = \frac{[FeF_2][K]^2}{[Fe][KF]^2}\ ;\ [Fe] = 1;\ [KF] = 1$$

$$[K] = 2[FeF_2]\ ;\ K = 4[FeF_2]^3$$

$$\log [FeF_2] = \frac{\log K - \log 4}{3} = -\frac{17.3}{3} = -5.8\ .$$

The value of ΔF = +84 kcal used here is obtained by extrapolation of the function

$$\Delta F = \frac{\Delta F - \Delta H_{298}}{T}\ T + \Delta H_{298}\ ,$$

from values of $(\Delta F - \Delta H_{298})/T$ at 500 and 1000°K and ΔH_{298}, for 2KF and FeF_2. The values refer to solid rather than liquid fluorides, but it was felt that the much larger extrapolation of data for the liquids below the freezing points of the pure salts would be subject to larger errors than the substitution of the data of the solids for those of the liquids. For the reaction $Cr + 2KF = CrF_2 + 2K$, a CrF_2 concentration of $10^{-4.8}$ is obtained in an analagous way that is considerably higher than for FeF_2. However, for NiF_2 the concentration becomes considerably smaller, namely $10^{-6.3}$. At 920°K, the concentration of FeF_2 is down to less than 10^{-7}, for CrF_2 it is 10^{-6}, and for NiF_2 it is 10^{-8}. Thus, in all cases, considerably more than 90%, or practically all the amount formed at 1500°F (1100°K), is unstable at 1200°F (920°K) and must thus be converted back into the free transition metal by reaction with the stoichiometric amount of potassium metal, both of which may be assumed to be

(7) M. A. Bredig, J. W. Johnson, and D. S. Jessman, *Chemistry Division Quarterly Progress Report for Period Ending June 30, 1951*, ORNL-1116, p. 65.

(8) L. Brewer and collaborators in Vol. IV, 19B of the National Nuclear Energy Series, *The Chemistry and Metallurgy of Miscellaneous Materials*, p. 76-375.

dissolved in the molten fluoride eutectic.

It may be assumed, at least for the sake of the discussion, that equilibrium is nearly established in the convection loops at both 1500 and 1200°F, in the time required for a given volume of the melt to pass through these temperature zones. With a flow rate of 8 to 10 ft/min and a hot-zone length of about 3 ft, the time amounts to approximately 20 seconds. For a loop having a total length of 8 to 10 ft, 6000 passes are made in 100 hr by the whole fluid charge of 2000 grams. Neglecting differences in molecular weight, a quantity of $6 \times 10^3 \times 2 \times 10^3 \times 10^{-5.7}$, or approximately 25 g of iron might be deposited in 100 hours. For nickel, or chromium, 6 g or 200 g, respectively, might be deposited if these metals were present in their standard states. The figures appear to be of the right order of magnitude, that is, within less than a factor of 10 when compared with the observations reported by the ANP groups. It is immediately clear from a consideration of the equilibrium constants that a concentration of 1%, for instance, of potassium metal maintained in the fluoride melt would reduce the equilibrium concentrations at 1500°F, of FeF_2, CrF_2, and NiF_2 to

$$(FeF_2) = 10^{-16.5}/10^{-2\times2} = 10^{-12.5}$$

or by a factor of 10^{-7},

or

$$(CrF_2) = 10^{-14}/10^{-2\times2} = 10^{-10} \text{ or by } 10^{-5}$$

or

$$(NiF_2) = 10^{-18.5}/10^{-2\times2} = 10^{-14.5} \text{ or by } 10^{-8}.$$

Therefore, it is expected that a comparatively minor concentration of alkali metal dissolved in the fluoride melt would substantially reduce mass transfer from a hot to a cold part of the stainless steel system.

When UF_4 is present it may be considered the major corrosive agent. The free energy change, ΔF, for the reaction $Fe + 2UF_4 = FeF_2 + 2UF_3$ is of the order of +6 kcal, which compares with 84 kcal for the reaction $Fe + 2KF = FeF_2 + 2K$, above, leading to an equilibrium constant of $\log K = -1$ that compares with −17 for the case of KF. There will be a more detailed discussion in a future report, but it may be pointed out briefly that the thermodynamic data seem to explain the fact that the corrosion and mass transfer observed in the convection loops, although somewhat higher than without UF_4, does not appear to be of a different order of magnitude in spite of the large difference in the equilibrium constants.

Similarly, thermodynamic data pertinent to conditions in the presence of BeF_2 and ZrF_4 are being examined and will be discussed in the near future.

The experimental work on the fluoride-metal system was started with an investigation of the solubility of potassium metal in the sodium fluoride-potassium fluoride eutectic mixture of 60 mole % KF and 40 mole % NaF that is reported to melt at 710°C. Potassium rather than sodium metal was chosen because, in agreement with thermodynamic data and with measurements by Rink,[9] sodium was found in a preliminary experiment[1] to partly reduce potassium fluoride.

An interesting observation, relative to the validity of the thermodynamic

[9] E. Rinck, *Ann. de Chemie* **18**, 395-531 (1932).

reasoning of the previous paragraph, was made when the eutectic mixture without potassium metal was prepared by heating sodium fluoride and potassium fluoride in a vacuum in a stainless steel crucible. After heating to 1000 °C the salts were found to have evaporated and to be redeposited at colder parts of the crucible. On opening the apparatus, slight explosions occurred such as are common when small amounts of finely divided alkali metal are exposed to air. In addition, dark-colored material within the mass of the white salts exhibited considerable ferromagnetism, indicating the presence of metallic iron and/or nickel. The stainless steel crucible walls must have been the source of the metal, since they were found to have been considerably corroded in the hot parts in a few hours. It seems that reactions such as $Fe + 2KF = FeF_2 + 2K$, as discussed above with partial reversal at the lower temperature, can explain the observations. Repetition by heating in an argon atmosphere prevented, as expected, the occurrence of the phenomena. It also yielded a eutectic temperature of 716 °C.

The potassium used (2.45 g) for determining the solubility of the metal in the molten salt eutectic (23 g) contained approximately 1/2 of 1% of sodium as a contaminant. The tests were conducted in type 309 stainless steel capsules pretreated for corrosion resistance with a 50% mixture of HF and HNO_3, rinsed with distilled water and acetone, and then dried and flamed. The eutectic salt was placed on top of the potassium metal in the capsule. After evacuation, crimping, and welding, the capsules were heated in a tube furnace at a temperature of 850 °C in an argon atmosphere for a period of 2 hr and then quenched in water. On opening the tubes under dry hexane three separate phases were observed: the dark purplish-grey salt phase, the solid metal phase (potassium metal), and some liquid metal phase, the latter resulting from some reduction of NaF by K producing liquid Na-K alloy. Free metal adhering to the surface of salt lumps was removed by reaction with alcohol. The lumps were then dried, weighed, dissolved in more alcohol and finally water, and the excess metal dispersed throughout the salt was determined by the alkalinity developed in the aqueous solution. Values of 3.0 and 3.1 mole % potassium were found to have dissolved in the molten eutectic salt phase at 860 °C. The figures may be low because of the pretreatment with alcohol for removal of loosely adhering metal. The amount of 3 mole % is believed to be more than ample to suppress corrosive mass transfer under the conditions of the ANP reactor or of the experimental convection loops. (See the thermodynamic estimates above.)

DETERMINATION OF THE HIGH-TEMPERATURE GLASERITE-TYPE CRYSTAL STRUCTURE OF SOME A_2BX_4 COMPOUNDS

R. D. Ellison M. A. Bredig

A Patterson synthesis on the basis of x-ray intensity data obtained with the Weissenberg camera of the projections of the atomic distances onto the *xy* plane of the hexagonal unit cell of glaserite $(K, Na)_2SO_4$, isotypic with αNa_2BeF_4 and αK_2BeF_4, has been accomplished. The interpretation of the resulting vector map, although still incomplete, indicates agreement with the results of a linear Fourier synthesis made earlier in that the *x* and *y* parameters of the Na, K, S, and of the two of the eight oxygen atoms are those given by Gossner.[10] Thus far, no clear indication of the *x* and *y* parameters of the other six

[10] Gossner, *N. Jahrb. Min.* **57A**, 89-116 (1928).

oxygen atoms has been found. The z parameters of the S, O and two of the three K atoms are uncertain.

MISCELLANEOUS X-RAY DIFFRACTION WORK

R. D. Ellison M. A. Bredig

The work performed in connection with problems of various groups of the Chemistry and Chemical Technology Divisions is being reported by the groups concerned. Investigations of technetium and rhenium compounds, of zirconium oxychloride hydrates, thorium hydroxy perchlorate, metal-metal halide preparations, and others are included.

In an attempt to determine possible chain structures in liquid solutions of thorium nitrate in tributyl phosphate (for the Chemical Technology Division) an x-ray monochromater was set up. An exposure of 250 hr with silver K_α radiation produced with only 33 kv peak voltage, the maximum available at present, at 15 to 20 ma, did not produce a satisfactory diffraction pattern of liquid tributyl phosphate. The experiment is being repeated with copper K_α radiation of considerably higher intensity.

INSTRUMENTS

GAMMA-RAY ENERGY RESOLUTION WITH SODIUM IODIDE SCINTILLATION SPECTROMETERS

C. J. Borkowski

Various methods have been tried in the last year for obtaining a stable NaI-TlI scintillation spectrometer with good energy resolution, that is, less than 8% full width at half maximum for a 670-kev photoelectric peak. In early attempts Lucite light pipers were used with aluminum foil as a reflector. Most of the assemblies showed a drift in pulse size over a period of weeks. The following method of crystal preparation and mounting has given long-time surface stability of the NaI-TlI and good energy resolution.

Crystal Preparation and Mounting. In most of the applications cylindrical crystals 1 1/2 in. in diameter and 1 in. in thickness were used. A radius was turned on one face of one crystal to conform to the curvature of the photocathode. This was done on the lathe while the crystal was kept wet with mineral oil. After the radius had been turned, all subsequent operations on the crystal were made in a dry box having a relative humidity of less than 10%. After surplus mineral oil was removed from the crystal with Kleenex, the crystal was ground dry with 180-grit carborundum or emery paper. No polishing was done, since diffuse reflection has given better energy resolution than specular reflection, especially for the larger crystals. All surfaces were rough ground. The crystal was optically coupled to the photocathode with Dow-Corning DC 200 fluid having a viscosity of 60,000 centipoises. However, if the crystal makes a very good fit to the photocathode, Dow-Corning silicone stopcock grease is preferred as the optical coupling medium.

Magnesium oxide is superior to aluminum foil as a reflector, especially for the larger crystals from which 30% more light was obtained. Prior to use, the magnesium oxide should be dried in an oven at 120°C. Figure 22 shows the method used for mounting the crystal on the type-5819 photomultiplier. The magnesium oxide

should be firmly packed between the crystal and the thin aluminum tube. An aluminum housing was slipped over the thin aluminum tube and crystal and sealed to the glass photomultiplier envelope with Apiezon Q. Black Scotch electrical tape was then wrapped around the Apiezon seal, the aluminum housing, and the remainder of the glass envelope to create a light-tight, hermetically sealed assembly. The top of the aluminum housing should be kept thin, about 0.015 inch.

Scintillation spectrometers with this type of seal have given over six months of service with negligible change in resolution or pulse size. Several portable scintillation counters made for uranium ore prospecting for the U. S. Geological Survey were sealed in the same manner; they have given good service.

An alternate method of mounting that does not require machining of the sodium iodide crystal is the following: a flat, glass disk 1 1/2 in. in diameter and about 0.060 in. in thickness (made from photographic glass plate) is cemented to the photocathode with Gelva resin, which is highly transparent and has a melting point of 65°C. The photomultiplier, resin, and glass disk are heated to about 75°C in an oven to obtain optical coupling between the photocathode and glass disk. Heating to this temperature produces no change in the photomultiplier characteristics. The flat end of the 1 1/2- by 1-in., cylindrical, sodium iodide crystal is optically coupled to the flat, glass disk with silicone stopcock grease and mounted as shown in Fig. 22.

Lucite light pipers were not used because long-time surface stability of the sodium iodide could not be obtained with them. No improvement in resolution is obtained by using light pipers when magnesium oxide is used as a reflector.

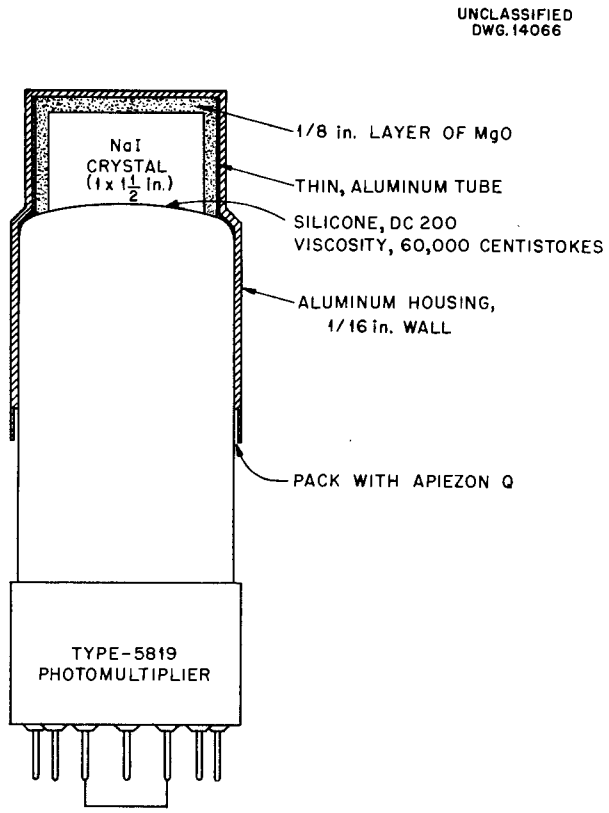

Fig. 22. Sodium Iodide Scintillation Spectrometer Crystal Mounting.

Effect of Crystal Surface Treatment and Reflectors. The effect of surface treatment of the sodium iodide crystal and a comparison of magnesium oxide and aluminum-foil reflectors are shown in Table 24.

If the photomultiplier used gives a width around 9.0%, there is very little difference between solvent-polished and rough-polished crystals when the crystal is relatively small, that is, 1 1/2 by 1 in., and when magnesium oxide is used as the reflector. However, when a photomultiplier that gives excellent resolution, that is, 7.5% width, is used, better results are obtained with rough-polished crystals than with solvent-polished crystals. The preferred procedure is to rough grind all surfaces of the crystal and to use magnesium oxide as a reflector.

Table 24

EFFECT OF SURFACE TREATMENT OF SODIUM IODIDE CRYSTALS AND A COMPARISON OF MAGNESIUM OXIDE AND ALUMINUM-FOIL REFLECTORS

CRYSTAL SIZE	SURFACE TREATMENT	TYPE OF REFLECTOR	RELATIVE PULSE SIZE	HALF WIDTH FOR Cs^{137} (%)	PEAK-TO-VALLEY RATIO	PHOTO-MULTIPLIER TUBE NO.
1½- by 1-in. cylinder	180-grit emery paper	MgO	100	9.5	28:1	650-265
	Acetone solvent polish	MgO	100	9.5	28:1	650-265
	Acetone solvent polish	Al	78	13.0	23:1	650-265
1½- by 2-in. cylinder	180-grit emery paper	MgO	100	9.8	30:1	650-265
	Acetone solvent polish	MgO	79	10.9	31:1	650-265
	Acetone solvent polish	Al	63	13.6	21:1	650-265
1½- by 1-in. truncated cone	180-grit emery paper	Al	90	9.7	38:1	650-265
	600-grit emery paper	MgO	100	9.0	42:1	650-265
	Acetone solvent polish	MgO	100	9.0	42:1	650-265
1½- by 1-in. cylinder	180-grit emery paper	MgO	100	7.5	56:1	152-154
	180-grit emery paper	Al	73	8.6	45:1	152-154
	600-grit emery paper	MgO	100	8.3	48:1	152-154
1½- by 1-in. cylinder with ¾-in. Lucite light piper	600-grit emery paper	MgO	66	9.2	38:1	152-154
	Acetone solvent polish	MgO	100	8.8	37:1	152-154
	Acetone solvent polish	Al	76	10.2	29:1	152-154

Energy Resolution. Figure 23 indicates the kind of resolution (7.2% half width) that is obtained for the 670-kev gamma ray from Cs^{137} with the use of a selected type-5819 photomultiplier and a 1 1/2- by 1-in. crystal. Figure 24 shows that a crystal 1 1/2 by 2 in. gives essentially the same resolution as a crystal half as thick. Using a 3- by 3-in., cylindrical, sodium iodide crystal with magnesium oxide as a diffuse reflector, a 9.0% width was obtained on Cs^{137}, as shown in Fig. 25. The 3- by 3-in. crystal was mounted in somewhat the same manner as that shown in Fig. 22. Since the crystal was much larger than the photocathode of the type-5819 photomultiplier, all crystal surfaces not in contact with the photocathode were surrounded with magnesium oxide.

Figure 26 shows the two Co^{60} gamma rays well resolved. The Compton distribution for the 1.33-Mev gamma ray can be seen on the tail of the 1.17-Mev Compton distribution.

Figures 27 and 28 show the difference in the energy distribution of recoil electrons, pairs, and photoelectrons from the gamma rays of Na^{24}. The data were obtained by using a 1- by 1 1/2-in. and a 3- by 3-in. sodium iodide crystal. Note the absence of an "annihilation escape peak" for the larger crystal and the relatively small Compton recoil contribution. No collimation of the source was used in any of these experiments.

As shown by Morton,[1] the number of electrons actually entering the multiplier can be determined by extrapolating the integral pulse-height distribution curve to zero pulse height. Such a curve was obtained for a type-5819 photomultiplier tube that had a photocathode efficiency of 60 μa per lumen. To ensure that the pulses being counted originated at the photocathode and not at the first or second dynode, a small amount of light was directed on the photocathode. The dark-current pulse background was deducted from the illuminated photocathode pulse distribution to give the curve shown in Fig. 29. The pulse height in volts that correspond to a single photoelectron is found by taking the area under the distribution curve and dividing it by the number of photoelectrons entering the photomultiplier. For these particular conditions, a pulse height of 10.4 v corresponds to a single average electron. Using a 41.6-kev x-ray source and the sodium iodide crystal mounting shown in Fig. 22, an electron energy loss of 200 ev in the crystal releases a single photoelectron from the photocathode of this particular tube.

Figure 30 shows the dark-current pulse background as a function of electron energy loss in the crystal. It can be seen that even at 2 kv a background of only 34 cpm is obtained at room temperature for a good tube.

Variation in Energy Resolution of Photomultipliers. Table 25 shows the variation in energy resolution for 50 photomultiplier tubes (type 5819).

Table 25

VARIATION IN ENERGY RESOLUTION FOR 50 PHOTOMULTIPLIER TUBES

FULL WIDTH AT HALF MAXIMUM FOR Cs^{137} PHOTO PEAK (%)	PERCENTAGE OF TUBES
7 to 8	11
8 to 9	23
9 to 10	18
10 to 12	26
over 12	22

[1] G. A. Morton, *R. C. A. Review* **10**, 525 (1949).

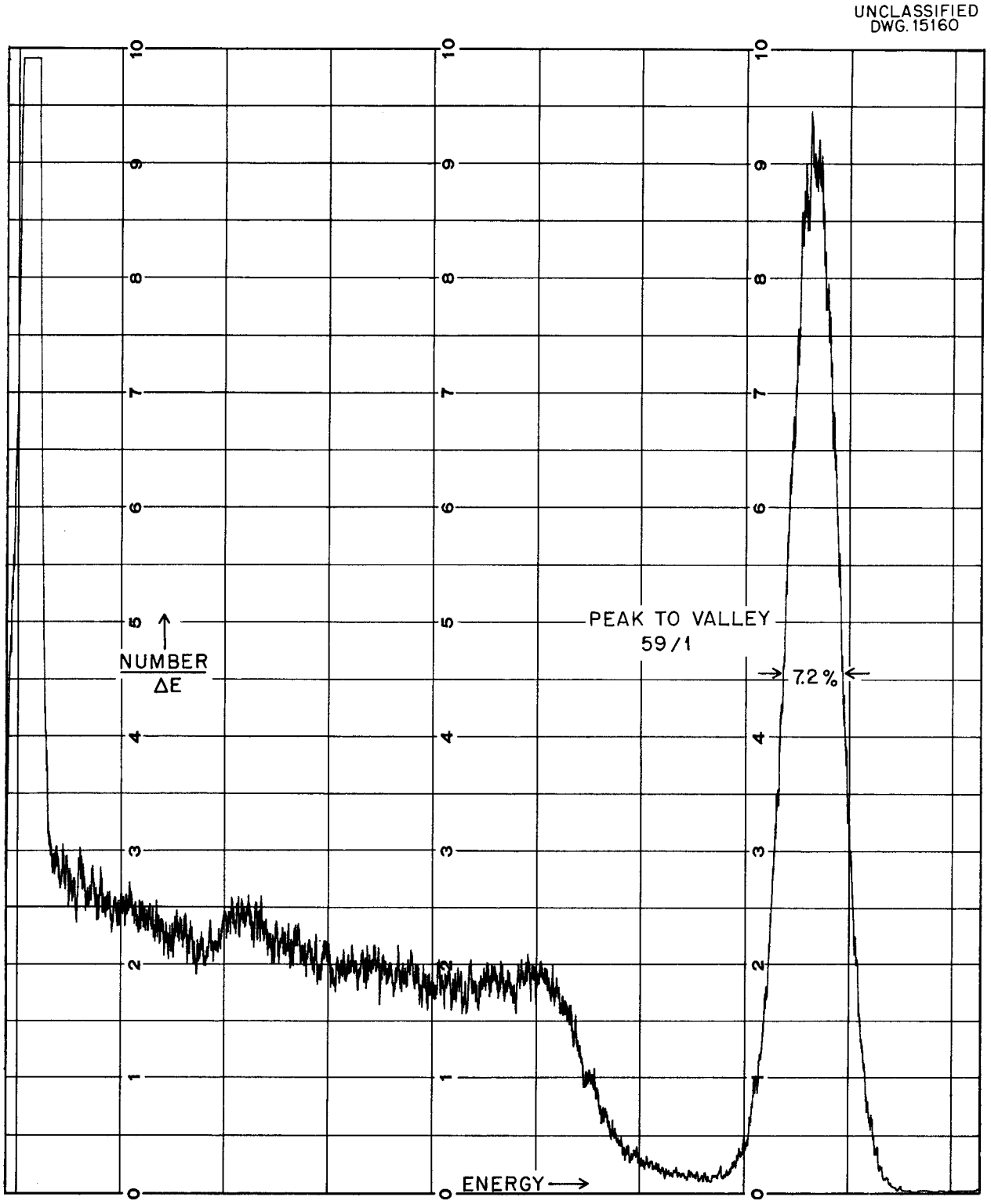

Fig. 23. Resolution of 670-kev Gamma Ray from Cs^{137} Obtained with a Type-5819 Photomultipler and a 1½- by 1-in. Sodium Iodide Crystal.

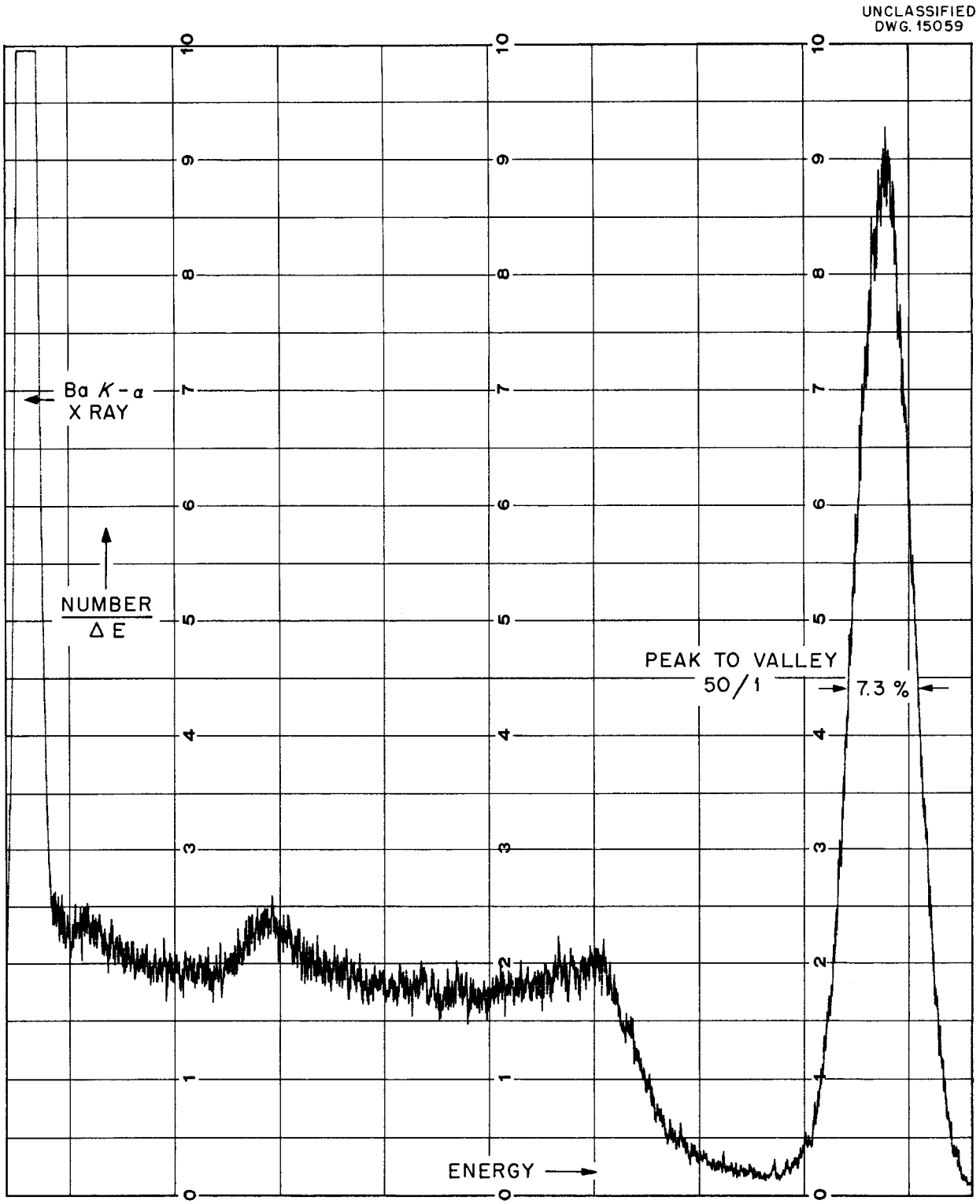

Fig. 24. Resolution of 670-kev Gamma Ray from Cs^{137} Obtained with a Type-5819 Photomultipler and a 1½- by 2-in. Sodium Iodide Crystal.

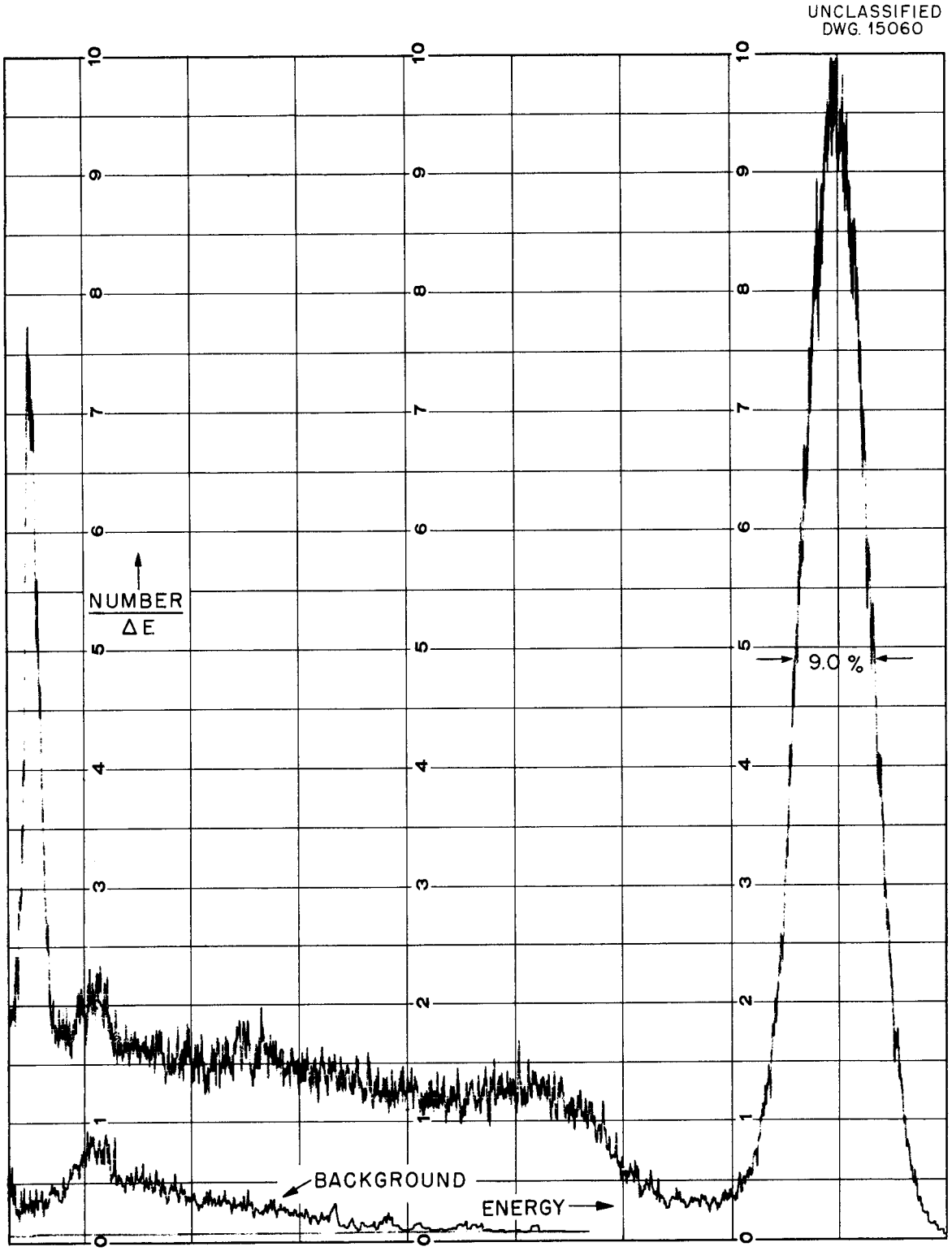

Fig. 25. Resolution of 670-kev Gamma Ray from Cs^{137} Obtained with a Type-5819 Photomultipler and a 3- by 3-in., Cylindrical, Sodium Iodide Crystal with Magnesium Oxide as a Diffuse Reflector.

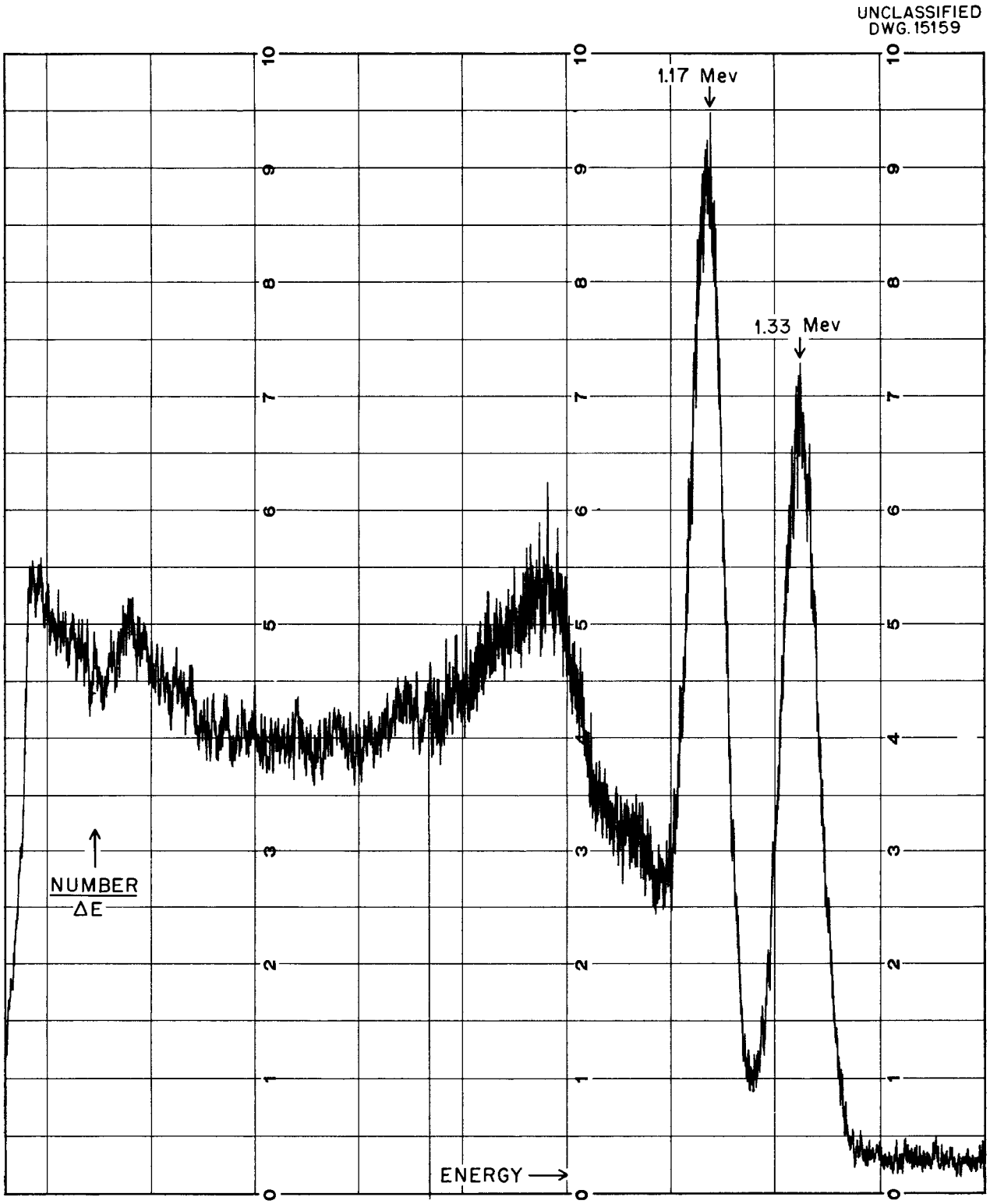

Fig. 26. Resolution of Two Co^{60} Gamma Rays Obtained with a Type-5819 Photomultipler and a 1½- by 1½-in. Sodium Iodide Crystal.

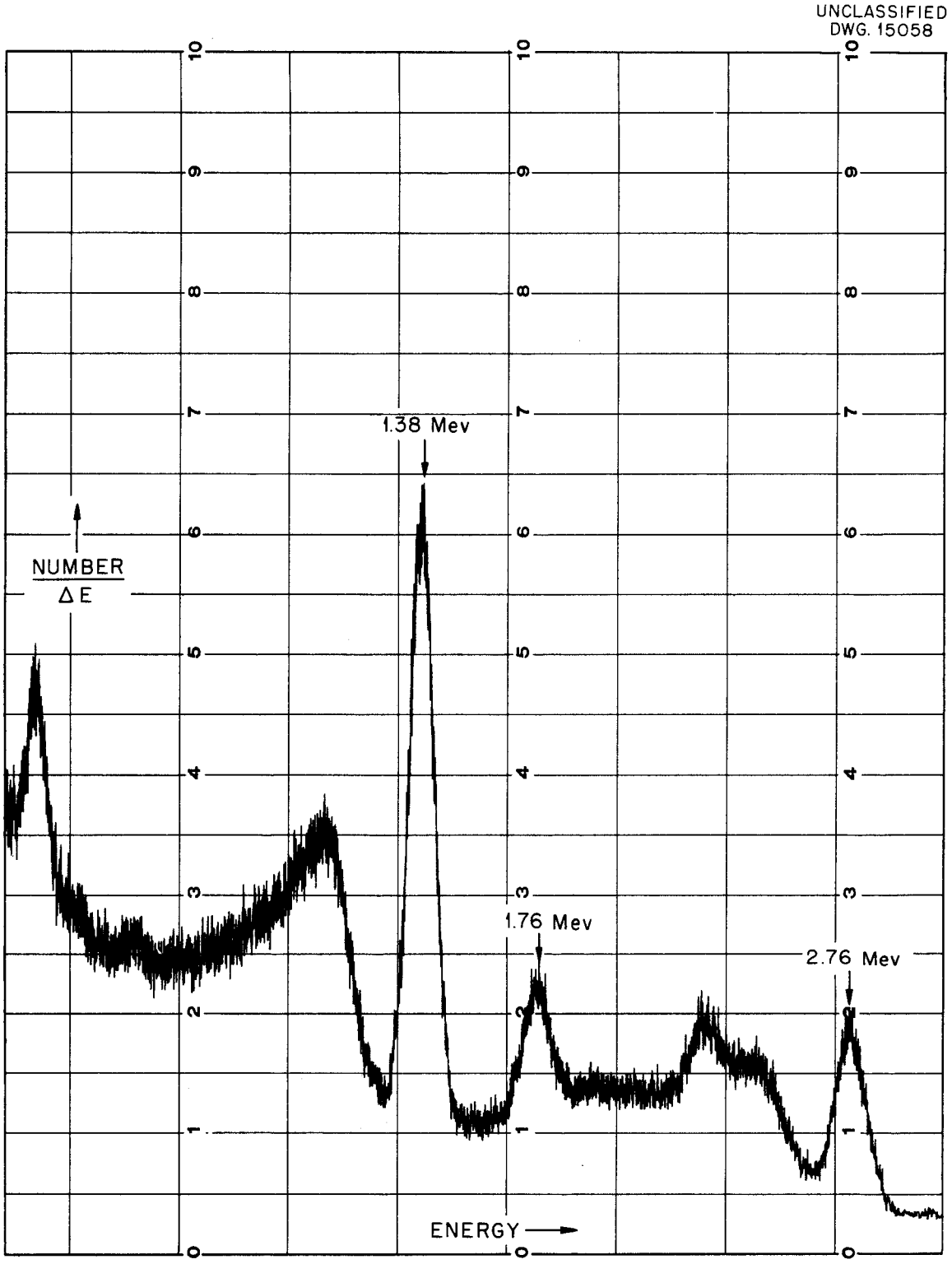

Fig. 27. Resolution of Na^{24} Gamma Rays Obtained with a Type-5819 Photomultipler and a 1- by 1½-in. Sodium Iodide Crystal.

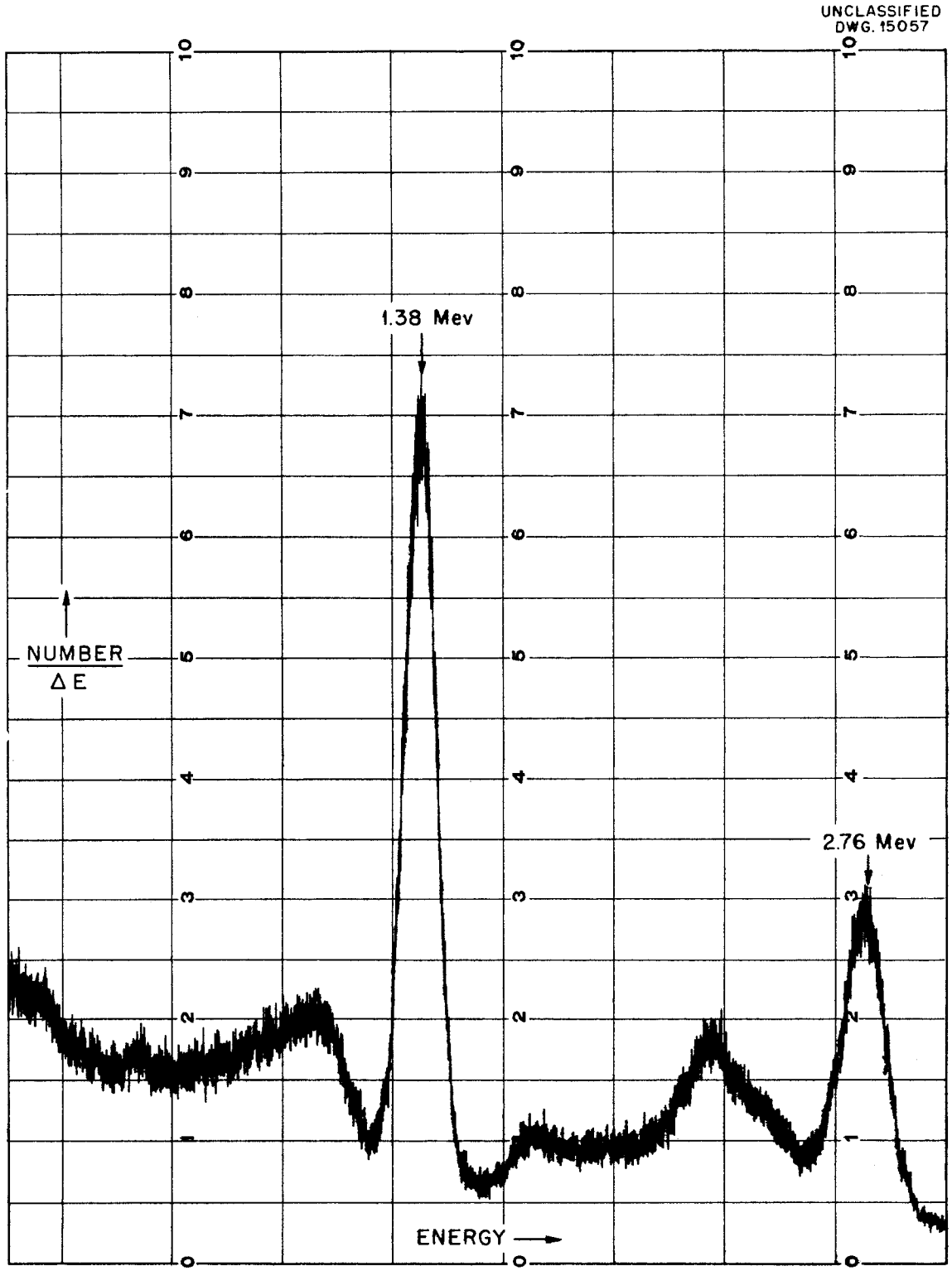

Fig. 28. Resolution of Na^{24} Gamma Rays Obtained with a Type-5819 Photomultipler and a 3- by 3-in. Sodium Iodide Crystal.

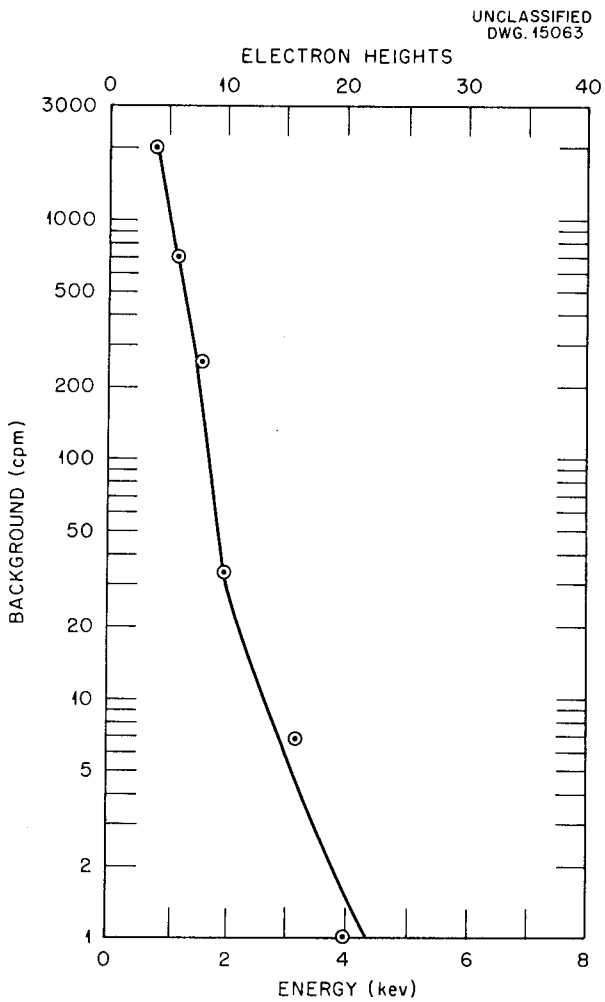

Fig. 29. Dark-Current Pulse Background for Type-5819 Photomultipler at Room Temperature.

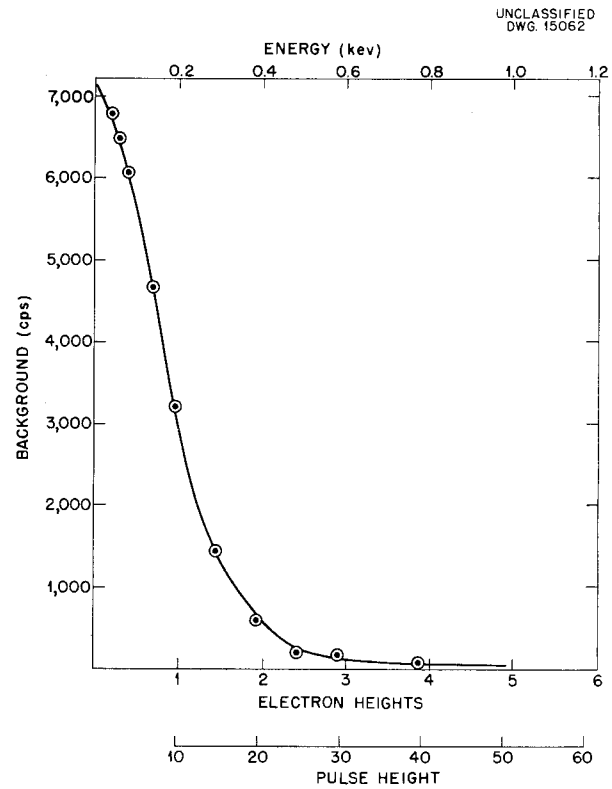

Fig. 30. Pulse-Height Distribution of Photoelectrons from Illuminated Photocathode of the Type-5819 Photomultiplier.

In general, tubes with the highest photocathode efficiency gave the best energy resolution. However, there were exceptions to this rule. In many of the exceptions the photocathode was visually nonuniform. In all the tests a 5-1-1-etc., photocathode to first dynode to second dynode voltage ratio was used. The over-all voltage was 600 to 700 volts.

Variation in Harshaw Sodium Iodide Crystals. Table 26 indicates the variation in pulse size and energy resolution of 1 1/2- by 1-in., cylindrical, sodium iodide crystals.

Variations in energy resolution and pulse size for the various crystals is primarily due to variations in thallium iodide content and foreign inclusions in the crystal that absorb light. The crystals that showed no slight yellowish discoloration, which indicated a low TlI content, invariably gave poor resolution and low light output.

A single-channel sweep type of differential discriminator designed by Fairstein and described in ORNL-1036[2] was used for all pulse height distributions shown.

[2] E. Fairstein, *Chemistry Division Quarterly Progress Report for Period Ending December 31, 1950*, ORNL-1036, p. 65.

Table 26

VARIATION IN PULSE SIZE AND ENERGY RESOLUTION OF 1½- BY 1-in., CYLINDRICAL, SODIUM IODIDE CRYSTALS

CRYSTAL NO.	FULL WIDTH AT HALF MAXIMUM FOR Cs^{137} PHOTO PEAK (%)	PEAK-TO-VALLEY RATIO	RELATIVE PULSE SIZE
1	7.6	52:1	82
2	7.8	46:1	95
3	8.0	35:1	80
4	8.0	45:1	85
5	8.3	42:1	89
6	8.4	37:1	90
7	9.0	37:1	78
8	9.1	40:1	78
9	9.5	28:1	53
10	9.7	38:1	72
11	9.7	29:1	83
12	11.7	32:1	84
13	13.2	16:1	61
14	14.0	13:1	64

The author wishes to express his thanks to R. L. Clark for the preparation and mounting of the crystals and his help in obtaining much of the counting data.

LINEAR AMPLIFIER FOR SCINTILLATION SPECTROMETRY

E. Fairstein

A new amplifier was described in the last quarterly report. The problem of building a practical unit with the desired characteristics has proved to be quite difficult, but success is definitely within sight.

Most of the difficulty has been associated with the problem of getting good overload characteristics. After testing 10 or 12 different circuit configurations, none of which were satisfactory, one was finally evolved and is quite successful. The basic circuit contains four pentodes. The first two are connected as a cathode-coupled pair. When operated in this manner, the input tube can accept large-amplitude signals without drawing grid current. The last two tubes are cascaded as conventional R-C coupled amplifiers. The output signal is fed back to the grid of the second tube in the cathode-coupled pair. The unusual feature of this circuit is that the grid resistors of the last two stages are less than one-tenth the size of the preceding plate-load resistors. There are two beneficial effects: (1) the time constant of the coupling network when

grid current is being drawn is only 5% different from the no-grid-current condition, thus solving the blocking problem, (2) the very-wide bandwidth of two of the stages compared with the third makes possible 20 db of feedback with absolute amplifier stability.

The remaining problems center around the designs of an efficient power output stage and a differential discriminator.

Nuclear Quadripole Resonance Equipment. Approximately half of the last quarter was spent in investigating detector circuits and designing associated amplifiers and oscillators to be used by Livingston in work on nuclear quadripole resonances.

REACTOR CHEMISTRY

HOMOGENEOUS RECOMBINATION OF HYDROGEN AND OXYGEN IN SOLUTIONS

H. F. McDuffie E. L. Compere
H. H. Stone

Studies during the past quarter of the solution recombination of hydrogen and oxygen in the absence of radiation were concerned with the firm evaluation of the catalysis of the process by copper ion, the improvement of techniques and the interpretation of results, and the testing of the possible catalytic effect of other ions. It was found that the diffusion of gases into the solution affected the recombination rate, and mathematical interpretations of the phenomena have been made. The diffusion effect is now removed by mechanical agitation of the apparatus. The geometric term relating the rate of pressure-drop to the solution-recombination rate has been evaluated. Copper remains the best catalyst yet found, but silver ion may be promising under unusual conditions because of a second-order (or higher) behavior and a lower dependence on temperature.

A standard copper-uranyl sulfate aqueous solution was used in much of the work. The composition of the solution is given in Table 27.

Table 27

COMPOSITION OF COPPER-URANYL SULFATE SOLUTION

TEMPERATURE (°C)	$CuSO_4$ (moles per liter)	UO_2SO_4 (g of U per liter)
25	0.0025	40
250	0.00205	32.9

The reactions were carried out by placing a weighed quantity of the solution in a 30-ml, type 347 stainless steel bomb connected to a gas manifold and to a Baldwin strain gage attached to a Brown recorder. Hydrogen at 600 psi and oxygen at 300 psi were charged to the bombs at room temperature. The bombs, in an aluminum-block thermostat, were then heated to reaction temperature, usually 250°C. When agitation was desired, the thermostat blocks containing the bombs were rocked over a ±30-deg angle from the horizontal at 57 cpm; rocking was started after the reaction temperature was reached. Two blocks were available so it was possible to carry out six runs simultaneously.

The bombs and their liquid contents were weighed before and after each run; a loss in weight suggested steam loss due to leaks in the system, whereas a gain in weight showed water formation by recombination. Only those runs where no substantial leak was indicated were used.

The rate of pressure drop was observed as the reaction proceeded. The rate of pressure drop is related to the solution rate of recombination by the following equation, if the solution is assumed to be saturated with hydrogen gas:

$$\frac{d\,(\pi - A)}{dt} = k_\pi = k(\text{soln})\ F_G .$$

where

k_π = logarithmic rate of observed pressure drop (hr^{-1}),

k(soln) = first-order recombination rate constant in solution (hr^{-1}),

π = total observed pressure (psi),

A = partial pressure of inert gases, steam, excess oxygen, etc. (psi),

F_G = geometric factor, moles H_2 in solution at saturation per total moles H_2 in system.

The constant k(soln) is the sum of constants for all recombination reactions.

The geometric term F_G is evaluated on the basis of a material balance, by assuming Henry's law and the ideal gas law and by accounting for the small, but unavoidable, cool, external volumes in connecting tubing, etc.

$$F_G = \frac{\dfrac{V(l)}{V(g)}}{\dfrac{V(l)}{V(g)} + \dfrac{\alpha}{RT} + \dfrac{V(\text{ext})\ \alpha\pi}{V(g)\ R\ T(\text{ext})\ (\pi - Pw)}} .$$

where

$V(l)$ = volume of liquid solution (ml),

$V(g)$ = volume of gas space in bomb (ml),

V(ext) = volume of cool, external gas space in connectors, etc. (ml),

α = Henry's law constant for hydrogen solubility in solution (psia-ml/mole),

R = gas constant, 1206 psi-ml/°K (g mole),

T = absolute temperature (°K),

Pw = steam partial pressure (psi).

The value of the Henry's law constant, α, for gas solubility in the solution is not known exactly. Previously reported[1] data for the solubility of hydrogen in pure water were used in the calculations, and it is believed that they represent a good approximation.

Good straight lines were obtained when the logarithm of net gas pressure ($\pi - A$) was plotted against time, which indicated a first-order behavior of the recombination in terms of gas consumption. The slope of the line measured k_π.

Effect of Type 347 Stainless Steel Surface. An experiment without agitation was carried out at 250°C in which 15 g of the standard 0.0025 *M* Cu plus UO_2SO_4 solution was placed in each of two 30-ml bombs. Twenty five 2-in. pieces of 1/16-in. type 347 stainless steel rod, sufficient to increase the metal surface from 34 to 104 cm^2, were placed in one of the bombs. A solution recombination rate of 1.35 hr^{-1} was observed for the bomb containing the rods, whereas a

[1] H. A. Pray, C. E. Schweickert, and B. H. Minnich, *The Solubility of Hydrogen, Oxygen, Nitrogen, and Helium in Water at Elevated Temperatures*, BMI-T-25 (May 15, 1950).

rate of 1.47 hr^{-1} was found for the bomb that did not contain the rods. The agreement shows that the additional type 347 stainless steel surface did not exert appreciable effect on the recombination rate.

Effect of Hydrogen-Oxygen Ratio. Three experiments at 250 °C in which 5 g of the standard solution was added to 30-ml bombs, with gas pressures of 600 psi of hydrogen and 300 psi of oxygen (25 °C), gave solution-recombination-rate constants of 4.00, 3.80, and 4.07 hr^{-1}, without agitation. Under similar conditions, partial pressures of 400 psi of hydrogen and 400 psi of oxygen (at 25 °C) gave solution-recombination rates of 4.07 and 4.10 hr^{-1}, when calculated on the basis of first-order hydrogen disappearance. This shows that the rate is first order in hydrogen and is not influenced by the hydrogen-to-oxygen ratio at these levels.

Effect of Total Pressure on Reaction Rate. Two-to-one hydrogen-oxygen gas mixtures were placed with 5 g of the standard solution in 30-ml bombs under total pressures of 300, 600, and 1800 psi. The recombination was carried out with rocking agitation; at 248 °C, the solution-recombination rates were 9.57, 9.95, and 9.46 hr^{-1}, respectively, when calculated on the basis of first-order hydrogen disappearance. The agreement shows that the reaction is first order with respect to the gas mixture; since the reaction is independent of oxygen pressure, the belief that the reaction rate is first order in hydrogen is confirmed.

Factors Leading to Diffusional Concept. A number of experiments was carried out in unagitated 30-ml bombs at 250 °C and 600-psi H_2 and 300-psi O_2, and the standard Cu-UO_2SO_4 solution was used, in an effort to establish the geometric factor. The experiments, however, lead first to the recognition of the influence of diffusion on the reaction rate, as shown in Table 28. The experiments were carried out under similar conditions in vertical, unagitated bombs except for two, in which bombs containing 15 g of solution were placed in a horizontal position. Each of the horizontal experiments gave solution-recombination rates of 7.80 per hour. Thus, it was apparent that the solution depth or area of gas-liquid interface influenced reaction rate; the interpretation follows.

The gas phase contained from 90 to 99% of the hydrogen in the system.

Table 28

SOLUTION RECOMBINATION RATE CONSTANTS

AMOUNT OF SOLUTION (g)	TYPE OF BOMB	k_π/F_G (hr^{-1})
5	Vertical	4.01 (mean of five experiments)
10	Vertical	2.42
15	Vertical	1.64 (mean of four experiments)
20	Vertical	0.98
15	Horizontal	7.80 (two experiments)

The recombination in solution was rapid enough to cause a deficiency of dissolved gas deep in the solution that was made up by diffusion of the gas downward from the surface. If the diffusion was sufficiently slow, it controlled the rate.

A mathematical equation may be developed to describe the situation if an element of area perpendicular to the direction of diffusional flow from the liquid surface is considered and the flow is regarded as one dimensional. Dissolved gas may diffuse in and out of the element and may also disappear in the element by recombination that will be regarded as a first-order process. The case in which additional gas is produced, as is true for in-reactor experiments, is discussed in another section of this report (cf., "Gas Kinetics of In-Reactor Radiation Studies"). -p.99

The basic differential equation for such a situation, provided an inexhaustible source of diffusing substance is present,[2] is:

$$\frac{D\ d^2c}{dx^2} - kc = \frac{dc}{dt}$$

where

c = concentration (moles/l),

t = time (sec),

D = diffusion coefficient (cm^2/sec),

x = distance in direction of diffusion (cm),

k = first-order solution reaction rate constant (sec^{-1}).

The solution of a similar equation for heat flow in a rod is given by Jeffries:[3]

Under the boundary conditions that at $X = 0$, $c = c_0$, and at $X = L$, $dc/dx = 0$,

$$c = c_0\ e^{-X\sqrt{k/D}}\left\{\tfrac{1}{2}\left(1 - \operatorname{erf}\frac{X - 2t\sqrt{Dk}}{2\sqrt{Dt}}\right) + \tfrac{1}{2}\ e^{2X\sqrt{k/D}}\left(1 - \operatorname{erf}\frac{X + 2t\sqrt{Dk}}{2\sqrt{Dt}}\right)\right\}$$

where

$$\operatorname{erf} W = \frac{2}{\sqrt{\pi}}\int_0^W e^{-Z^2}\ dZ,$$

which is the error function. The terms within the brackets approach 1 for sufficiently large values of time. In particular, for 15 g of 0.0025 M $CuSO_4$ at 250 °C, in a 30-ml bomb, the steady state will be substantially established before 5% of the gas in the system has disappeared by reaction.

Consequently, it is justifiable within a very good approximation, to regard the steady-state concentration gradient as being set up rapidly with a more or less inexhaustible gas reservoir that slowly drifts away. The gradient maintains an equilibrium with the gas reservoir as recombination occurs. For smaller quantities of solution or slower reaction, the approximation is even better.

Therefore the steady-state solution may be written as

$$c = c_0\ e^{-x\sqrt{k/D}} = c_0\ e^{-x/\sqrt{D/k}},$$

[2] T. K. Sherwood and C. E. Reed, *Applied Mathematics in Chemical Engineering*, McGraw-Hill, New York, 1939, p. 47.

[3] H. Jeffreys, *Operational Methods in Mathematical Physics*, p. 70, Cambridge University Press, London, 1931.

where c_0 is the saturation concentration at the gas-liquid interface. It will be noted that the factor $\sqrt{D/k}$ represents an exponential length in which the concentration drops by a factor $(1/e)$.

A value for the diffusion coefficient D may be estimated from the equation for the diffusion of hydrogen in water at high pressures and temperatures as given by Ipatiev:[4]

$$D = 1.83 \times 10^{-2}\ e^{-5100/RT}\ \text{cm}^2/\text{sec}.$$

At 250 °C, $D = 1.34 \times 10^{-4}$ cm²/sec. The exponential length $(\sqrt{D/k})$ is seen to be 2.1 mm if a representative value of $k = 11.0\ \text{hr}^{-1} = 3.06 \times 10^{-3}\ \text{sec}^{-1}$ is used. At a distance 2.1 mm from the surface, the hydrogen concentration would be $1/e$ = 37% of saturation. It can be seen that in unagitated bombs the greater part of the reaction occurred in the first few millimeters near the surface. The basic rate equation must therefore be corrected by a diffusional factor, F_D = moles of gas actually in solution per moles of gas in solution at saturation.

$$F_D = \frac{c}{c_0} = \frac{\int_0^L c\,dx}{c_0 \int_0^L dx}$$

$$\frac{1}{Lc_0}\int_0^L c_0\ e^{-x/\sqrt{D/k}}\ dx$$

$$F_D = \frac{\sqrt{\frac{D}{k}}}{L}\left(1 - e^{-L/\sqrt{D/k}}\right)$$

and at $L/\sqrt{D/k} > 5$, $F_D \sim \sqrt{D/k}/L$. The rate equation for the interpretation of pressure changes in terms of the recombination reaction rate now becomes

$$\frac{d \ln (\pi - A)}{dt} = k_\pi = k(\text{soln})\ F_G\ F_D.$$

The results in Table 28 are corrected in Table 29.

It thus appears that good agreement between values under various conditions has been obtained by application of the diffusional concept. However, the uncertainties involved in the estimation of F_D make it preferable to eliminate the necessity for the term by experimental means. Accordingly, the heater block was arranged so that it could be rocked at 57 cpm, 30 deg above and below horizontal during the course of the reaction. One run with 5 g of solution and another with 15 g of solution, at 250 °C, gave rate constants of 12.8 and 12.4 hr⁻¹, respectively (the mean of 11 runs gave 11.0 hr⁻¹). Evidently, the rocking technique did remove the diffusional effect, and the geometric term F_G gave consistent results. More rapid shaking (144 one-inch horizontal strokes per minute) did not increase the reaction rate.

Recombination Catalysis by Copper. Seven rocked-bomb experiments using the standard Cu-UO_2SO_4 solution (0.0025

Table 29

CORRECTED SOLUTION RECOMBINATION RATE CONSTANTS

AMOUNT OF SOLUTION (g)	TYPE OF BOMB	k(soln) (hr⁻¹)
15	Vertical	10.2
15	Horizontal	10.0
5	Vertical	10.3

[4] V. N. Ipatiev, Jr. and V. P. Teodorovitch, *J. Phys. Chem.* (*U.S.S.R.*) **10**, 712-718 (1937).

M $CuSO_4$, 40 g of uranium per liter) gave a mean k(soln) = 11.0 hr^{-1} at 250 °C or k_{Cu} = k(soln)/[Cu] = 5340 $(mole/l)^{-1}$ hr^{-1} (range 4990 to 6310).

Four experiments in which the copper concentration was 0.0005 *M* (with UO_2SO_4 at a concentration of 40 g of uranium per liter) gave values of k(soln) = 2.22 hr^{-1} at 250 °C, k_{Cu} = 5420 $(mole/l)^{-1}$ hr^{-1}.

The consistency of the values of k_{Cu} confirms first-order behavior of the reaction with respect to the copper ion. Copper also has been shown to give the same catalytic rate constant in the absence of uranyl sulfate. It may be noted that in-reactor studies at copper concentrations as high as 0.05 *M* also indicate recombination-rate constants consistent with first-order copper behavior.

Experiments at 190 and 220 °C, as well as with 250 °C, permit the reaction-rate constant for copper ion to be expressed

$$k(\text{soln}) = [\text{Cu}]^{1.0} \times 5.9 \times 10^{13} \cdot e^{-24000/RT}\ \text{hr}^{-1}\ (\pm 20\%)\ .$$

Catalysis by Silver. Silver ion may have possibilities as a catalyst at high reactor flux or at low temperatures, according to preliminary indications. The available data on silver catalysis of the recombination, consisting of seven experiments, fit the following empirical equation:

$$k(\text{soln}) = [\text{Ag}]^{2.45} \times 2.2 \times 10^{10} \cdot e^{-9000/RT}\ \text{hr}^{-1}\ (\pm 20\%)\ .$$

An order of 2 with respect to silver might be expected, but there is some doubt that the order is as high as 2.5. Even second-order behavior, however, may permit silver to be of interest under conditions of high flux, and the diminished thermal sensitivity of the reaction could make it attractive at lower temperatures.

Catalysis by Iodine. Iodide ion showed some catalytic activity, appearing as free iodine in the solution at the end of an experiment. Iodine is about 10% as active as copper and exhibits first-order behavior. The data from five runs fit the following empirical equation:

$$k(\text{soln}) = [\text{I}]^{1.0} \times 1.2 \times 10^{11} \cdot e^{-18500/RT}\ \text{hr}^{-1}\ (\pm 20\%)\ .$$

Other Ions. Other ions that were tested and showed no significant activity are Co, Zn, Cd, Pb, As, Li, Rb, Cl, K, Br, and Mg.

The recombination reaction in uranyl sulfate solution alone is not completely understood. It is so slow that the separation of the effects due to uranyl sulfate from other experimental factors has not been completed. Further work is under way.

Proposals for future work include investigation of the uranyl fluoride system and copper catalysis in this system, an extended search for other possible recombination catalysts, and a consideration of the catalytic effect of various ion pairs.

KINETICS OF THE DECOMPOSITION OF HYDROGEN PEROXIDE IN URANYL SULFATE SOLUTIONS

H. F. McDuffie M. D. Silverman

As indicated in the previous quarterly report,[5] consideration of the role of hydrogen peroxide in the fission-fragment decomposition of water, such as would be experienced

[5] J. W. Boyle *et al.*, *Chemistry Division Quarterly Progress Report for Period Ending December 31, 1951*, ORNL-1260, p. 120.

by an operating, aqueous, homogeneous reactor, suggested the need for studies of the thermal decomposition of hydrogen peroxide at various temperatures in solutions of interest.

The studies have been undertaken during the past quarter, by employing standard experimental techniques in kinetics. Analyses for hydrogen peroxide are made with standard ceric sulfate, using a back titration with ferrous sulfate, and orthophenanthroline as the indicator. Solutions of the reagents as low as 0.002 *N* have been employed satisfactorily in the presence of uranyl sulfate. Experiments thus far have been conducted in 0.0045 to 0.17 *M* uranyl sulfate solutions at 78°C, in which the initial hydrogen peroxide concentration has been varied from 4×10^{-4} to 5×10^{-3} *N*.

The pertinent data are given in Table 30, and the results of several typical experiments are shown in Fig. 31. Examination shows that the rate is first order with respect to peroxide concentration and apparently independent of uranyl sulfate concentration from 0.0175 to 0.176 *M*. The rate constants, *k*, in the fourth

Table 30

DECOMPOSITION OF HYDROGEN PEROXIDE IN AQUEOUS URANYL SULFATE SOLUTIONS AT 78.0°C

EXPERIMENT	UO_2SO_4 CONCENTRATION (*M*)	STARTING H_2O_2 CONCENTRATION ($M \times 10^3$)	k ($sec^{-1} \times 10^4$)	REMARKS
A	0.162	3.84	4.70	
B	0.162	4.37	5.07	
C	0.162	4.32	4.78	
D	0.176	1.02	4.60	
E	0.162	4.95	4.90	
F	0.0486	4.08	6.00	Supersaturated solution
G	0.0486	4.60		Heavy precipitate
H	0.0497	3.80	6.39	Small precipitate
J	0.0497	4.02	5.97	Small precipitate
K	0.0526	1.24	4.94	
L	0.0526	1.27	5.05	
M	0.0176	0.976	5.29	
N	0.0176	1.14	5.30	
O	0.0175	1.37	5.26	
P	0.0178	0.496	4.09	
Q	0.0178	0.420	4.07	
R	0.0045	0.380	3.35	
S	0.0045	0.463	4.26	
AA	0	5.19	0.0685	
BB	0	4.72	0.0748	

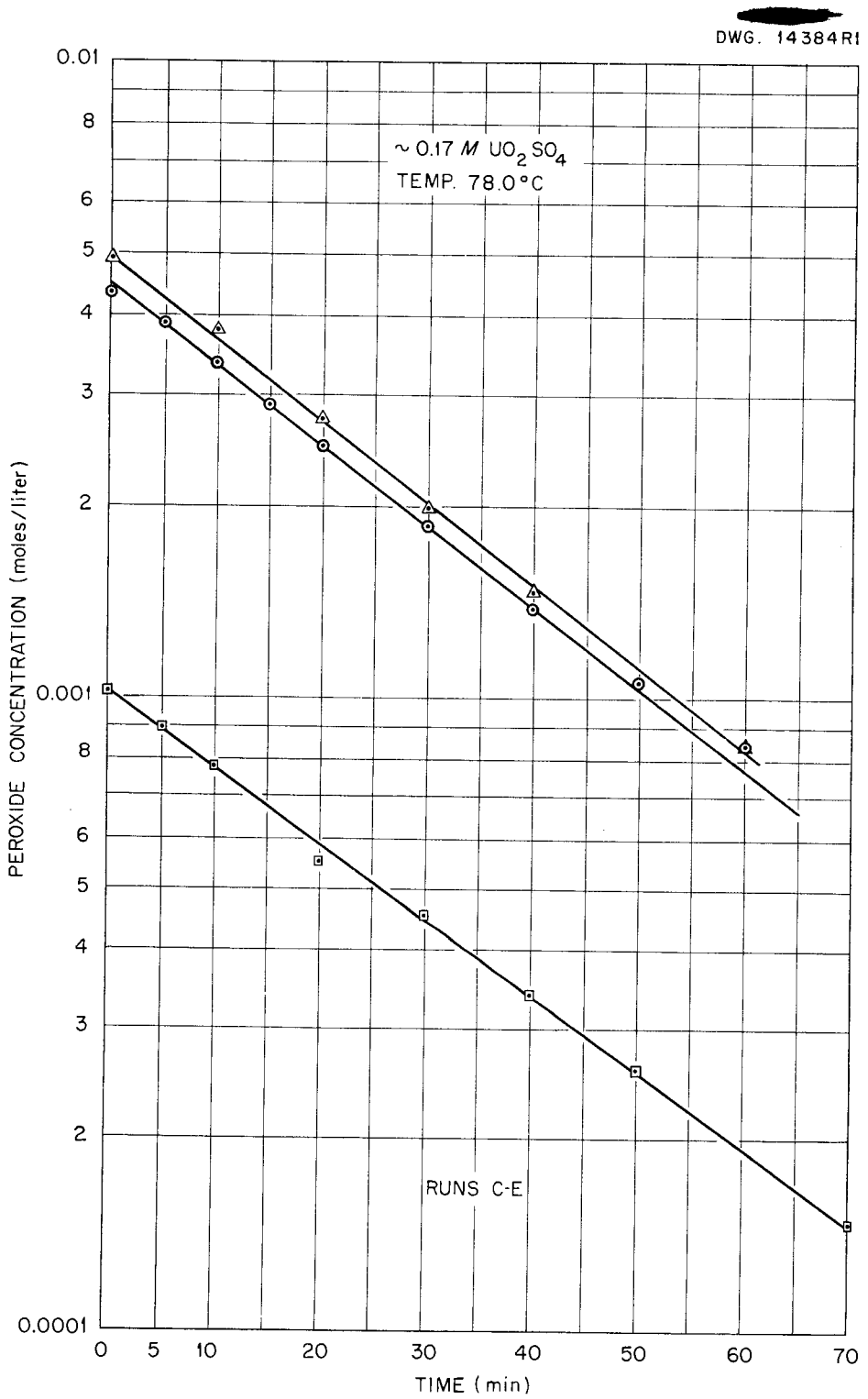

Fig. 31. Decomposition of Hydrogen Peroxide in Uranyl Sulfate Solutions.

column of the table have been calculated on that basis by using the equation

$$\frac{d\,(H_2O_2)}{dt} = k(C_{H_2O_2}) .$$

The large difference between rates of decomposition in water and in uranyl sulfate solutions suggests catalysis by uranyl sulfate or its ions. Since k is independent of uranium concentration above 0.0045 M, the activity of the reacting species may have become constant. The phenomenon is being compared with a similar lack of dependence on concentration for electrical conductivity and the catalysis of the recombination of hydrogen and oxygen, which is currently being investigated.

During the next quarter, larger quantities of pure uranyl sulfate will be prepared for use in studying the effects of changes in pH, uranyl and sulfate ion concentrations, and temperature.

RADIATION CHEMISTRY OF AQUEOUS REACTOR SOLUTIONS

H. F. McDuffie J. W. Boyle
W. F. Kieffer

Uranyl Sulfate. The initial rate of gas production for pure uranyl sulfate solutions has been determined as a function of temperature, concentration, and isotopic enrichment. The work is almost completed and has been reported.[5,6] To summarize briefly, the rate of gas production under constant neutron flux decreases with an increase in uranyl sulfate concentration and a decrease in enrichment (U^{235} content). The rate of gas production is independent of temperature between 30 and 250°C.

The reason for the decrease in G (molecules of H_2 produced per 100 ev expended in solution) with an increase in uranyl sulfate concentration (1.7 at 1 g of uranium per liter to 0.5 at 800 g of uranium per liter) has been the object of some thought. In order to determine whether the change is related to a characteristic of the uranyl ion or to a less specific property, such as mass of solute, two solutions were made up consisting of UO_2SO_4 and Cs_2SO_4. Cs_2SO_4 was chosen for two reasons: (1) since Cs is an alkali metal, it would be expected to behave as an inert material; (2) it is noted that the ratio of Cs to SO_4 in Cs_2SO_4 is 265.8 to 96 and the ratio of UO_2 to SO_4 in UO_2SO_4 is 267 to 96, so that for each SO_4 ion the cation mass is very nearly equal. By comparing columns 3 and 4 in Table 31, it is found that G decreases with an increase in uranium concentration but is not changed when an equivalent mass is added as Cs^{++} ion. The experiment demonstrates that the decrease in G with increase in uranyl sulfate concentration is specific for uranyl ion and does not depend upon mass of solute cation.

The interest in Cu^{++} ion as a possible pressure inhibitor in homogeneous reactors prompted an examination of solutions of UO_2SO_4 with added Cu^{++} ion to determine whether the copper depressed the rate of gas formation. It was found that Cu^{++} does not decrease the rate of gas formation but rather increases the rate slightly, as would be predicted from previous data.[7] The decrease in equilibrium pressure over fissioning UO_2SO_4 solutions containing copper is caused by a chemically induced back reaction – the recombination of hydrogen and oxygen gases to form water. Table 32 shows that the gas production is actually

(6) H. F. McDuffie *et al.*, *Homogeneous Reactor Project Quarterly Progress Report for Period Ending November 15, 1951*, ORNL-1221, p. 117.

(7) A. O. Allen *et al.*, *Decomposition of Water and Aqueous Solutions Under Pile Radiation*, ORNL-130 (Oct. 11, 1949).

Table 31

EFFECT OF URANYL ION ON *G* VALUES FOR H_2 PRODUCTION

COMPOSITION OF SOLUTION			
Uranium Concentration 93% Enriched (mg/ml)	Cs_2SO_4 Concentration (mg/ml)	*G* (observed)	*G* FOR UO_2SO_4 SOLUTION (Concentration equivalent to column 1 plus column 2)
4.03	0	1.66	1.66
6.74	155.3	1.63	1.32
6.23	324.2	1.64	1.06

Table 32

***G* VALUES FOR H_2 PRODUCTION AS INFLUENCED BY Cu^{++} IN UO_2SO_4 SOLUTION CONTAINING 40 g OF URANIUM PER LITER, 93% ENRICHED**

Cu CONCENTRATION (*M*)	TEMPERATURE (°C)	*G* VALUE
0	120	1.52
0.05	120	1.61
0.03	120	1.56
0.03	190	1.55
0.03	210	1.54
0.03	210	1.56 (type-347 stainless steel present)

increased by adding Cu^{++}. The experiments were carried out in silica ampoules, with chromate-pretreated stainless steel present in the last experiment. Two ampoules were prepared with the stainless steel present, one with the metal completely submerged and the other with half of the metal in the gas phase and half in the solution. The two ampoules gave the same results.

Uranyl Fluoride. The *G* values for uranyl fluoride solutions have been measured in a manner identical to that employed for the UO_2SO_4 studies. The concentration range was from 4 to 406 mg of uranium per milliliter. The same temperature (120 °C) and the same relative enrichments were maintained as were used in the comparable UO_2SO_4 investigations. The data are summarized in Table 33 and Fig. 32. They are to be compared with Table 31 (this report) and with Fig. 29 of ORNL-1260.[5] It will be noted that although the same trend is apparent in the decrease of *G* with increasing concentration of UO_2^{++} ion, the effect is less in the presence of F^- ion than in the presence of equivalent amounts of $SO_4^=$ ion.

Table 33

G VALUES FOR H_2 PRODUCTION FROM AQUEOUS UO_2F_2 SOLUTIONS IRRADIATED AT 120 °C

G	TOTAL URANIUM (mg/ml)	U^{235} (mg/ml)	ENRICHMENT (%)	RATIO OF FISSION ENERGY TO TOTAL ENERGY
1.63	4.25	3.96	93.2	0.959
1.58	40.1	37.3	93.2	0.995
1.36	118.8	37.1	31.3	0.995
1.11	272.1	37.2	13.7	0.995
1.00	405.7	42.3	10.4	0.996

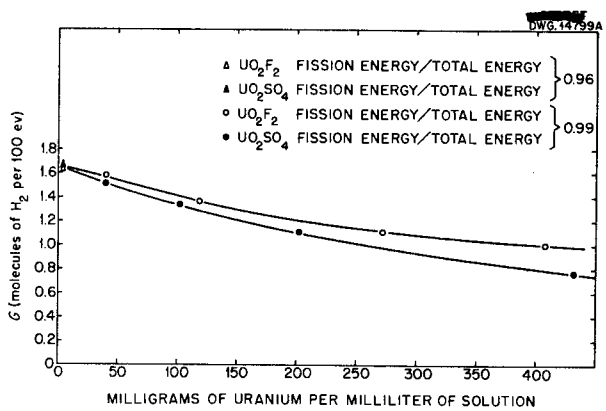

Fig. 32. Variation of G with Uranium Concentration for Enriched Uranyl Solutions.

GAS KINETICS OF IN-REACTOR RADIATION STUDIES

C. H. Secoy
H. F. McDuffie
D. M. Richardson
L. F. Woo
F. H. Sweeton
J. W. Boyle
J. F. Manneschmidt
W. E. Hill
W. C. Yee
A. W. Smith

For purposes of discussion, a closed system containing a water solution of fissionable atoms and a vapor space and exposed to a thermal neutron flux is assumed. Along the fission-recoil tracks, water molecules are dissociated to form free radicals that, in turn, may interact to re-form H_2O molecules or to form hydrogen and hydrogen peroxide molecules. The hydrogen peroxide will thermally decompose to yield oxygen and water. The over-all result is the production of a 2:1 hydrogen-oxygen gas mixture.

The rate of production of hydrogen in such a system has been shown to be independent of temperature (or very nearly so) and proportional to the fission density in the solution. The yield is often expressed by the quantity G, defined as the number of molecules of hydrogen produced per 100 ev of absorbed energy. The production at a particular flux, ϕ, and for a solution containing $[U^{235}]$ moles of uranium-235 per liter can be expressed by

$$k = \frac{\phi\, \sigma_{235}\, E\, [U^{235}]\, G}{100} \quad \text{moles } H_2 \text{ per liter per sec} \qquad (1)$$

where E = 168 Mev, the fission recoil energy per fission.

Simultaneously with the production of gas, and apart from the recombination of free radicals in the fission-recoil track, a molecular recombination of hydrogen and oxygen occurs, the rate depending on the temperature of the system, the concentration of hydrogen in solution, and the presence of certain ions that serve as homogeneous catalysts. The rate of recombination of hydrogen is given by the expression

$$\frac{-d\ [H_2]}{dt} = k(\text{soln})\ [H_2] \qquad (2)$$

wherein the bracketed quantities indicate concentrations in moles per liter and k(soln) is the solution molar rate constant. If the assumption is made that there are no concentration gradients in the solution, Eqs. 1 and 2 combine to give the net change of hydrogen concentration as,

$$\frac{d\ [H_2]}{dt} = k - k(\text{soln})\ [H_2]\ . \qquad (3)$$

From a knowledge of the solubility of hydrogen and oxygen and the relative gas-to-liquid volumes in the system, it is possible to relate the hydrogen concentration to the partial pressure of hydrogen and oxygen, and Eq. 3 can be written as,

$$\frac{dP}{dt} = k_1 - k_2 P\ . \qquad (4)$$

Equation 4 is the simplified equation, the form that has been proved to be correct by the data from a number of in-reactor experiments. According to Eq. 4, a plot of dP/dt vs. P should yield a straight line, the intercept on the dP/dt axis being the production rate, k_1, and the slope of the line representing the recombination rate constant, k_2. The effect of increased temperature (or any other factor that accelerates the recombination) is to increase the slope of the lines. If, on the other hand, factors affecting the recombination rate remain the same but the production rate is changed, for example, by precipitation of uranium from solution, the slope of the line will remain unaltered but the dP/dt intercept will change. The intercept on the P axis ($dP/dt = 0$) gives the steady-state pressure of the system (Fig. 33).

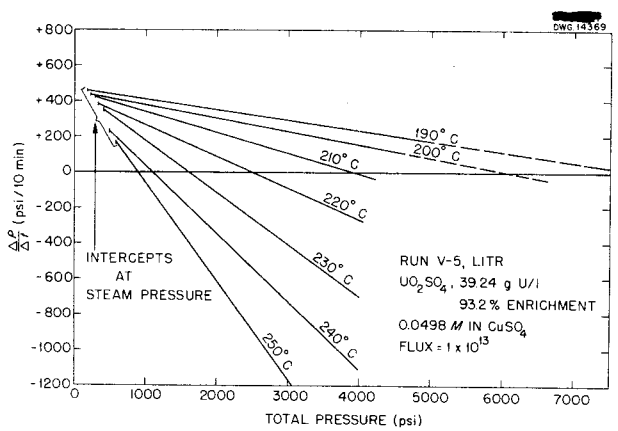

Fig. 33. Relationship Between $\Delta P/\Delta t$ and P at Various Temperatures.

Equation 4 has been found to be correct in its general form and the effects mentioned are in agreement, at least qualitatively, as described. However, before a quantitative treatment is possible, the details of Eq. 4 must be examined more carefully: first, the procedure in transforming Eq. 3 to Eq. 4 and second, the effect of concentration gradients as a result of finite diffusion rates.

Assuming that the gas obeys the ideal gas law, Henry's law, and Dalton's

law, it is possible to write for each gas:

$$N_i(g) = \frac{P_i \; V(g)}{RT}, \tag{5a}$$

$$N_i(l) = \frac{P_i \; V(l)}{\alpha_i}, \tag{5b}$$

$$P = P_{H_2} + P_{O_2}. \tag{5c}$$

Also, because 2 moles of hydrogen are produced (or recombined) with 1 mole of oxygen,

$$N_{H_2} = 2N_{O_2}, \tag{6a}$$

$$\frac{dN_{H_2}}{dt} = 2\frac{dN_{O_2}}{dt}. \tag{6b}$$

By multiplying Eq. 3 by $V(l)$, the liquid volume, and since the assumption is made that all reaction takes place in the liquid phase,

$$\frac{dN_{H_{2(l)}}}{dt} = \frac{dN_{H_2}}{dt} = V(l)\;k - k(\text{soln})\;N_{H_{2(l)}}. \tag{7}$$

From Eqs. 5a and 5b:

$$N_{H_2} = N_{H_{2(g)}} + N_{H_{2(l)}} = \left(\frac{V(g)}{RT} + \frac{V(l)}{\alpha_{H_2}}\right) P_{H_2},$$

$$N_{O_2} = N_{O_{2(g)}} + N_{O_{2(l)}} = \left(\frac{V(g)}{RT} + \frac{V(l)}{\alpha_{O_2}}\right) P_{O_2}. \tag{8}$$

Taking the derivative,

$$\frac{dN_{H_2}}{dt} = \left(\frac{V(g)}{RT} + \frac{V(l)}{\alpha_{H_2}}\right)\frac{dP_{H_2}}{dt} = Q_{H_2}\frac{dP_{H_2}}{dt},$$

$$\frac{dN_{O_2}}{dt} = \left(\frac{V(g)}{RT} + \frac{V(l)}{\alpha_{O_2}}\right)\frac{dP_{O_2}}{dt} = Q_{O_2}\frac{dP_{O_2}}{dt}. \tag{9}$$

From Eq. 5c:

$$\frac{dP}{dt} = \frac{dP_{H_2}}{dt} + \frac{dP_{O_2}}{dt}. \tag{10}$$

Proper substitutions from Eqs. 6b, 9, and 10 into Eq. 7 yield:

$$\frac{dP}{dt} = \left(\frac{1}{Q_{H_2}} + \frac{1}{2Q_{O_2}}\right) \cdot \left[V(l)\;k - k(\text{soln})\;N_{H_{2(l)}}\right]. \tag{11}$$

Partial expansion of Eq. 11 and further substitutions from Eqs. 5c, 6a, and 8 yields,

$$\frac{dP}{dt} = \left(\frac{1}{Q_{H_2}} + \frac{1}{2Q_{O_2}}\right) \cdot V(l)\;k - \frac{V(l)\;P\;k(\text{soln})}{\alpha_{H_2}\;Q_{H_2}}. \tag{12}$$

An expression for k was given in Eq. 1, and k(soln) can be expressed as equal to k_{Cu} [Cu] when the experiment is carried out in the presence of cupric ions. All other quantities in Eq. 12 are known constants or can be determined in the course of an experiment. Values of Henry's constant,

α, have not been determined for the salt solution but have been measured for hydrogen and oxygen in water.

The next consideration is the effect of diffusion on the rate processes. For simplification any radial-diffusion gradients (in a cylindrical bomb) will be neglected, and the x axis is made to lie along the axis of the cylinder. In a column element of unit cross section and depth dx, four processes are occurring. In time dt they are:

1. production $= K\ dx\ dt$

2. diffusion in $= -D \dfrac{dc}{dx}\ dt$

3. diffusion out $= -D \left[\dfrac{dc}{dx} + d\ \dfrac{dc}{dx} \right] dt$

4. reaction $= \dfrac{-d(c\ dx)}{dt}\ dt = kc\ dx\ dt$.

The net over-all change in moles of hydrogen is given by the combination of the four terms integrated over the length of the bomb, L, and multiplied by the cross-sectional area, A, giving

$$\frac{dN_{H_2}}{dt} = A \int_0^L K\ dx + D\ d\ \frac{dc}{dx} - kc\ dx. \qquad (13)$$

If c were not a function of x – if there were no diffusion gradient for example – Eq. 13 would readily integrate to give Eq. 12. In order to express c as a function of x, consider the steady-state case

$$K\ dx + D\ d\ \frac{dc}{dx} - kc\ dx = 0\ . \qquad (14)$$

Dividing by dx and transposing gives

$$D \frac{d^2 c}{dx^2} = kc - K\ . \qquad (15)$$

Defining y as the difference in concentration from the steady-state concentration, $y = c - K/k$, and substituting, the equation becomes,

$$\frac{d^2 y}{dx^2} = \frac{k}{D}\, y$$

and the solution is

$$y = A_1\ e^{-x\sqrt{k/D}} + A_2\ e^{x\sqrt{k/D}}\ . \qquad (16)$$

At $x = 0$ (the liquid-gas interface) $y = y_0$; therefore,

$$y_0 = A_1 + A_2\ . \qquad (17)$$

A second boundary condition results from the fact that regardless of whether the system is above or below the steady state, y must always decrease with increasing x. Therefore, A_2 must be zero and,

$$y = y_0\ e^{-x\sqrt{k/D}} = y_0\ e^{-x/\lambda}\ . \qquad (18)$$

A diffusion factor, F_D, is defined by,

$$F_D \equiv \frac{y}{y_0} = \frac{\int_0^L y\ dx}{\int_0^L dx} = \frac{\lambda}{L}(1 - e^{-L/\lambda})\ , \qquad (19)$$

in which y is the mean effective value of the concentration difference from steady-state concentration, and λ is the distance in which the concentration falls off by a factor e and can be

referred to as the diffusion length. When L is large in comparison with λ, which is true in this application, $F_D \cong \lambda/L$.

The relation between y and the partial pressure of hydrogen is given by,

$$P_{H_2} = \alpha_{H_2} C_0$$

$$P_{H_2} - P_{H_{2(ss)}} = \alpha_{H_2}(C_0 - C_{(ss)}) = \alpha_{H_2} y_0 . \quad (20)$$

Returning now to the nonsteady-state case,

$$\frac{dN_{H_2}}{dt} = \int_0^L -V(l)\ k(\text{soln})\ y\ dx . \quad (21)$$

The steps in solving Eq. 21 and converting to the pressure variable are completely analogous to those given above and will not be repeated. The final equation is,

$$\frac{dP}{dt} = 36\ \phi\ \sigma_f\ E\ [U^{235}]\ V(l)\ G\ F_D \left(\frac{1}{Q_{H_2}} + \frac{1}{2Q_{O_2}}\right) - \frac{V(l)\ F_D}{\alpha_{H_2}\ Q_{H_2}} P \sum k_i C_i^{n_i} . \quad (22)$$

The molar-rate constant for the ith ion is k_i, the concentration is C_i, and the order of the recombination reaction for the ith ion is n_i. The quantity is summed for all ionic species that have an effect on the reaction rate. All other quantities in Eq. 22 have been defined. It should be pointed out that in the derivation of expression 19 for F_D, entrance effects at the liquid-gas interface have been ignored and transient effects and eddy diffusion have been neglected. Equation 19 can hardly be expected to hold well in the in-reactor experiments in which much internal heating occurs. In fact, the experiments indicate that the mixing is about ten times better than that given by simple diffusion.

Equation 22 can be applied to the pressure data obtained from in-reactor irradiation studies for two purposes. First, the solution molar-rate constant can be calculated from the steady-state pressure, and, second, the gas-production rate can be calculated from the extrapolated dP/dt value at $P = 0$, provided the diffusion factor is known.

Cupric-Ion Molar-Rate Constant. The cupric ion has been shown to have a very high specific-rate effect in comparison with uranyl ion, and in the experiments to be described the effect of the uranyl ion can be neglected. At the steady state $dP/dt = 0$, upon rearrangement and cancellation of common terms Eq. 22 yields,

$$k_{cu} = Q_{H_2}\left(\frac{1}{Q_{H_2}} + \frac{1}{2Q_{O_2}}\right) \frac{36\ \phi\ \sigma\ E\ [U]\ G\ \alpha_{H_2}}{[Cu]\ P_{(ss)}} . \quad (23)$$

In the temperature range under consideration (190 to 260°C), the solubilities of H_2 and O_2 are nearly the same and no serious error is introduced by setting $Q_{H_2} = Q_{O_2}$, giving

$$k_{Cu} = \frac{54\ \phi\ \sigma\ E\ [U]\ G\ \alpha_{H_2}}{[Cu]\ P_{(ss)}}, \text{ hr}^{-1} . \quad (24)$$

Table 34 gives the experimentally determined steady-state pressures for four experiments, two of which were carried out in the graphite reactor and two in the LITR. The copper

Table 34

CUPRIC ION MOLAR RATE CONSTANT

TEMPERATURE (°C)	α_{H_2} (psi/mole/l)	$P_{(ss)}$ (psia)	k_{Cu} (hr^{-1})	LOCATION AND CONDITIONS OF EXPERIMENT
Experiment 363				
194	15,000	2000	495	Hole 12; graphite reactor
209	13,200	860	1010	$\phi = 5 \times 10^{11}$
229	10,800	300	2380	[U] = 0.16 *M*
239	9,800	185	3500	[Cu] = 0.009 *M*
249	8,700	103	5580	
259	7,750	60	8530	
Experiment 371				
210	13,100	3400	1140	Hole 60; graphite reactor
215	12,500	2420	1530	$\phi = 5 \times 10^{11}$
222	11,700	1806	1920	[U] = 0.16 *M*
226	11,250	1448	2310	[Cu] = 0.002 *M*
230	10,800	1148	2800	
236.5	10,000	894	3320	
241	9,530	649	4360	
Experiment V-5				
190	15,400	7668	467	Hole C-44; LITR
200	14,300	5855	567	$\phi = 1 \times 10^{13}$
210	13,100	3598	846	[U] = 0.1557 *M*
220	11,900	2140	1290	[Cu] = 0.0498 *M*
230	10,800	1205	2080	
240	9,650	595	3770	
250	8,600	304	6570	
Experiment V-7				
210	13,100	4873	1060	Hole C-44; LITR
220	11,900	3104	1510	$\phi = 1 \times 10^{13}$
230	10,800	1414	3000	[U] = 0.158 *M*
240	9,650	890	4260	[Cu] = 0.0299 *M*
250	8,600	428	7890	
260	7,650	305	9850	
Out-of-Reactor Experiments				
190			244*	
220			1349**	
250			5365***	

*Mean of 3 experiments, range 226 to 258.

**Mean of 3 experiments, range 1246 to 1450.

***Mean of 11 experiments, range 4860 to 6310.

concentration differed in the experiments from 0.002 M in experiment 371 to 0.05 M in experiment V-5. The calculated values for k_{Cu}, also given in Table 34, are plotted on semilogarithmic paper against $1/T$ in Fig. 34. Values of k_{Cu} at three temperatures obtained from out-of-reactor experiments are also shown. The calculated energy of activation is 23 kcal, and k_{Cu} can be expressed as a function of temperature by,

$$2.3 \log k_{Cu} = \frac{-23,000}{RT} + 30.88 \ . \quad (25)$$

Although there is considerable scatter to the points in Fig. 34, the data are quite satisfactory in view of the experimental difficulties and the approximations involved in the calculation. The values of α_{H_2} were obtained from BMI-T-25[1] and apply to the solubility of hydrogen in water. The values of k_{Cu} must be corrected when data for the solubility in the appropriate solution become available.

The fact that the three points from out-of-reactor experiments all lie below the line in Fig. 33 is not believed to be evidence for the existence of a radiation effect on the reaction rate, since they also lie within the range of variation of the in-reactor results. In the calculation of k_{Cu} from the out-of-reactor experiments, the application of the geometric correction factor, Q, is necessary, and the diffusion factor, F_D, must either be applied or diffusion effects eliminated by adequate agitation of the vessel. Some uncertainty is involved in the Q factor when estimating the volume of the external system. During the experiments the bombs were agitated and no diffusion factor was used. Therefore there remains a question as to whether the agitation was adequate to ensure complex mixing. The degree of agreement of the results with the in-reactor data, however, indicates that neither of the factors is seriously in error.

Diffusion Factor, F_D. As previously mentioned, if a true value of the "mixing coefficient" is available for an in-reactor experiment, values of G, the gas production can be calculated from the dP/dt value at $P = 0$. Equation 19 has been derived for the diffusion factor from simple diffusion theory, but there remains the question of whether simple diffusion can account for the actual mixing obtained in an experiment. Since a dependable value of G has been obtained by other experiments, a comparison of theoretically calculated diffusion factors (Eq. 19) and experimentally determined mixing factors appears in order.

Table 35 gives the values of the required mixing factor, designated as F_D^*, for experiments V-5 and V-7 calculated from the dP/dt intercepts by using G = 1.5 molecules H_2 per 100 ev. Values of F_D calculated by Eq. 19 are given for comparison. The only available data for D, the diffusion coefficient, are those of Ipatiev and Teodorovich[4] for the diffusion of gases in water and were used in the calculation of F_D. Values of the mixing factor and the diffusion coefficient as a function of temperature are shown graphically in Fig. 35.

The conclusions from these calculations are: (1) mixing is actually about ten times better than that resulting from simple diffusion and is about 70% complete at 200°C, becoming less complete at higher temperatures; and (2) the mixing factors other than pure diffusion are relatively independent of temperature, as indicated by the similarity in shape of the curves of Fig. 35. The first conclusion seems reasonable in view of the complexity of thermal gradients in the system and the possibility of actual

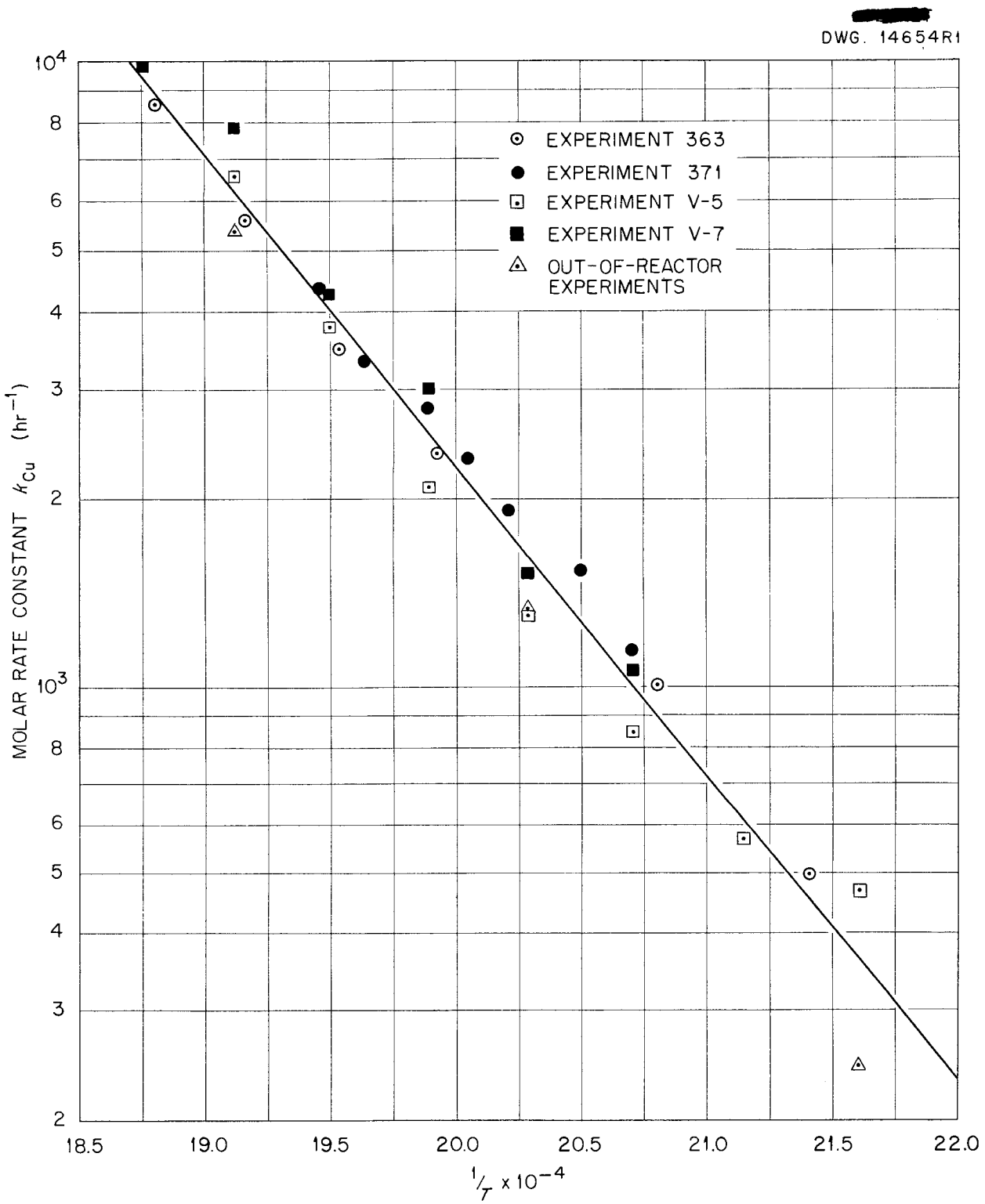

Fig. 34. Molar Rate Constant for Cupric Ion vs. Reciprocal of Absolute Temperature.

Table 35

CALCULATED MIXING COEFFICIENTS AND DIFFUSION FACTORS

TEMPERATURE (°C)	$(dP/dt)_{P=0}$ (psi/hr)	MIXING FACTOR, F_D,* FOR G = 1.5	DIFFUSION FACTOR, F_D
Experiment V-5			
190	2748	0.765	0.069
200	2610	0.707	0.066
210	2550	0.673	0.057
220	2292	0.589	0.048
230	2100	0.526	0.040
240	1380	0.337	0.031
250	1008	0.240	0.024
Experiment V-7			
210	2045	0.514	0.065
220	1941	0.475	0.057
230	1894	0.451	0.042
240	1636	0.380	0.037
250	1159	0.262	0.028
260	690	0.152	0.026

bubble formation, both factors giving rise to increased mixing. Furthermore, there is no obvious reason why the factors should display much variation over the temperature range employed.

In conclusion, emphasis should be given to the value of the concepts advanced, particularly as exemplified in Eq. 4, in the interpretation of pressure data during the course of an experiment. The nature of a dP/dt vs. P graph immediately indicates the conditions in the system. This has proved to be a most useful tool in the experimental program.

PLUTONIUM SOLUBILITIES IN URANYL SALT SOLUTION

K. S. Warren H. W. Wright

Stability of Plutonium Sulfate in Uranyl Sulfate Solutions. The investigation of the stability of plutonium(IV) sulfate in aqueous uranyl sulfate has been continued. Previously experiments had been conducted to determine the amount of plutonium remaining in solution after heating samples of a stock solution of uranyl-plutonium sulfates for various periods of times

-1285
3/52

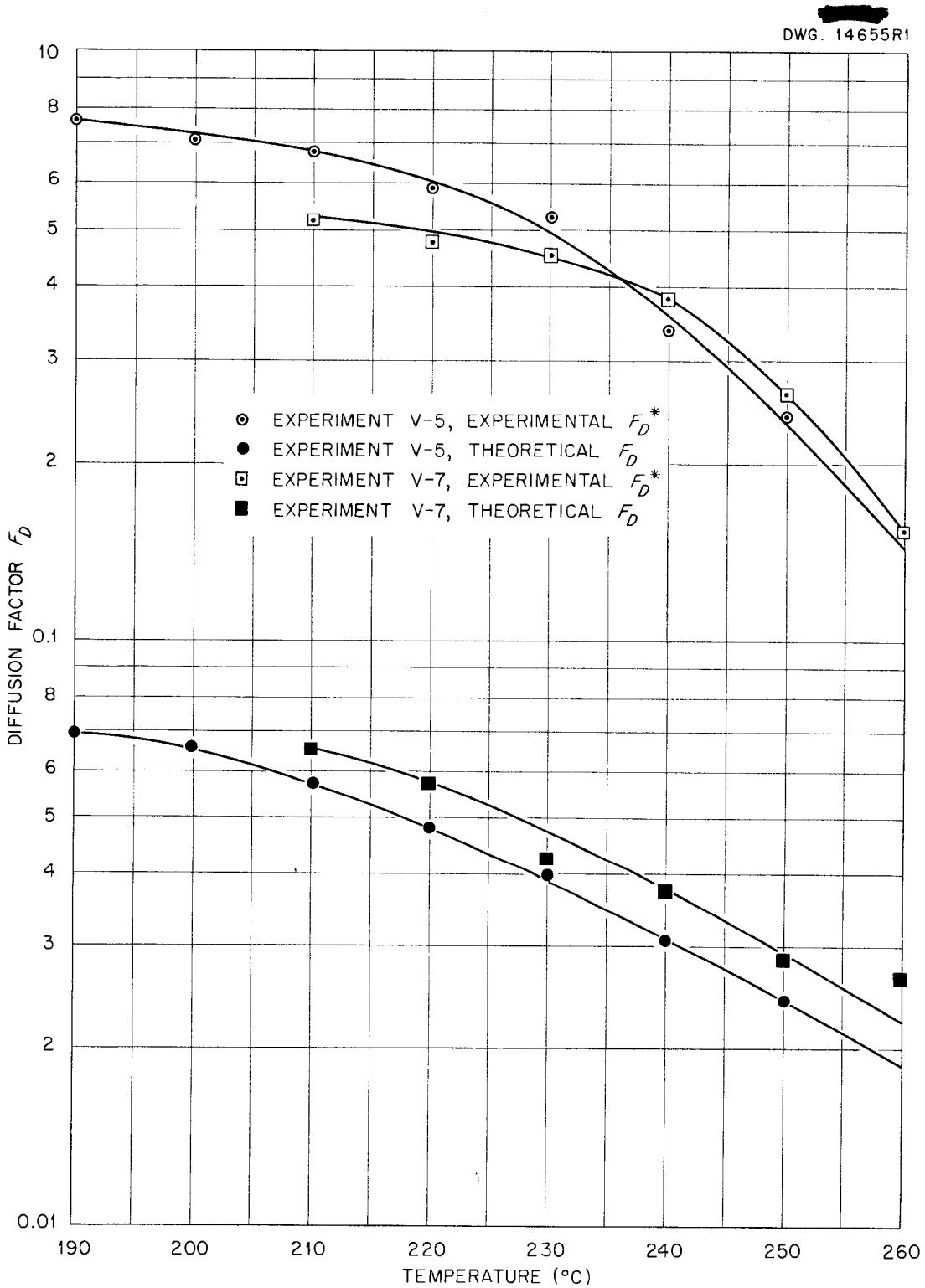

Fig. 35. Experimental and Theoretical Diffusion Factors for Experiments V-5 and V-7.

and at several temperatures.[8] Additional work showed that equilibrium was not attained as rapidly at the lower temperatures, and accordingly a determination of reaction rates appeared desirable.

A stock solution of about 0.5 g of plutonium(IV) per liter in UO_2SO_4 (650 g of uranium per liter of solution) was prepared in a manner similar to that employed for the preparation of the 1.26 *M* UO_2SO_4 stock solution.[8] Small amounts of the stock solution were sealed in glass ampoules and placed in an aluminum heater for the desired periods of time, and then removed, centrifuged, and analyzed. Details of the procedure have been described.[8] The data obtained at 100, 110, 125, and 150°C were plotted (see Fig. 36) and the reaction rate, *k*, for each of the four temperatures was calculated. It appeared that first-order-reaction treatment of the data was applicable, at least as a first approximation. From the straight line derived from log *k* plotted vs. $(1/T)$, the energy of activation was calculated to be about 31 kilocalories. The value for the energy of activation of the hydrolysis reaction applies specifically to plutonium dissolved in 2.73 *M* UO_2SO_4 and heated in pyrex glass ampoules with no more oxygen present than was originally contained in the enclosed air above the liquid sample. For future studies in which other types of container, lower concentrations of uranium, and higher concentrations of oxygen will be variables, see "Proposed Work," below.

Stability of Plutonium Ion in Fluoride Solutions. A solution of plutonium(IV) (0.53 g of plutonium per liter) in UO_2F_2 was prepared from plutonium peroxide and a solution of UO_2F_2 containing 398 g of uranium per liter. An exploratory investigation of the stability of the plutonium(IV) ion in the solution was conducted at 130°C in the same manner that the plutonium sulfate solutions had previously been studied. Plutonium precipitated from solution, behaving similarly to the sulfate under the experimental conditions, as may be observed in Table 36. A linear relationship between the *logarithm of the concentration* of plutonium ion and *time* has been derived from the data in Table 36, suggesting a first-order reaction.

Table 36

STABILITY OF PLUTONIUM ION IN FLUORIDE SOLUTIONS

TIME OF HEATING AT 130°C (days)	AMOUNT OF Pu REMAINING IN SOLUTION (g/liter)
0	0.53
0.75	0.34
5	0.04
10	0.006

During attempts to prepare a suitable sample for the stability investigation, a light-yellow precipitate was obtained in every case. The precipitate has not been identified.

Effect of Radiation on the Valence State of Plutonium. There is little definite information concerning the ability of intense gamma-radiation fields to change the valence of plutonium ions in solution. A few experiments were planned for the purpose of studying the subject, since it would have a direct bearing on the homogeneous reactor program. Samples of plutonium(III) and plutonium(VI) were prepared by electrolyzing plutonium sulfate in a glass cell by using platinum electrodes without stirring

[8] K. S. Warren and H. W. Wright, *op. cit.*, ORNL-1221, p. 97.

-1285 3/52

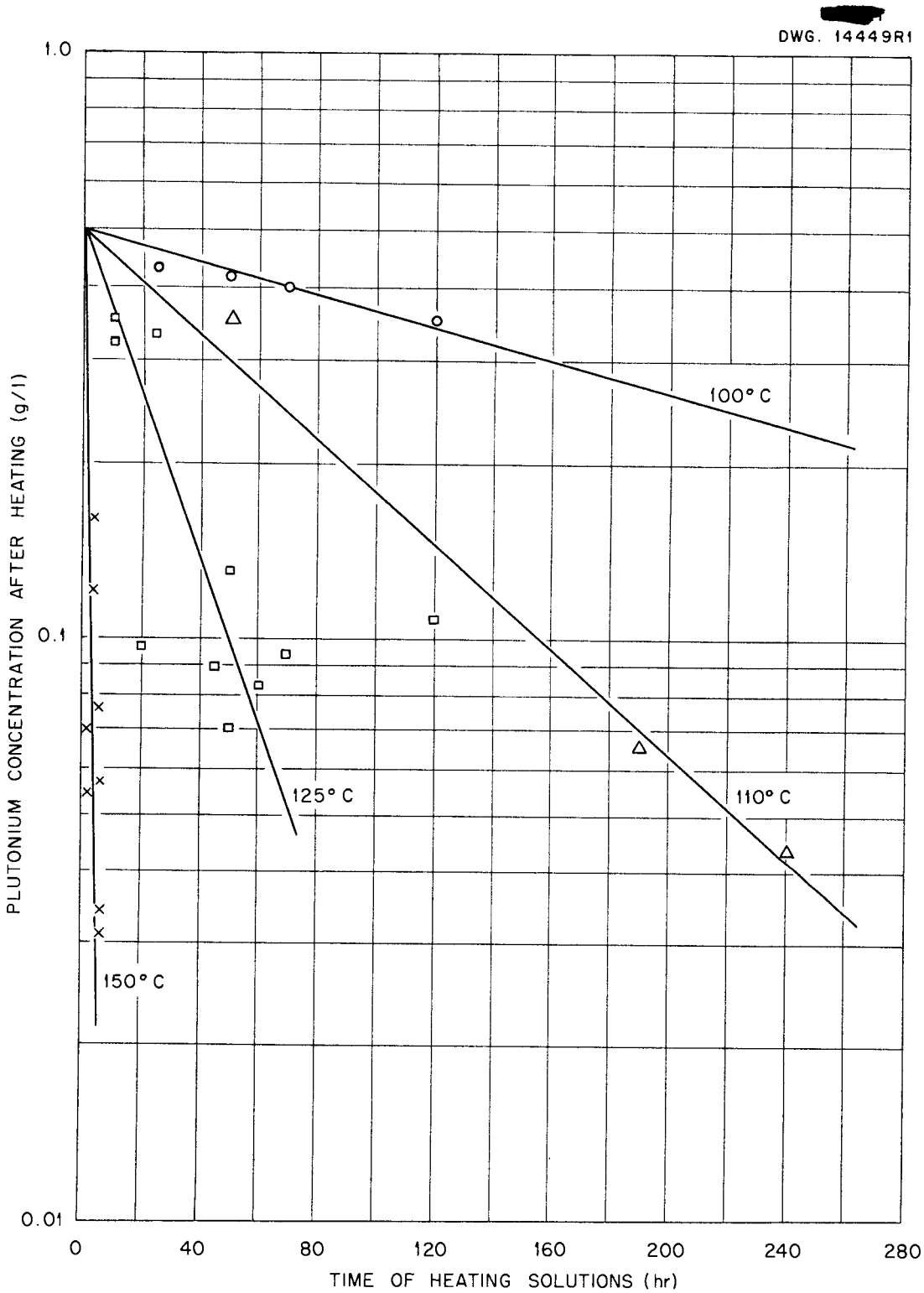

Fig. 36. Change of Concentration of Plutonium Sulfate in 2.73 *M* Uranyl Sulfate During Heating at Various Temperatures.

and a current density of 0.55 ma per cm^2 of electrode surface. Portions of the electrolyte were removed from the anode and cathode compartments and sealed in pyrex glass ampoules. The ampoules were irradiated for 67 hr in a gamma field at 12,000 r/min. After irradiation the samples were kept at room temperature for three days before opening and diluting with 0.1 *M* H_2SO_4. Absorption measurements on the diluted samples were made with a Beckman quartz spectrophotometer. An inspection of the absorption curves showed that the high and low valence states of the control samples tended to "drift" back to the original IV state while standing under room conditions. However, the valence states of the irradiated samples changed more rapidly to the stable IV state. The experiment should be repeated at least once before arriving at more quantitative conclusions.

Proposed Work. Plutonium-solubility investigations using stainless steel bombs are planned. A parallel set of experiments in titanium bombs will be added if they appear warranted. The effect of oxygen on the solubility of plutonium is of considerable interest in view of recent work by Tomlin of the Chemical Technology Division. A stainless steel bomb has been fabricated for the first of the new series of investigations.

A second irradiation study is being made in connection with plutonium valence changes. The time elapsed between irradiation and absorption analysis will be held to a minimum to eliminate "post-irradiation" drifts that may be in opposition to the effects of the gamma radiation.

A plutonium-uranyl phosphate solution is being prepared for solubility investigations similar to those made with the corresponding sulfates.

FISSION-PRODUCT SOLUBILITIES IN URANYL SULFATE SOLUTIONS

E. V. Jones

Cesium Sulfate. The silica-tube synthetic method has been applied in the study of the solubility of Cs_2SO_4 in 0.126 and 1.26 *M* UO_2SO_4 solutions as a function of temperature. A partial report on the work and on other solubility studies has appeared previously.[9]

The corrected data are given in Table 37 and are shown in Fig. 37 along with the data of Lietzke and Stoughton[10] for the solubility of Cs_2SO_4 in water. The extremely low solubility for Cs_2SO_4 in 1.26 *M* UO_2SO_4 has been noted and will be investigated further.

Cadmium Sulfate. The solubility of $CdSO_4$ in 1.26 *M* UO_2SO_4 has been studied as a function of temperature by using the synthetic method. The data are given in Table 38 and Fig. 38. For purposes of comparison, the solubilities by Lietzke and Stoughton[10] and Benrath[11] in water and in 0.126 *M* UO_2SO_4 are included in Fig. 38.

Cadmium sulfate shows a negative temperature coefficient of solubility and considerable supersaturation. The temperatures recorded are those at which the last crystals dissolved on very slow cooling.

Silver Sulfate. The solubility of Ag_2SO_4 is being studied in 0.126 and 1.26 *M* UO_2SO_4 by the synthetic method. Silver sulfate shows a positive temperature coefficient of solubility. In 0.126 *M* UO_2SO_4 a reversible reaction yielding a reddish precipitate occurs at about 150°C. Plans have been made to investigate the nature of the red

(9) E. V. Jones, *ibid.*, p. 99.

(10) M. H. Lietzke and R. W. Stoughton, *The Measurement of the Solubility of Fission Product Sulfates at High Temperatures and Pressures*, ORNL-970 (March 13, 1951).

(11) I. A. Benrath *et al.*, *Z. anorg. allgem. Chem.* **231**, 285 (1937).

-1225
3/52

product. At present there is some uncertainty in the data. For that reason, the completed work will be withheld until the next report.

Interpretation of Data. Solubility data for $Y_2(SO_4)_3$, $La_2(SO_4)_3$, Cs_2SO_4, $CdSO_4$, Ag_2SO_4, and $Ce(SO_4)_2$ in water, 0.126 *M*, and 1.26 *M* UO_2SO_4 were considered. The data were obtained from the current investigation, work by Lietzke, Zemel, and Stoughton of this laboratory, and previously published literature data on studies

Table 37

SOLUBILITY OF Cs_2SO_4 IN UO_2SO_4 SOLUTIONS

IN 0.126 *M* UO_2SO_4		IN 1.26 *M* UO_2SO_4	
Temperature (°C)	Cs_2SO_4 (wt %)	Temperature (°C)	Cs_2SO_4 (wt %)
53.8	64.19	167.7	0.30
61.6	66.00	178.5	0.33
77.3	67.12	187.3	0.37
84.2	67.55	214.8	0.44
104.8	68.58	245.3	0.49
140.2	70.07	285.6	0.54
177.5	71.66	Two liquid layers at 288.6	
228.6	73.48	Much undissolved	0.78

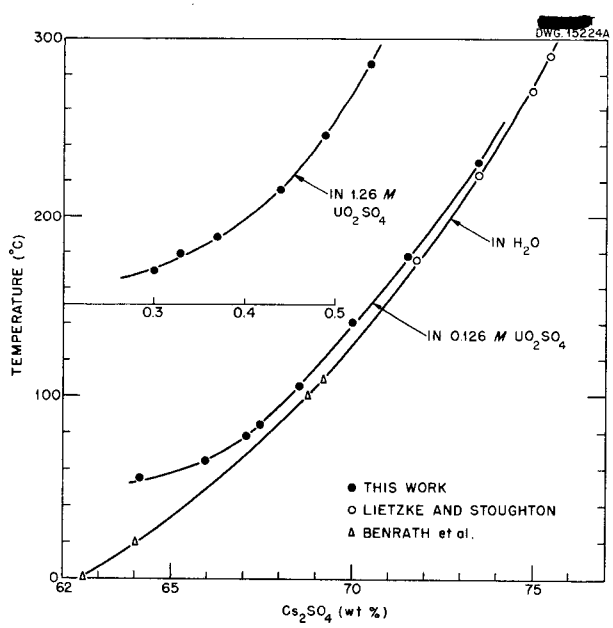

Fig. 37. The Solubility of Cs_2SO_4 in UO_2SO_4 Solutions.

Table 38

SOLUBILITY OF $CdSO_4$ IN 1.26 *M* UO_2SO_4

TEMPERATURE (°C)	$CdSO_4$ (wt %)
21	31.62
47.8 (209)*	31.33
84.2	30.50
102.9 (215.8)*	30.12
215.8	29.37
216.8	29.69
220.8	28.68
228.7	26.54
230.6	25.83
244.3	22.51

*Double solubility points.

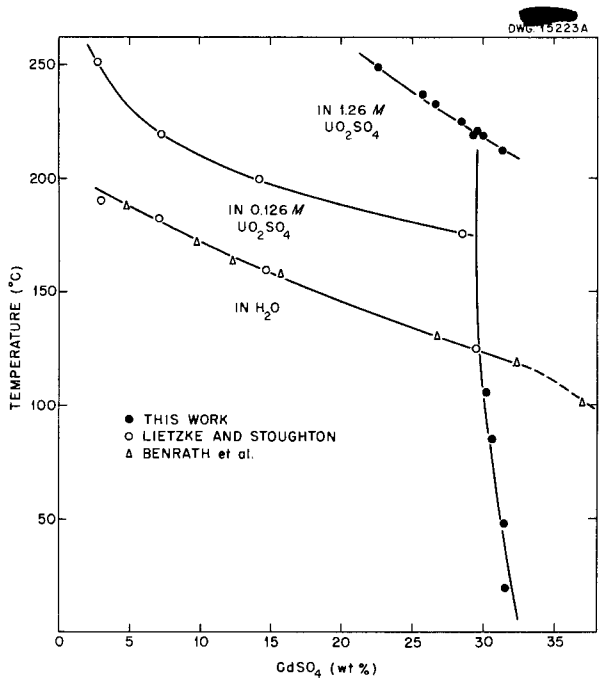

Fig. 38. The Solubility of $CdSO_4$ in UO_2SO_4 Solutions.

in water. The data have been plotted by using the Van't Hoff isochore, $d \log N/d(1/T) = -\Delta H/2.3R$. In most cases the plot yielded straight-line relationships. Differential heats of solution for the fission-product sulfates (in the saturated solution) obtained are given in Table 39. In considering the data, the change in ΔH with respect to molarity of UO_2SO_4 was positive for all the above salt systems.

CALCULATED FISSION-PRODUCT BUILDUPS FOR A HOMOGENEOUS REACTOR - EXPERIMENTAL SOLUBILITIES OF FISSION-PRODUCT MIXTURES IN URANYL SULFATE SOLUTIONS

J. S. Gill W. L. Marshall

The actual expected amounts of fission products for a typical reactor were calculated to provide a basis for

Table 39

SOME DIFFERENTIAL HEATS OF SOLUTION OF FISSION-PRODUCT SULFATES IN WATER AND IN URANYL SULFATE SOLUTION ABOVE 100°C

SALT	ΔH(soln) in kcal/mole		
	In H_2O	In 0.126 M UO_2SO_4	In 1.26 M UO_2SO_4
$Y_2(SO_4)_3$	-27	-16	-9
$La_2(SO_4)_3$	-23	-12	-8
$CdSO_4$	-17	-14	-5.4
$Ce(SO_4)_2$	-10	- 6.9	
Ag_2SO_4	+ 1.1	+ 2.3	+3.7
Cs_2SO_4	+ 0.20	+ 0.20	+1.5

-1285
3/52

an investigation of fission-product solubilities and to make the elimination of certain fission products from solubility consideration possible. Continuous operation periods of one month and one year were chosen since they should be greatly in excess of actual processing intervals. The behavior of fission products in the relative amounts indicated by the calculations is being studied at 250°C in uranyl sulfate solutions.

Fission-product buildups were calculated for a 50 kw/liter reactor running continuously at full power for the specified times. All fission chains producing a given element were considered. The chains together with fission yields were obtained from the plutonium-project data.[12] Standard equations involving buildups of stable and unstable isotopes were used; however, approximations were made where no significant change would occur in the final summation for a given element. The values given in Table 40 were calculated for the case in which no gaseous fission products were removed and for 100% removal. The actual amounts should be between the two limits, depending on the percentage of gaseous fission product removal during reactor operation. To determine buildups for other power levels, the values in Table 40 should be multiplied by the appropriate power ratio, for example, for a 25 kw/liter reactor, the buildups would be halved.

Synthetic mixtures of ten of the solid fission products with highest yield (Ce, Zr, Cs, Mo, Ru, Ba, Sr, La, Nb, and Y) as chlorides or nitrates

[12] J. M. Siegel, *J. Am. Chem. Soc.* 68, 2411 (1946).

Table 40

CALCULATED SOLID FISSION-PRODUCT BUILDUPS FOR A 50 kw/liter HOMOGENEOUS REACTOR CONTINUOUSLY OPERATED

ELEMENT	FISSION-PRODUCT BUILDUP (g/l)			
	One Month		One Year	
	0% Gas Removal	100% Gas Removal	0% Gas Removal	100% Gas Removal
Cerium	0.2	0.06	2	0.7
Neodymium	0.2	0.07	2	0.8
Zirconium	0.2	0.08	2	0.6
Cesium	0.1	0.0	2	0
Molybdenum	0.1	0.1	1	1
Ruthenium	0.1	0.1	1	1
Barium	0.09	0.0001	0.8	0.001
Strontium	0.08	0.007	0.8	0.1
Lanthanum	0.07	0.0	0.7	0.0
Praseodymium	0.04	0.0	0.6	0.0
Niobium	0.04	0.004	0.5	0.1
Yttrium	0.04	0.0	0.3	0.0
Technetium	0.03	0.03	0.5	0.5
Rubidium	0.03	0.007	0.3	0.01
Promethium	0.02	0.02	0.2	0.2
Rhodium	0.006	0.006	0.3	0.3

were fumed to dryness with a 1:1 HNO_3-H_2SO_4 mixture. An amount of the dry mixture equivalent to one year's production, assuming no gas removal, was added to 0.125 and 1.25 *M* UO_2SO_4 solutions, respectively, and the resultant solution heated to 250°C. The experiments were conducted in titanium bombs with platinum filters; the apparatus was developed by B. Zemel and R. W. Stoughton and has been described in previous reports. By means of the apparatus the solutions were filtered at 250°C from the solid, and the various soluble components were determined by separation-tracer and spectrographic techniques.

The variation in analytical data from a standpoint of the individual runs and between the tracer and spectrographic data is quite marked, therefore, the individual values will not be reported until more consistent results are obtained. From the data, however, it does appear justifiable to state that cerium, zirconium, ruthenium, barium, and niobium will be the first of the elements studied to precipitate. Any interaction of the elements or others with the reactor surfaces is not considered.

TWO-LIQUID-PHASE TEMPERATURES FOR THE DEUTERIUM OXIDE-URANYL SULFATE AND URANYL FLUORIDE SYSTEMS

E. V. Jones

Two liquid phase transition temperatures were determined for various concentrations of uranyl sulfate and uranyl fluoride in deuterium oxide. For purposes of comparison, similar measurements were made in normal water for both the sulfate and fluoride systems.

Uranyl sulfate was prepared by Lietzke and Griess[13] at this Laboratory by the current method that consists of adjusting a H_2SO_4-UO_3 Mallinckrodt solution to the stoichiometric ratio. Approximately anhydrous UO_2SO_4 was prepared by dehydrating the salt at 350°C with a stream of dried air as prescribed by Mansfield of the Chemical Technology Division. Analysis for uranium indicated 97.6% anhydrous UO_2SO_4. The solid was dissolved in 99.8% D_2O to make the required UO_2SO_4-D_2O solutions. The UO_2SO_4-H_2O solutions were made with both the dehydrated UO_2SO_4 and $UO_2SO_4 \cdot 3H_2O$ solid. No transition temperature difference was noted with either sample.

Uranyl fluoride prepared at the Y-12 Plant was dried at 135°C to give 99.9% UO_2F_2. The solid was dissolved in 99.8% D_2O and also in H_2O to make the two solutions.

Experimental runs were made in 4-mm-ID silica tubing in rocker apparatus similar to that used in all previous solubility studies. The Brown temperature recorder and thermocouple was calibrated both by potentiometric methods and by melting points of naphthalene (79°C), tin (232°C), and bismuth (271°C).

The data for UO_2SO_4 are shown in Table 41 and Fig. 39. Two significant results were obtained. First, the two-liquid-phase appearance temperature was lowered about 10 deg in D_2O as compared with the water system; the minimum critical-solution temperature for the D_2O system is 275°C. Second, the values obtained in water are about 10°C below those previously reported for this system,[14] that is, 285°C instead of 295°C for the minimum critical-solution temperature.

One possible explanation for the difference between past and present results in water is that prior to

[13] M. H. Lietzke and J. C. Griess, *Homogeneous Reactor Project Quarterly Progress Report for Period Ending August 15, 1951*, ORNL-1121, p. 124.

[14] C. H. Secoy, *J. Am. Chem. Soc.* **72**, 3343 (1950).

-1285
3/52

Table 41

TWO-LIQUID-PHASE TEMPERATURES FOR URANYL SULFATE IN WATER AND IN DEUTERIUM OXIDE

IN H_2O		IN D_2O	
Temperature (°C)	UO_2SO_4 (wt %)	Temperature (°C)	UO_2SO_4 (wt %)
304.7	3.77	282.7	7.80
303.7	3.88	277.7	12.07
300.8	4.02	274.7	20.03
287.6	11.56	274.7	36.05
284.7	20.01	276.3	43.53
284.7	32.15	278.8	50.54
285.0	34.90	286.6	59.02
288.1	48.28	305.5	66.46
294.5	59.34		

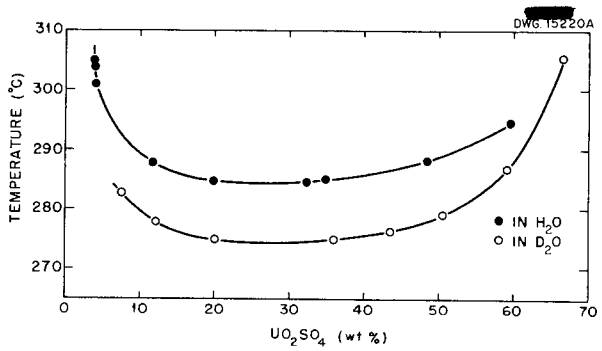

Fig. 39. The Two-Liquid-Phase Region of UO_2SO_4 in H_2O and in D_2O.

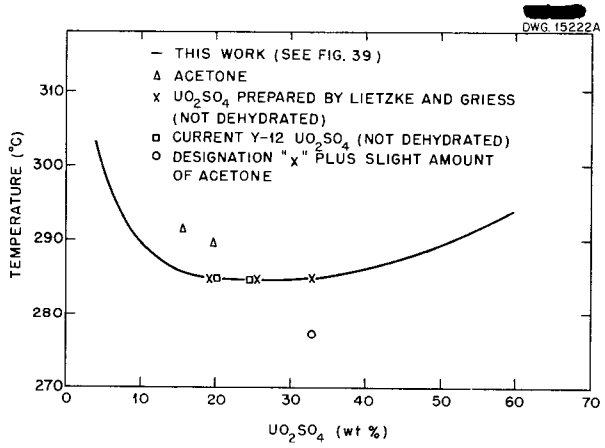

Fig. 40. The Two-Liquid Phase Region of UO_2F_2 in H_2O and in D_2O.

July, 1951, all UO_2SO_4 used in the work was prepared by the acetone precipitation process.[15] To test this explanation, together with that of the possible decomposition of UO_2SO_4 upon drying at 275°C, several variables were introduced. Two runs were made with the UO_2SO_4 solution prepared at Y-12. Three runs were made with Lietzke-Griess UO_2SO_4 solution and two runs were made with acetone-precipitated UO_2SO_4. A final run was made after adding one drop of acetone to the Lietzke-Griess UO_2SO_4 solution. The results given in Fig. 40 indicate that there is no temperature effect from the use of other samples of uranyl sulfate prepared by stoichiometric combination of UO_3 and H_2SO_4. However, the acetone-precipitated material did give a 5-deg elevation in temperature. Free acetone added to the Lietzke-Griess solution lowered the two-liquid-phase temperature. Degassing

[15] L. Helmholtz and G. Friedlander, *Physical Properties of Uranyl Sulfate Solutions*, LAMS-30R (Dec. 15, 1943).

some solutions (not containing acetone) appeared to have very little effect on the transition temperatures.

The data for uranyl fluoride are given in Table 42 and are shown in Fig. 41. There is the significant 10-deg lowering of the liquid-phase transition temperature for the D_2O system as compared with water. Values for the UO_2F_2-H_2O system alone are about 2 deg higher than previously reported.[16] No satisfactory values for the fluoride system were obtained for concentrations below about 15 to 20% because of the previously observed reaction with the silica tube.[16]

[16] W. L. Marshall, J. S. Gill, and C. H. Secoy, *Chemistry Division Quarterly Progress Report for Period Ending June 30, 1950*, ORNL-795, p. 22.

Impurities apparently have a large effect on the two-liquid-phase transition temperatures. This conclusion was drawn after noting the 10-deg-lowering effect of 95 to 100% D_2O, the

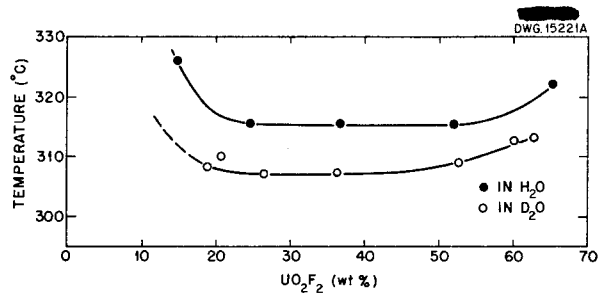

Fig. 41. Some Effects of Different UO_2SO_4 Solutions on the Two-Liquid-Phase Region of UO_2SO_4-H_2O.

Table 42

TWO-LIQUID-PHASE TEMPERATURES FOR URANYL FLUORIDE IN WATER AND IN DEUTERIUM OXIDE

IN H_2O		IN D_2O	
Temperature (°C)	UO_2F_2 (wt %)	Temperature (°C)	UO_2F_2 (wt %)
No transition up to 350	4.42	Crystals at 328	5.24
326.2	14.73	No transition up to 340	
315.8	24.77	Crystals at 309	16.12
315.8	36.99	No transition up to 340	
315.3	51.90	308.4	18.67
322.2	65.15	310.4	20.85
		307.4	26.01
		307.4	36.25
		308.7	52.43
		312.6	59.86
		313.1	62.80

large difference in two-liquid-phase appearance temperature between the currently prepared UO_2SO_4 and previously prepared acetone-precipitated UO_2SO_4, the effect of excess acid, and fission-product effects (cf., previous *Chemistry Division Quarterly Progress Reports*).

CONDUCTIVITY OF URANYL SULFATE AND URANYL FLUORIDE IN AQUEOUS SOLUTION

R. D. Brown

The experimental measurement of the conductivity of aqueous solutions of uranyl sulfate and uranyl fluoride, described in previous quarterly progress reports, has been continued. Conductivity data are now available for uranyl sulfate solutions in concentrations from 0.0001 to 6 *N* at 0, 25, 50, 90, and 125°C. Similar data are available for uranyl fluoride solutions in concentrations from 0.0001 *N* to 6.0 *N* at 0, 25, 50, and 90°C.

Tables 43 and 44 summarize the equivalent conductances of uranyl sulfate and uranyl fluoride solutions.

Figures 42 and 43 show a plot of equivalent conductance (Λ) vs. $\sqrt{C}$, where C is equivalents per liter at 25 °C for uranyl sulfate and uranyl fluoride.

The data show that both uranyl sulfate and uranyl fluoride are weak electrolytes in aqueous solution. Uranyl fluoride is the weaker of the two; its conductivity at 90°C is approximately equal to that of uranyl sulfate at 0°C. The fluoride, however, shows a much greater relative increase in equivalent conductivity than does the sulfate, which indicates that the increase is not simply a viscosity function. No detailed theoretical treatment of the data has been made, but it would appear that uranyl sulfate is more highly dissociated than uranyl fluorides.

VAPOR PRESSURES OF URANYL SULFATE SOLUTIONS

H. O. Day, Jr.

The vapor pressures of pure water were checked as preliminary measurements prior to making accurate vapor-pressure measurements on uranyl salt solutions from 50 to 150°C. The water was degassed by freezing and melting several times under vacuum and subliming the ice from one container to another a number of times. The pressure measured at the triple point before the water was distilled into the pressure vessel checked with the literature value to a high degree of accuracy. After the water was distilled into the pressure vessel, measurements were made up to 100 and 110°C. Unfortunately the vapor pressures at these temperatures were lower than the true values by an amount larger than the experimental accuracy of the the apparatus. The error possibly resulted from cleaning the pressure vessel with a mixture of sodium dichromate and sulfuric acid. There is a good chance that the glass walls adsorbed enough impurities to cause later errors in the vapor pressure measurements. New cleaning methods are now used.

During the preliminary runs two pressure vessels cracked because of errors in the water-loading technique. When new vessels were built an improved design was used in an effort to prevent breakage and also to attain better stirring.

Measurements of the vapor pressures of saturated solutions of UO_2SO_4 have been started and measurements have been made at 50, 60, 70, 80, 90, and 100°C. The values obtained will not

Table 43

CONDUCTIVITY OF URANYL SULFATE

URANYL SULFATE CONCENTRATION (eq./l at 25°C)	EQUIVALENT CONDUCTANCE ($ohms^{-1}$)				
	At 0°C	At 25°C	At 50°C	At 90°C	At 125°C
0.0001		175.65	288.0	505	600
0.0005	66.28	127.40	197.0	280	320
0.001	57.86	106.70	157.9	220.0	236
0.005	40.04	63.30	85.20	104.0	110.4
0.01	29.54	49.31	64.74	77.0	81.4
0.025	22.26	44.18			
0.05	17.71	27.70	35.66	43.80	48.6
0.1	14.24	22.22	29.01	37.30	42.08
0.5		14.45	20.34	28.64	
1.0	(0.4 *N*) 9.37	11.61	16.88	24.43	26.78
2.52	(3 *N*) 2.51	6.16	9.59	14.49	18.00
4.66	(6 *N*) 0.465	2.78	4.69	7.77	10.07
7.28			1.02		

Table 44

CONDUCTIVITY OF URANYL FLUORIDE

URANYL FLUORIDE CONCENTRATION (eq./l at 25°C)	EQUIVALENT CONDUCTANCE ($ohms^{-1}$)			
	At 0°C	At 25°C	At 50°C	At 90°C
0.0001	34.45	73.54		
0.0005	18.39	35.70	62.48	104.2
0.001	12.47	26.10	44.22	71.30
0.005	6.16	12.31	19.51	30.40
0.01	4.62	9.17	14.41	22.70
0.05	2.73	5.43	8.60	13.52
0.1	2.37	4.74	7.50	11.88
0.5	1.87	3.75(3.80)*	5.96	9.50
1.0	1.61	3.22(3.22)*	5.10	8.15
3.0			3.12	4.91
6.0			1.40	2.27

*G. R. Dean, *Properties of Uranyl Fluoride*, Metallurgical Project, CC 2092 G (Sept. 11, 1944).

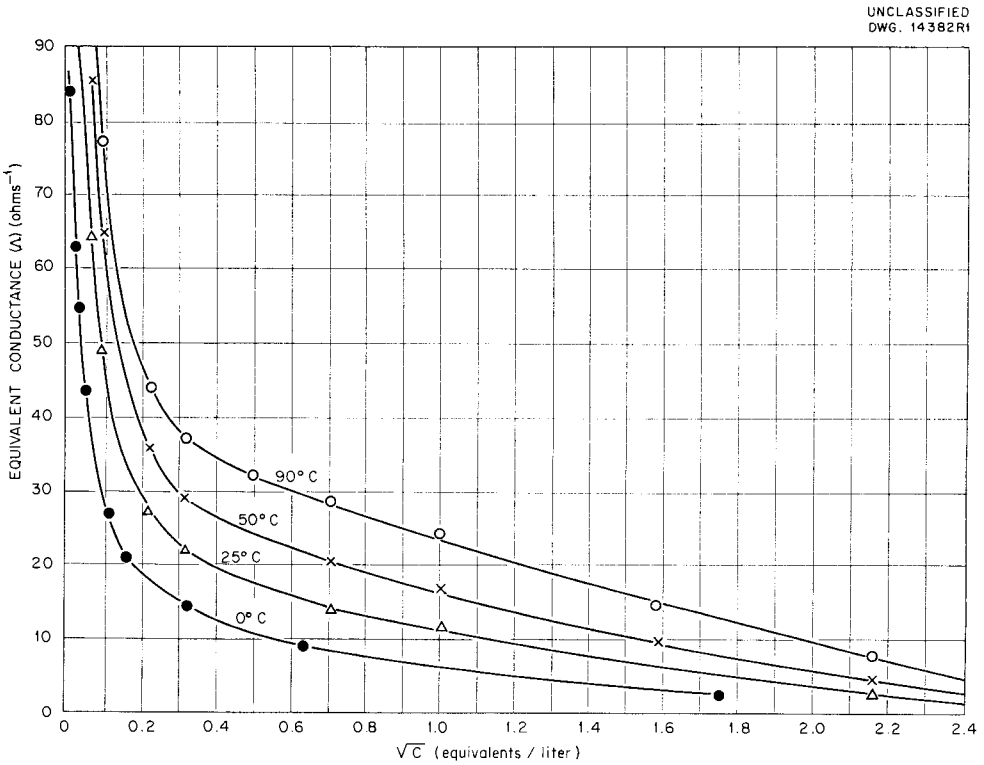

Fig. 42. Conductivity of Uranyl Sulfate.

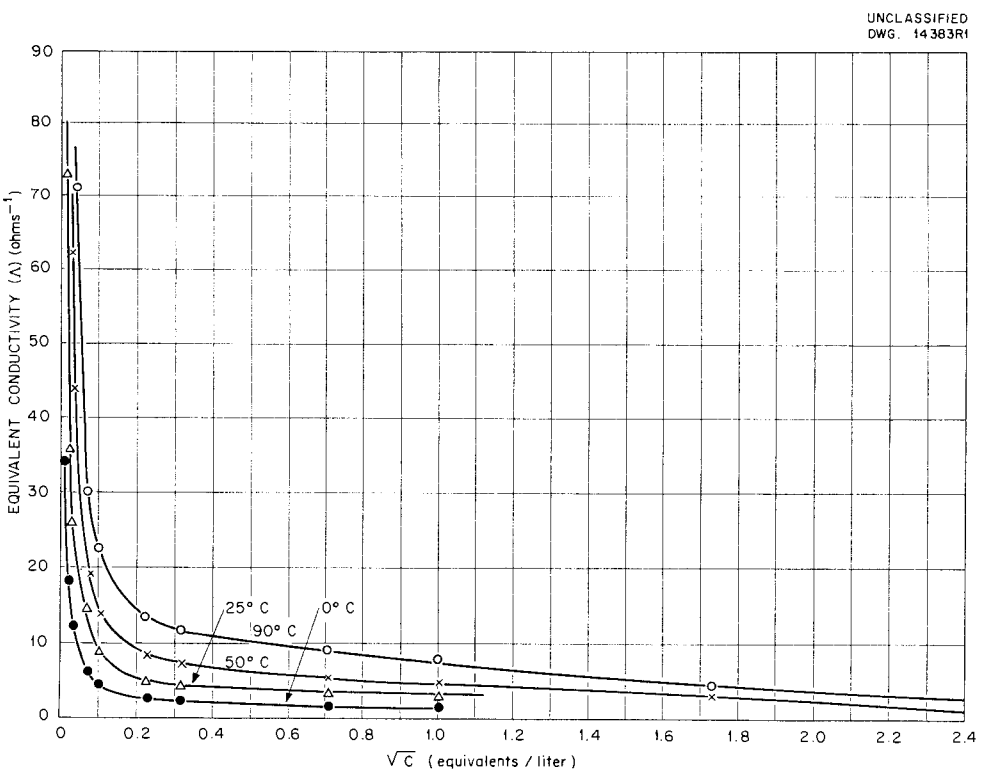

Fig. 43. Conductivity of Uranyl Fluoride.

be given until more data are collected. Difficulty has been encountered in attaining true saturation in the constant-pressure measurements. Work on uranyl sulfate solutions is being continued.

DENSITY-WEIGHT PERCENT-MOLARITY RELATIONSHIPS AT 25°C AND BETWEEN 100 AND 300°C FOR AQUEOUS URANYL SULFATE SOLUTIONS

W. L. Marshall

Empirical density-weight percent-molarity conversion equations have been determined for uranyl sulfate-water solutions at 25.0°C and between 100 and 300°C from available density data. The equations together with origins of data and with detailed derivations are included in a Homogeneous Reactor Quarterly Report.[17] A few of the significant equations from the work are given below.

The equations for UO_2SO_4-H_2O solution applicable at 25.0 ± 0.2°C are:

$$d = 0.9970 + 0.316_5\, M \quad ,$$

accuracy:

$$d \text{ to } \pm 0.45 \left(1 - \frac{1}{d}\right) \% \quad ,$$

$$M \text{ to } \pm 0.45\% \quad ,$$

$$d = \frac{0.9970}{1 - 0.00864_5\, S} \quad ,$$

accuracy:

$$d \text{ to } \pm 0.45\,(d - 1)\ \% \quad ,$$

$$S \text{ to } \pm 0.45\% \quad ,$$

$$\frac{1}{M} = \frac{36.7_2}{S} - 0.3174 \quad ,$$

accuracy:

$$M \text{ to } \pm 0.45 \left(\frac{37M}{S} - 1\right) \% \quad ,$$

$$S \text{ to } \pm 0.45 \left(\frac{S}{37M} - 1\right) \% \quad ,$$

where,

d = density of solution in g/cm³ at 25.0°C,

M = molarity at 25.0°C,

S = wt % UO_2SO_4.

An equation applicable between 100 and 300°C is:

$$d^t_{soln} = \frac{1}{\dfrac{120.9}{S} - 1.046} + d^t_{H_2O}$$

accuracy:

d^t_{soln} to ±0.5% from 25 to 300°C for UO_2SO_4-H_2O solutions not over 10 wt % UO_2SO_4,

d^t_{soln} to ±1.0% between 120 and 250°C for concentration greater than 10%,

d^t_{soln} to ±2.0% between 25 and 280°C for concentration above 10%,

where

$d^t_{H_2O}$ = density of water at t°C (at saturated vapor pressure) .

The following equations for UO_2SO_4-D_2O solutions are derived by the

[17] W. L. Marshall, *Homogeneous Reactor Quarterly Progress Report for Period Ending March 15, 1952*, ORNL-1280, p. 188.

-1285 3/52

substitution of D_2O density for H_2O density in the foregoing relationships. There are no experimental data available to justify the correctness of the equations.

At 25.0 ± 0.2°C,

$$d_{soln} = 1.1044 + 0.316_5\, M$$

$$d_{soln} = \frac{1.1044}{1 - 0.008645\, S}$$

$$\frac{1}{M} = \frac{33.14}{S} - 0.286_6 \ .$$

Between 120 and 280°C,

$$d^t_{soln} = \frac{1}{\frac{109.2}{S} - 0.943_9} + d^t_{D_2O} \ .$$

EXPERIMENTS WITH HIGH-TEMPERATURE ELECTRODES

M. H. Lietzke R. W. Stoughton

The work[18] to develop a high-temperature reference electrode is being continued. Considerable difficulty has been experienced in setting up a $Pb,PbSO_4$ electrode that in combination with a Ag,Ag_2SO_4 or Hg,Hg_2SO_4 electrode will give a potential in agreement with the value calculated from thermodynamic data. Although amalgams and sulfuric acid of several different concentrations have been tried, the cell potentials measured with the lead electrodes in conjunction with a Ag,Ag_2SO_4 electrode have been at least 15 mv low. The difficulty is being investigated further. Both the Ag,Ag_2SO_4 and Hg,Hg_2SO_4 electrodes, however, seem to function properly and can be used as high-temperature reference electrodes in dilute H_2SO_4 solutions. It appears that the Ag_2SO_4 electrode can also be used as a reference electrode in UO_2SO_4 solution.

Experiments at temperatures from 25 to 50°C have indicated that the Ag,Ag_2SO_4 and Hg,Hg_2SO_4 electrodes in H_2SO_4 must be allowed to stand several days before equilibrium potentials are obtained. Figure 44 shows a plot of the potential of the Ag,Ag_2SO_4, Hg_2SO_4,Hg cell as a function of temperature. It was necessary to equilibrate the cell combination for two or three days to obtain each point on the line. The slope of the line gives

$$\frac{dE}{dT} = -0.345 \text{ mv/°C} \ .$$

Since $dE/dT = \Delta S/nF$, the value of ΔS for the cell reaction can be calculated. From the above slope

$$\Delta S = \frac{2\ (96{,}500)\ (-0.345)}{(4.1833)\ (1000)} = -16.2 \text{ e.u.}$$

This corresponds to the average value of ΔS for the reaction

$$2\ Hg_{(l)} + Ag_2SO_{4(s)} = Hg_2SO_{4(s)} + 2\ Ag_{(s)}$$

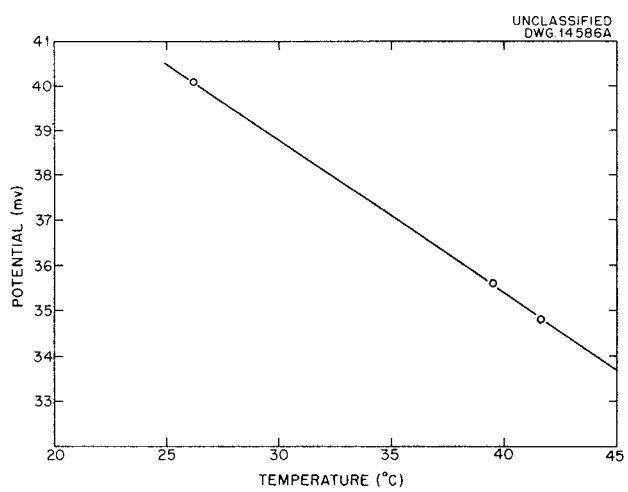

Fig. 44. Potential-Temperature Curve for Ag,Ag_2SO_4; Hg_2SO_4,Hg Electrode Combination.

[18] M. H. Lietzke and R. W. Stoughton, *Chemistry Division Quarterly Progress Report for Period Ending December 30, 1951*, ORNL-1260, p. 128.

over the region 25 to 45°C. The value for ΔS computed from individual entropies given in Latimer's tables[19] is -16.4 e.u. Hence the two values are in very good agreement, and the electrodes seem to be functioning properly. In future work, the high-temperature behavior of these electrodes will be studied and the value of ΔS for the cell reaction obtained as a function of temperature.

Figure 45 shows how the Ag, Ag_2SO_4 and the Hg, Hg_2SO_4 electrodes can be used to show the failure of the passive film on type 347 stainless steel in 0.05 *M* H_2SO_4 at high temperatures. The passive film was produced by heating with 1% HNO_3 for 24 hr at 250°C. As long as the film was intact the lower potential curves were obtained, but when the film broke the potentials shifted sharply to the values indicated in the upper curves. The upper curves represent the potential of the reference electrodes against the bare steel in 0.05 *M* H_2SO_4. The shift in potential amounted to over half a volt.

At present the Ag, Ag_2SO_4 electrode is being tried to show the failure of the passive film on type 347 stainless steel in UO_2SO_4 solution at high temperature. Curves have been obtained which show the break, but work on this phase of the problem is still incomplete. An attempt will be made to correlate the potential measurements with the durability of the passive film under various partial pressures of oxygen.

(19) W. M. Latimer, *Oxidation Potentials* (new edition to be published).

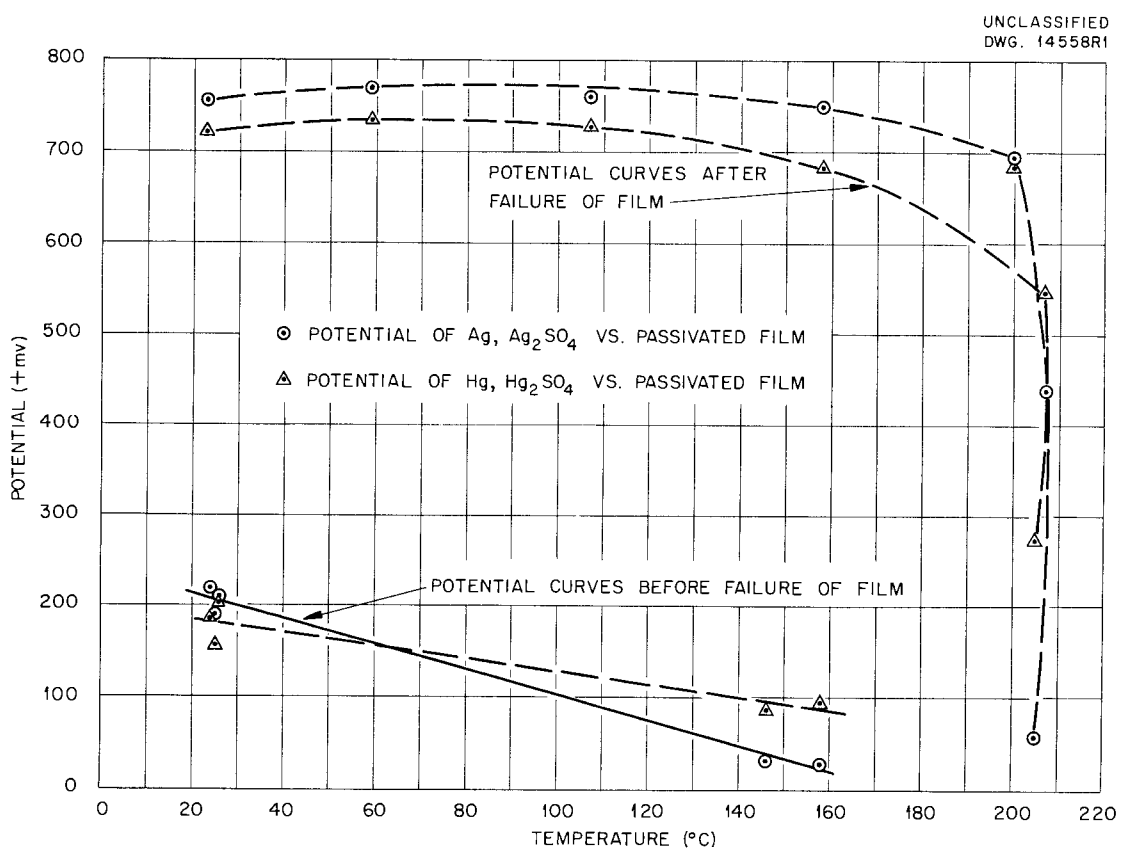

Fig. 45. Curves Showing Failure of Passive Film on Type 347 Stainless Steel in 0.05 *M* H_2SO_4.